PHD COURSE IN BIOMEDICAL SCIENCES AND BIOTECHNOLOGY

XXXI CYCLE

Title of the thesis

Respiratory Limitations to Exercise Tolerance and Performance in Obese Adolescent Patients

Supervisors

Prof. Bruno Grassi

Dr. Desy Salvadego

PhD Student

Hailu Kinfu Alemayehu

ACADEMIC YEAR 2018/2019

TABLE OF CONTENTS

ABSTRACT/SUMMARY

Obese adolescents (OB) have an increased O_2 cost of exercise, attributable in part to an increased O_2 cost of breathing. The increased O_2 cost of breathing could entail a "competition" between respiratory and locomotor muscles for the finite available O_2, leading to fatigue and premature exhaustion. This would contribute to the inactivity which represents one of the main causes of obesity, impeding the increased level of physical activity which is one of the cornerstones of the treatment of the disease. In order to interrupt this vicious circle, we followed two approaches, attempting to relieve the respiratory limitation in obese adolescents performing cycling/walking exercises.

In the first approach, respiratory muscles were acutely unloaded via normoxic helium-O_2 (HeO_2). Helium [He] has a lower density compared to nitrogen, and thereby HeO_2 breathing requires less respiratory muscle work than air breathing. This unloading lowered the O_2 cost of exercise and perceived exertion during moderate- and heavy-intensity cycling of relatively short duration (12 min). Following these findings, respiratory muscles were acutely unloaded by switching the inspired gas from ambient air (AIR) to normoxic HeO_2 (AIR+HeO_2) during constant work rate (CWR) cycling to exhaustion, in order to specifically evaluate the effects of the proposed intervention on exercise tolerance. The intervention extended exercise duration/improved exercise tolerance during both moderate (below the gas exchange threshold, <GET)- and heavy-intensity (above the gas exchange threshold, >GET) cycling exercises.

In the second approach, a standardized program of respiratory muscle endurance training (RMET) was superimposed on a standard multidisciplinary body mass reduction program; RMET decreased perceived exertion and O_2 cost of exercise during heavy-, but not during moderate-intensity cycling exercise, and improved peak cycling capacity. We then evaluated the hypothesis that the benefits of RMET on the O_2 cost of exercise and exercise tolerance would be more pronounced during walking on a treadmill compared to the effects described during cycling, and/or could be observed also at low intensities. Indeed, in OB a 3-wk RMET program markedly lowered the O_2 cost of moderate- and heavy-intensity walking and improved exercise tolerance. By contrasting the vicious circle of obesity → early fatigue → reduced exercise tolerance → reduced physical activity → obesity, the intervention more specifically directed to the respiratory function, such as RMET programs, could represent a useful adjunct in the control of obesity. Longer periods of RMET should be investigated.

LIST OF PUBLICATIONS

Alemayehu HK., Salvadego D, Isola M, Tringali G, De Micheli R, Caccavale M, Sartorio A, Grassi B. Three weeks of respiratory muscle endurance training improve the O_2 cost of walking and exercise tolerance in obese adolescents. *Physiol Rep,* 6 (19): e13888, 2018.

Beretta E, Lanfranconi F, Simone G, Bartesaghi M, **Alemayehu HK**, Miserocchi G. Reappraisal of DLCO adjustment to interpret the adaptive response of the air-blood barrier to hypoxia. *Respir Physiol Neurobiol* 238: 59–65, 2017.

Beretta E, Lanfranconi F, Simone G, Bartesaghi M, **Alemayehu HK**, Pratali L, Catuzzo B, Giardini G, Miserocchi G. Air blood barrier phenotype correlates with alveolo-capillary O_2 equilibration in hypobaric hypoxia. *Respir Physiol Neurobiol* 246: 53–58, 2017.

MANUSCRIPTS IN PREPARATION

Giovanelli Nicola, Biasutti Lea, Salvadego Desy, **Hailu K. Alemayehu**, Grassi Bruno, Lazzer Stefano. Changes in skeletal muscle oxidative capacity after a trail running race.

Bruno Grassi, Michael C. Hogan, William G. Aschenbach, **Hailu K. Alemayehu**, Jason J. Hamann, Kevin M. Kelley, Peter D. Wagner, L. Bruce Gladde. Enhanced peripheral O_2 diffusion by hyperoxia and right-shifted O_2-Hb dissociation curve slows down skeletal muscle $\dot{V}O_2$ kinetics to $\dot{V}O_{2max}$.

Manuscript from chapter 3 and 4 of this thesis.

ABBREVIATIONS

ANOVA	Analysis of variance
BMI	Body mass index
BMI-SDS:	SD score of body mass index
CWR	Constant work rate
ECG	Electrocardiography
ERV	Expiratory reserve volume
$FEF_{25\%-75\%}$,	Forced expiratory flow between 25 % and 75 % of FVC
FEV_1	Forced expiratory volume in 1 second
fR	Respiratory rate
FRC	Functional residual capacity
FVC	Forced vital capacity
GET	Gas exchange threshold
HeO_2	Normoxic helium-O_2 mixture
MRI	Magnetic resonance imaging
PEF	Peak expiratory flow
$PETCO_2$	End tidal pressure of CO_2
$PETO_2$	End tidal pressure of O_2
R	Respiratory gas-exchange ratio;
RCT	Respiratory compensation threshold
RPE_L,	Rate of perceived exertion for leg effort
RPE_R,	Rate of perceived exertion for respiratory discomfort

RV	Residual volume
SIEDP	Italian society for pediatrics endocrinology and diabetics
SPSS	Statistical package for social sciences
TE	Time to exhaustion
TLC	Total lung capacity
$\dot{V}CO_2$	CO_2 production;
V_DV_T	Dead space-tidal volume ratio
$\dot{V}_E$	Pulmonary ventilation
$\dot{V}_E/\dot{V}CO_2$	Ventilatory equivalents for CO_2
$\dot{V}_E/\dot{V}O_2$	Ventilatory equivalents for O_2
$\dot{V}O_2$	Oxygen consumption
$\dot{V}O_{2max}$	Maximum oxygen consumption
$\dot{V}O_{2peak}$	Peak oxygen consumption
$\dot{V}O_{2SC}$	Slow component of O_2 uptake kinetics
WHO	World Health Organization
WOB	Work of breathing

CHAPTER 1. GENERAL INTRODUCTION

What is the definition of obesity?

The Merriam-Webster dictionary defines obesity as a condition characterized by the excessive accumulation and storage of fat in the body (Obesity. Accessed 6/5/2013, 2013, at http://www.merriamwebster.com/dictionary/obesity). Obesity is a chronic metabolic disorder characterized by an increase in the number and/or the size of fat cells. The World Health Organization (WHO) classification and U.S. dietary guidelines for obesity in adults define overweight as a BMI of 25–30 kg/m^2 and obesity as a BMI of 30 kg/m^2 or greater (93). Country-specific growth charts have been developed based on cross-sectional and longitudinal data. For example, the Italian society for pediatrics, endocrinology and diabetics (SIEDP)-2006 developed growth charts for height, weight and body mass index (BMI) that apply to the Italian population, taken as a whole or separately in two geographical areas (North-Central and South Italy) (12).

Prevalence

There has been a worldwide increase in obesity among people of all ages (93) and obesity rages like an epidemic that involves millions of people each year. The WHO has declared that around 39% of the world's population is overweight and that worldwide obesity has nearly tripled since 1975. Over the past 60 years there has been a dramatic increase in the prevalence of overweight in children and adolescents, ranging from 4% in 1975 to 18% in 2016 (73).This alarming evidence shows that obesity is one of the major public health problems of the twenty-first century (obesity complications are the cause of about 3 million deaths per year) and the most frequent nutritional disorder in the developed countries. A review of 21 surveys conducted in various European countries indicated a higher prevalence of overweight in western and southern Europe. The countries surrounding the Mediterranean showed prevalence rates for overweight children in the range of 20- 40%, whereas those in northern areas showed lower rates, in the range of 10–20% (59). Health Behavior in School-aged Children (HBSC) study

conducted on regionally representative samples in Italy found that 25.4% boys and 11.7% girls aged 15 yrs were overweight or obese (54).

Complications of childhood obesity

As with adults, obesity in youth is a multisystem disease with potentially catastrophic consequences. Adolescent obesity causes hypertension, dyslipidemia, chronic inflammation, increased blood clotting tendency, endothelial dysfunction, and hyperinsulinemia. This grouping of cardiovascular disease risk factors has been identified in children as young as 5 years of age (108). Among adolescents and young adults who died of traumatic causes, the presence of cardiovascular disease risk factors correlated with asymptomatic coronary atherosclerosis, and lesions were more advanced in obese individuals (25). Type 2 diabetes, once nearly unrecognized in adolescence, now accounts for as many as half of all new diagnoses of diabetes in some populations. This condition is almost entirely attributable to the pediatric obesity epidemic, though heredity and lifestyle factors affect individual risk. The emergence of type 2 diabetes in children represents an important development, in view of the macrovascular (heart disease, stroke, limb amputation) and microvascular (kidney failure, blindness) sequelae. Frequent pulmonary complications of childhood obesity include sleep disordered breathing, asthma, and exercise intolerance. Exercise intolerance is a condition of inability or decreased ability to perform physical exercise at what would be considered to be the normally expected level or duration. It also includes experience of unusually severe post-exercise pain, fatigue, nausea, vomiting or other negative effects. Exercise intolerance in an obese child can limit physical activity and thus cause further weight gain (25). To offer more effective treatment for this increasingly common health problem, a better understanding of the nature and source of exercise intolerance in obesity is required. The mechanisms of activity restriction in obesity are likely to be multifactorial but the role of respiratory impairment and the associated respiratory discomfort is thought to be important.

Breathing physiology in obesity

The broad deleterious effects of obesity on the respiratory systems were first described in the 1950's (14). It was postulated that noticeable obesity, in the absence of intrinsic pulmonary disease, may alter pulmonary function to such an extent that the effective alveolar ventilation is reduced and hypoxemia and secondary polycythemia result. This has led to the description of a clinical syndrome, dubbed the "Pickwickian syndrome" by Burwell and his associates (11). Since then scientists have investigated the substantial effects of obesity on the physiology of breathing (9, 14, 31, 35, 49, 50, 58, 63, 74, 97). The main respiratory alterations of obesity include, but are not limited to, decreased lung volumes and capacities, reduced respiratory compliance, altered breathing patterns, increased demand for ventilation, elevated work and O_2 cost of breathing, respiratory muscle inefficiency.

Lung volumes and capacities

Static lung volumes

The effects of obesity on lung volumes have been studied extensively. The most common and consistent indicator of obesity is a reduction in expiratory reserve volume (ERV). This occurs because of displacement of the diaphragm into the thorax by the obese abdomen and by the increased chest wall mass. This mass loading effect of obesity decreases Functional Residual Capacity (FRC) (74). Because FRC is reduced and the residual volume (RV) is not, ERV declines (see figure 1.1). ERV reduction is greatest in the supine position when the diaphragm ascends in the chest, and the weight of the lower thorax and the abdomen is applied to the lungs.

Studies on obesity related lung function alteration of non-asthmatic children presented data for FRC and showed either significantly lower FRC levels in subjects with obesity or a statistically significant inverse association between FRC and adiposity. From the studies that presented data for ERV and RV, it seems that both ERV and RV decreased with increasing adiposity. ERV increased by an average of 15% in severely obese individuals who lost weight following an intervention program (32).

How does obesity have these effects on lung volumes? One proposed mechanism is that abdominal fat displaces the diaphragm into the abdomen (49). This is supported by a study which showed that lung volumes were affected more in patients with a waist to hip ratio >0.95 ('upper' body fat distribution) (18). In addition, chest-wall adiposity may simply compress the thoracic cage, leading to lower lung volumes (49). This is supported by the similar pattern observed when lung volumes are measured after elastic strapping of the chest (13). Although there is some question as to whether obesity acts as a mass (threshold) load or an elastic load, it is likely that both play a role in decreasing lung volumes, and it would be difficult to isolate and study one component independently (58). A third possible mechanism for the effect of obesity on lung volumes could be exemplified by the following question: is there an increase in thoracic or mediastinal fat in obese patients? Normal weight subjects (BMI 25.0) were compared with obese subjects (BMI 38.8). The obese subjects were then divided into two groups: those with a TLC <80% of predicted (obese restricted) and those with a TLC >80% of predicted (obese normal). Although obese subjects did have more mediastinal fat than normal subjects, no difference in mediastinal fat was observed between the obese restricted and the obese normal subjects. In fact, the only apparent difference between the two obese groups was the intrathoracic volume at full breath hold; 124% of predicted TLC in the obese normal group, and 105% of predicted TLC in the obese restricted group. The authors hypothesized that a reduction in diaphragmatic excursion due to abdominal fat was responsible for the observed phenomenon (103).

Although MRI has become the preferred method for localizing and quantifying adiposity, no studies have been done yet on whether abdominal adiposity, as determined by MRI, is correlated with reduced lung volumes (58), but a preliminary study used MRI to compare end expiratory lung volume and fat distribution in obese men and women (BMI of 35±4 and 37± 2 kg/m^2, respectively) *versus* that in normal subjects. Surprisingly, that study showed little variation in the distribution of fat between normal subjects and obese subjects, for both men and women. This underscores the difficulty of teasing out the relative contributions of chest wall and abdominal fat to alterations in lung volumes. The study did show a significant relationship between visceral fat, that is, fat surrounding the abdominal organs, anterior subcutaneous fat (both abdominal and chest wall) and end-expiratory lung volume (expressed as % TLC) (4). The study also highlighted the fact that both chest wall and abdominal fat likely play a role in derangement of lung volume (58).

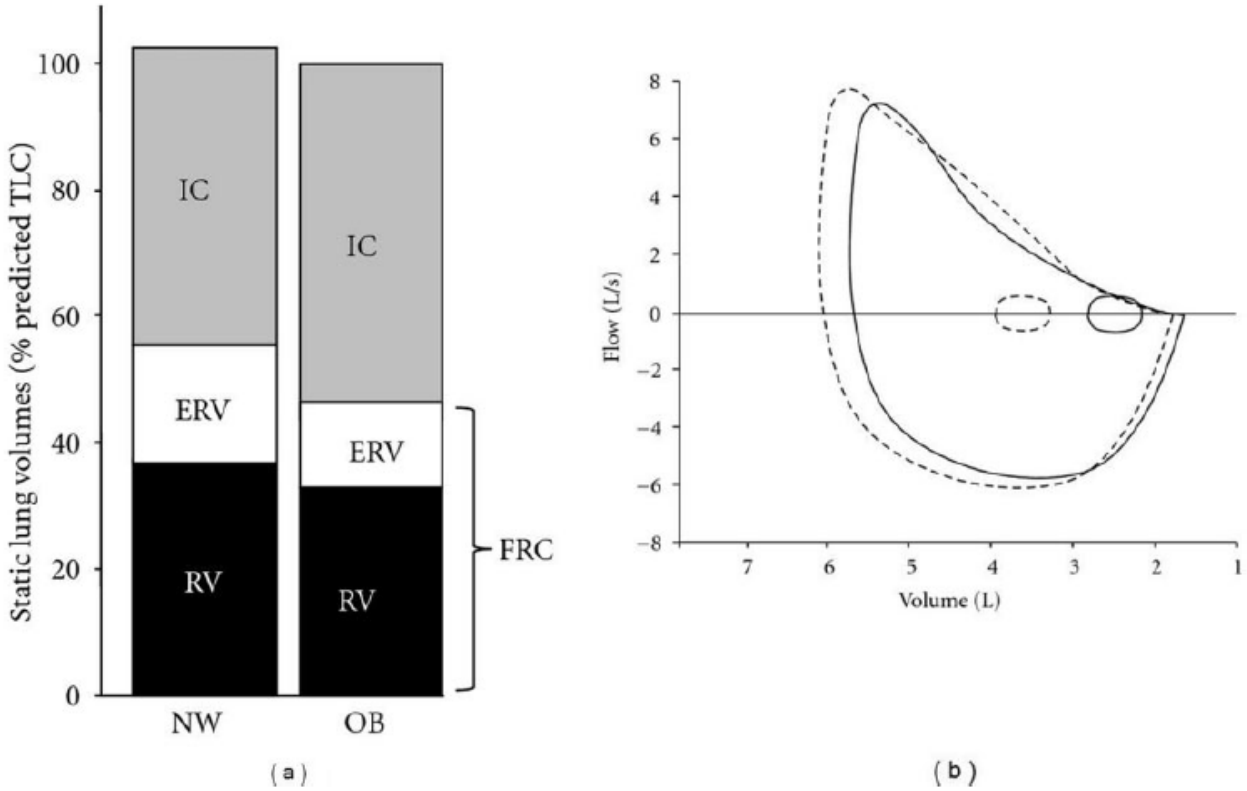

Figure 1.1 (a) Static lung volumes in obesity (OB) versus normal weight (NW) showing a reduction in ERV and FRC. (b) A typical flow–volume loop in an obese patient showing a rightward shift in the tidal flow–volume loop, with a suggestion of airflow limitation during tidal breathing. Reproduced from O'Donnell *et al* (71). Key: ----- Normal weight; _____Obese.

Dynamic Spirometry

In terms of spirometry some contrasting results have been reported. In general spirometry is normal in mild obesity. But in morbidly obese patients there are evidences that forced expiratory volume in 1 second (FEV_1) and forced vital capacity (FVC) are reduced (74). Another large French population-based study demonstrated that even mild abdominal obesity, even with a normal BMI, is associated with lower FVC and FEV_1 in men and women (56). FEV_1 to FVC ratio was normal and static lung volumes were reduced, suggesting the reduction

may be due to restriction as opposed to air flow obstruction. Lazarus *et al* (22) found that the FEV_1 to FVC ratio decreases with increasing BMI in overweight and obese individuals.

Again, findings of studies that investigated the relationship of overweight/obesity in children and/or adolescents with the spirometric variables of lung function are, to some extent, inconsistent. Few studies observed no differences in FEV_1, FVC, FV1/FVC and $FEF_{25\%-75\%}$ between obese and/or overweight and normal weight children. But a majority of studies revealed a statistically significant association between the degree of adiposity and at least one of the spirometric variables. In general, the results depict a trend of significantly decreased spirometric values in the individuals belonging to higher BMI centiles (32).

The physiologic mechanisms that cause the impact of obesity on lung function are not entirely understood. It seems that the thoracic and abdominal fat deposition limit the outward movement of the chest wall and the descent of the diaphragm (32). Additionally, obesity is associated with reduced compliance of the respiratory system, although it is not clarified whether both lung and chest wall compliance are reduced or not (58). More recent studies suggest that the adverse effects of obesity on lung function are due not only to mechanical reasons but also to the metabolic abnormalities encountered in obesity. Rastogi *et al* (81) found that insulin resistance was a significant determinant of FEV_1/FVC ratio and ERV in adolescents, even after adjusting for general and truncal adiposity. The main proposed mechanisms underlying reduced lung function in obese children are depicted in Figure 1.2.

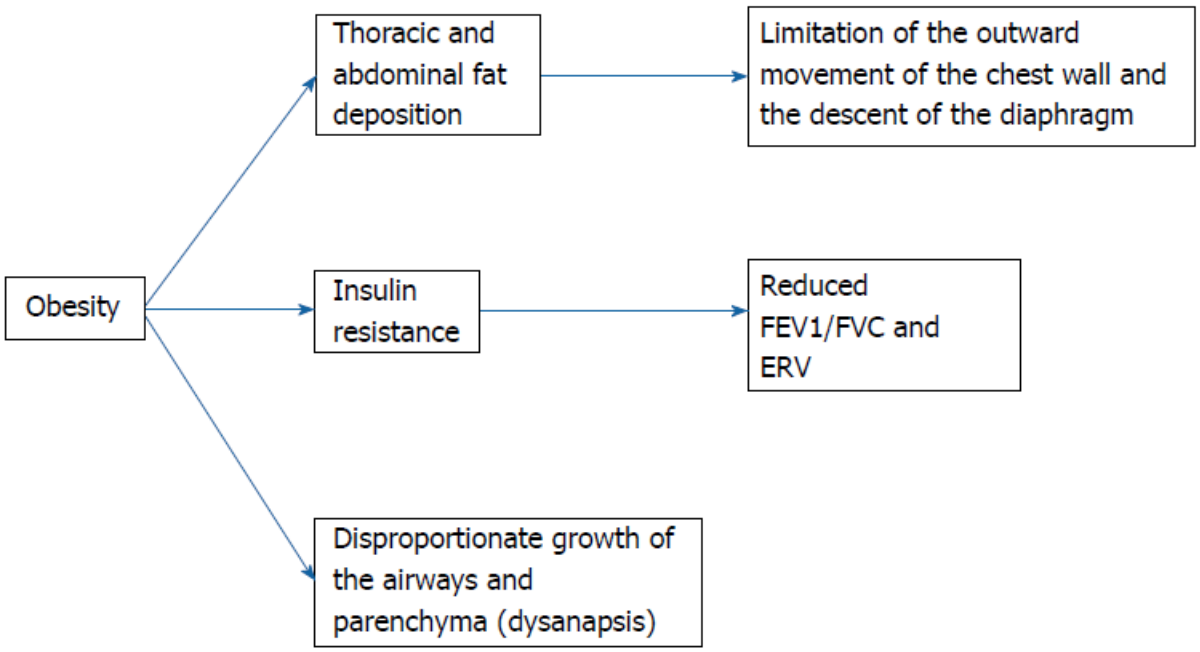

Figure 1.2. Mechanisms underlying reduced lung function in obese children/adolescents. ERV: Expiratory reserve volume; FEV_1: Forced expiratory volume in 1 s; FVC: Forced vital capacity. Reproduced from Fretzayas *et al* (32).

Respiratory compliance

The data presented by Naimark and Cherniack (70) indicate that the compliance of the total respiratory system is reduced in obese individuals. This reduction in compliance is almost entirely due to a reduction in compliance of the chest wall. In other words, there is an increase in elastic resistance to the distention of the chest wall in obese individuals. According to these authors' explanation, the respiratory muscles of obese individuals are performing more than twice as much work as those of normal individuals. One-third of this increase is due to increased elastic work done on the chest wall. The remainder of the increase must, therefore, be attributed either to invalidity of the assumption of a normal efficiency of the respiratory muscles in obese individuals, or to an increase in nonelastic work, or both. These findings support the hypothesis of other investigators that the increased oxygen cost of breathing in obesity is at least in part due to an increased mechanical work done to overcome elastic resistance of the chest wall.

The reduction in vital capacity in obese individuals is related to a reduction in the compliance of the total respiratory system, which is largely due to a reduced distensibility of extrapulmonary structures. It was expected that total respiratory compliance would also be related to a measure of the size of the respiratory system, such as FRC. It is notable that the compliance of the total respiratory system is reduced even further in the supine position in obese individuals. The increase in resistance to distention during recumbency is entirely due to an increased resistance offered by the chest wall in this position. Thus, while the resistance of the chest wall is an average of over 70 % of the total resistance to distention in the obese subject in the seated position, this is increased to over 80 % in the supine position (70).

On the other hand the study by Suratt *et al*. (95) indicates that the chest wall compliance in obese patients is not significantly different from that of normal subjects, and the increased work of breathing that is thought to occur in obese subjects could result from work done to overcome chest wall resistance or inertance, or from work performed on the airways and lung. Chest wall resistance and inertance have been difficult to measure; so there have been few reports of these variables in obese subjects. A study of chest wall resistance in obese subjects using two different methods yielded ambiguous results (91). Chest wall inertance, another component of the work of moving the chest wall, has not been measured directly in humans. Total respiratory inertance, however, has been reported to correlate with body weight (91), presumably because of an increase in tissue inertance in obese subjects. The low lung compliance that occurs in obesity is often thought to be a consequence of a stiff chest wall. It is postulated that the weight of the chest wall is applied to the lung, decreasing lung filling with each breath and leading to a low lung compliance. However, if chest wall compliance is normal in obesity though, why is lung compliance low? In addition, why do obese subjects breathe at lower tidal volumes and at higher respiratory rates than do normals? One explanation may be related to elevated pharyngeal and nasopharyngeal resistance in obese subjects. Using the pulse-flow method, scientists reported that resistance between the mouth and an esophageal catheter is correlated to BMI (72). Breathing through a narrow nasopharyngeal airway would increase the work of breathing and could lead the obese subject to breathe at a lower tidal volume and at a higher respiratory frequency in an attempt to lower the work of breathing. Another explanation for the low lung compliance may be related to the increased pulmonary blood volume in obese individuals (48).

The Work and Energy Cost of Breathing

The respiratory muscles

The respiratory muscles are the force-generators that drive the respiratory system (85). Regarded as the primary inspiratory muscle, the diaphragm accounts for approximately 70% of the tidal volume exchanged during normal conditions. Other inspiratory muscles that account for the balance of tidal ventilation are the external intercostal, parasternal, and scalene muscles. Contraction of these muscle fibers elevates the rib cage. The sternocleidomastoid muscles are major accessory inspiratory muscles that have a predominantly pump-handle action on the rib cage, which elevates the first rib and sternum (Fig 1.3). During quiet breathing, they are usually inactive but are always active during high levels of ventilation, as in exercise, as well as during respiratory muscle loading (6).

Expiratory muscles include the internal intercostal and abdominal muscles. On contraction, the internal intercostal muscles act to lower the ribs, thus deflating the lungs. The abdominal muscles are the most important and powerful muscles of exhalation. Four abdominal muscles important for ventilation are the external abdominal oblique, internal abdominal oblique, transverse abdominis, and rectus abdominis (Fig 1.3) (85). In general, when these muscles contract, the abdominal wall is pulled in, causing increased intraabdominal pressure that forces the diaphragm cephalad into the thoracic cavity (6). Also, the lower ribs are pulled down and medially, and the net effect of these actions is deflation of the rib cage. Normally, exhalation is a passive process, and the abdominal muscles are inactive. However, during increased muscle loads (e.g., increased airway resistance), the abdominal muscles are recruited, and exhalation becomes an active energy-consuming process (6).

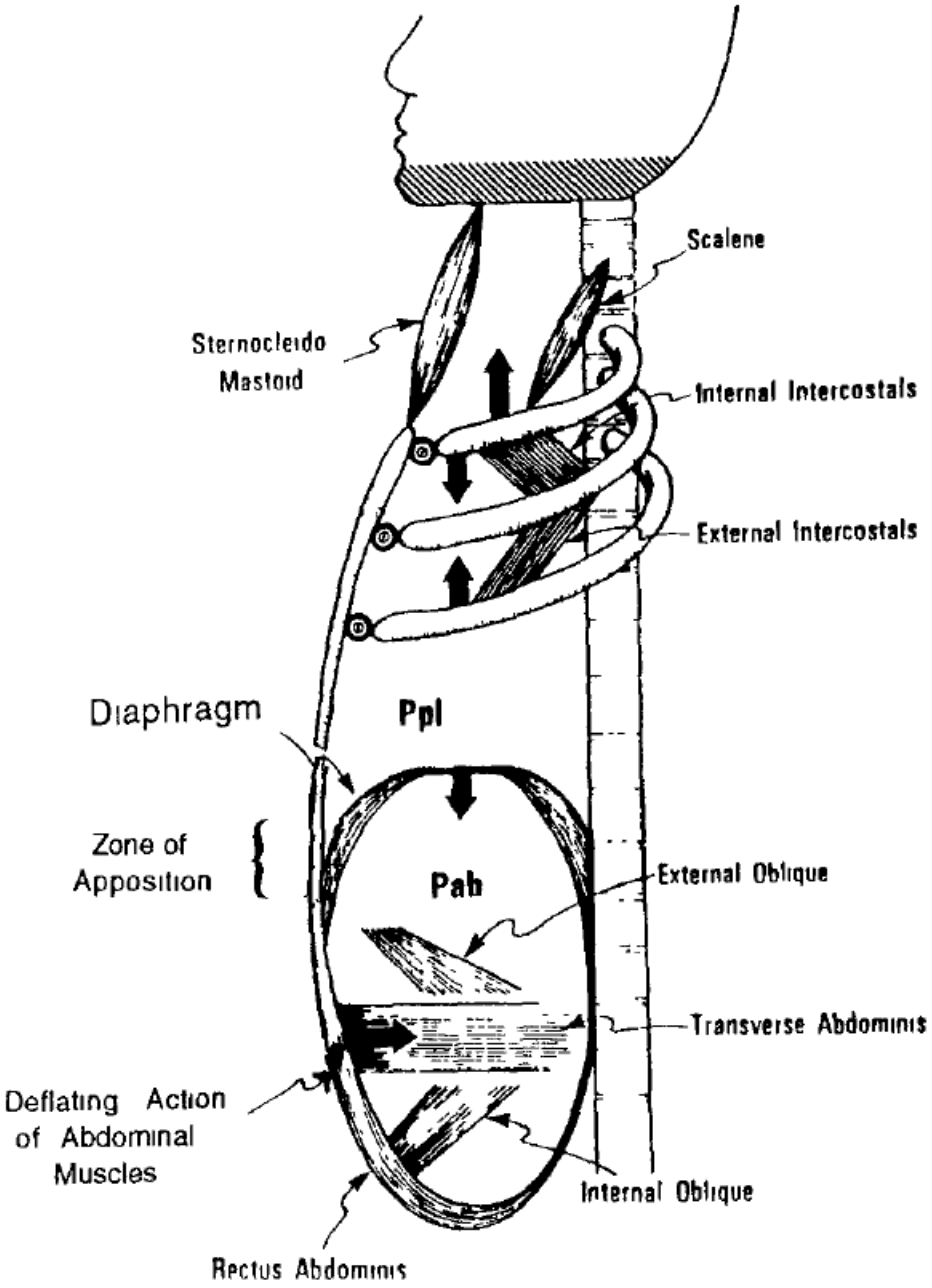

Fig 1.3. Diagrammatic representations of inspiratory and expiratory muscles are illustrated, arrows indicate direction of action Pab, abdominal pressure; Ppl, intrapleural pressure. Reproduced from Banner (6).

The work of breathing

As mentioned in previous sections, the most common and consistent pulmonary function tests abnormality seen in obese individuals is a reduction in FRC and ERV (74). Because breathing occurs at low FRC and in the less compliant portion of the pressure–volume curve, increased effort is needed to overcome respiratory system elasticity. Thus, obese individuals need to do more respiratory work to maintain appropriate levels of ventilation (57). Naimark and Cherniack (70) reported WOB values ~2.5 times greater in obese individuals (0.540 kg.m/L) compared to lean individuals (0.227 kg.m/L), while Pelosi et al. (76) reported values of 1.30 J/L and 0.52 J/L, respectively. This increased respiratory muscle force generation, and the concomitant increase in respiratory neural drive associated with increased ventilation are an important source of sensation of respiratory effort in obese subjects (89). Exertional dyspnea is an obstacle to the prevention and treatment of obesity and coexisting comorbidities. Many obese subjects without coexisting disorders are unable to exercise due to dyspnea on exertion, and thus cannot participate in regular physical activity (89). Obesity may also impair upper airway mechanical function and neuromuscular strength, and increase oxygen consumption, which in turn, may increase the work of breathing and impair the ventilatory drive. The combination of ventilatory impairment, excess CO_2 production and reduced ventilatory drive predisposes obese individuals to the “obesity hypoventilation syndrome” (57), summarized in figure 1.4.

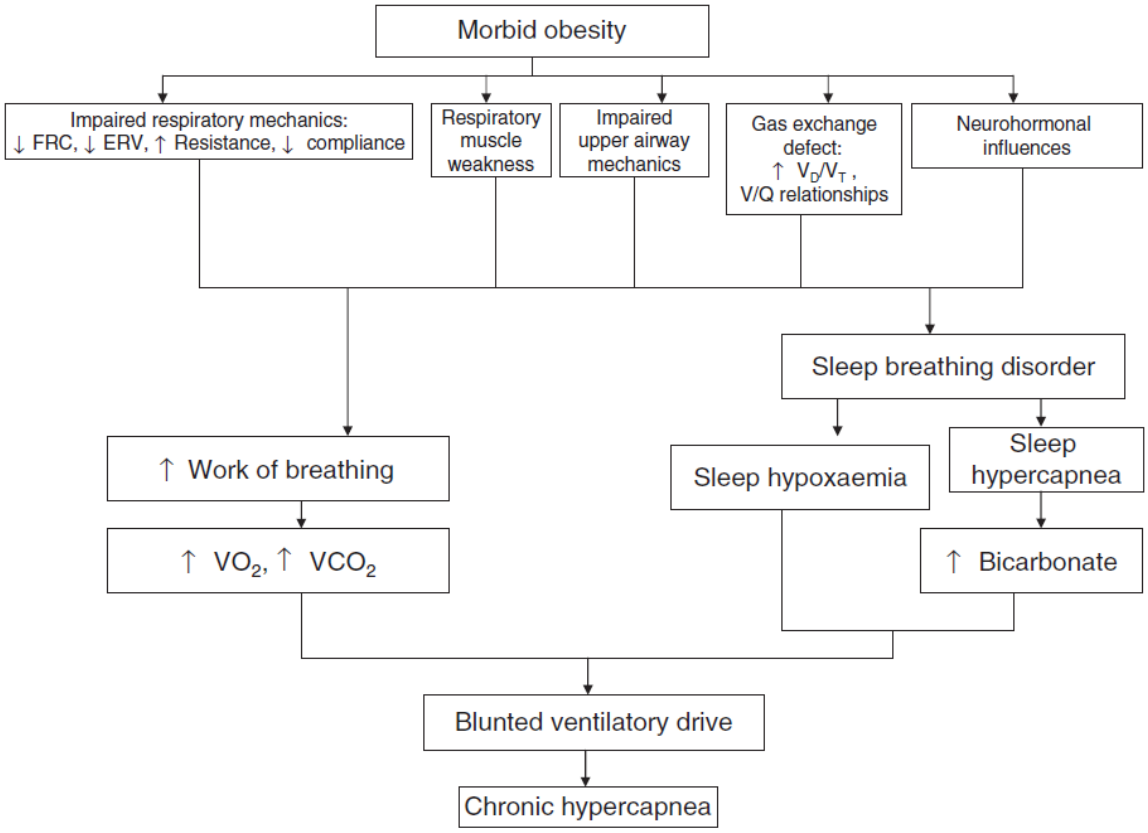

Figure 1.4. Possible mechanisms by which obesity can lead to blunted ventilatory drive and chronic daytime hypercapnia. ERV, expiratory reserve volume; FRC, functional residual capacity; $\dot{V}CO_2$, CO_2 production; V_DV_T, dead space-tidal volume ratio; VO_2, oxygen consumption. Reproduced from Lin and Lin (57)

The oxygen cost of breathing

The oxygen cost of breathing accounts for the total energy required by the respiratory muscles to overcome respiratory mechanical aspects, such as airway resistance and lung compliance, chest wall resistance, breathing inertia, antagonistic activity of respiratory muscles, chest wall distortion, gas compressibility, and work on the abdominal viscera (68). Many of these components are affected by the presence of an increased adipose tissue on the rib cage, the abdomen, and/or in the visceral cavity, especially during exercise (35, 50, 76). In healthy subjects the oxygen cost of breathing during eupnea is minimal and represent a small fraction of whole-body oxygen uptake. During dynamic exercise, however, as minute ventilation rises

the oxygen cost of breathing can represent 15% of maximum O_2 uptake (23). Morbidly obese patients dedicate a disproportionately high percentage of the total $\dot{V}O_2$ for respiratory work, even during quiet breathing (50). The rate of increase in $\dot{V}O_2$ for respiratory work is significant even with a slight increase in ventilation from resting levels; this rate increases swiftly at higher levels of ventilation like those encountered during exercise (14, 50). This relative inefficiency suggests a decreased ventilatory reserve and a predisposition to respiratory failure in the setting of even mild pulmonary or systemic insults (7).

Respiratory Muscle unloading

The lower density of helium (He) reduces the pressure needed to overcome airway resistance at higher flow rates by maintaining laminar flow. According to study by Segizbaeva (90) resistive unloading by normoxic HeO_2 in normal subjects obtained a decrease in mouth pressure, work of breathing and central inspiratory activity compared with air breathing. These results indicate that a lower neuromuscular output is required to achieve the same $\dot{V}_E$ and $PETCO_2$ during normoxic HeO_2 compared with air.

Studies have produced mixed results regarding the effects of loaded (via resistors) and unloaded breathing [via breathing normoxic helium-O_2 mixture (HeO_2) or via proportional assist ventilator (PAV)] on respiratory responses and exercise capacity. Cross et al. (19) found that, in trained cyclists breathing HeO_2 decreased the amplitude of the slow component of O_2 uptake kinetics ($\dot{V}O_{2SC}$) and operating lung volume when exercise was performed above, but not below, the threshold of respiratory compensation (i.e. the RCT). The reduction in operating lung volume was related to the decrease in the $\dot{V}O_{2SC}$ observed during the HeO_2 trials, relative to normal air. These findings suggest that operating lung volume, through altering the O_2 cost of breathing, plays an important role in the development of the $\dot{V}O_{2SC}$. Moreover, the impact of breathing HeO_2 on reducing operating lung volume, and thus the $\dot{V}O_{2SC}$, is more pronounced at work rates performed above, compared with below, the RCT. Other data from Powers and colleagues (77) also supported the notion that breathing a normoxic HeO_2 gas results in an increase in $\dot{V}O_{2max}$, improved exercise tolerance, higher $\%SO_2$, and greater minute ventilations during maximal exercise when compared with air breathing in aerobically trained subjects. A

similar study on male nonathletic subjects demonstrated a reduction in the ventilatory resistance to O_2 flow induced by HeO_2 breathing, which resulted in a significant increase in $\dot{V}O_{2max}$ during hypoxic exercise. This was not the case in normoxia (29). In contrary to results from most previous studies that have evaluated the effects of breathing a lighter gas on performance of exercise, study on trained cyclists reported that substituting helium for nitrogen in the hyperoxic ambient air did not improve the maximal performance of exercise during an incremental exercise test to exhaustion (2).

Respiratory Muscle Endurance Training

Most respiratory muscle (RM) training studies have employed two modes of training: (i) voluntary isocapnic hyperpnoea to improve RM endurance; or (ii) inspiratory resistive loading to improve RM strength, for reviews see references (8, 24, 92, 98, 99, 107, 27, 34, 36, 46, 55, 65, 80, 87). During isocapnic hyperpnoea training individuals maintain a given level of ventilation for up to 30 minutes. This regimen is carried out typically for 3 to 5 times per week for 4 to 5 weeks. Using this type of training, several investigators have shown improvements in RM endurance. Just to mention some of them, RMET reduced the perception of adverse respiratory sensations during volitional and exercise-induced hyperpnoea, in healthy subjects (98). Similarly, endurance training of respiratory muscles improved cycling performance in fit young cyclists (46). In highly-trained rowers, following respiratory muscle training, perceived breathlessness, HR and $\dot{V}_E$ were reduced during an incremental rowing test despite the absence of change in peak exercise performance. Another similar study demonstrated an increased respiratory muscle strength and a more efficient breathing characterized by a low respiratory rate in triathletes. After the training the athletes could tolerate higher workloads enhancing the exercise performance (8). When added on usual training sessions, RMET was more effective than usual training sessions alone in eliciting improvements in swimming performance. Data presented by Lemaitre *et al*., (55) suggested that RMET had also beneficial effects on pulmonary function, dyspnea and perceived exertion.

In a previous study by our group, (87) RMET superimposed on a standard multidisciplinary body mass reduction program slightly decreased perceived exertion and O_2 cost of exercise and improved peak exercise capacity during cycling in young obese patients. Other study by the

same group (60) found that a short multidisciplinary body weight reduction program including RMET applied to otherwise healthy obese adolescents contributes to increased exercise performance by changing static and dynamic chest wall configuration, lowering the abdominal load, unloading the respiratory muscles, and reducing dyspnea.

AIMS OF THE THESIS

My PhD research project focused on the respiratory factors that influence exercise tolerance/capacity in adolescents with mild-to-moderate obesity. In OB the increased O_2 cost of breathing could entail a "competition" between respiratory and locomotor muscles for the finite available O_2, leading to fatigue and premature exhaustion. This would contribute to the inactivity which represents one of the main causes of obesity, impeding the execution of exercise which is one of the cornerstones for the treatment of the disease. In order to interrupt this vicious circle, I followed two approaches, attempting to relieve the respiratory limitation in OB performing cycling/walking exercises.

A previous study by our group demonstrated that an unloading of the respiratory muscles by normoxic HeO_2 breathing was able to reduce the O_2 cost of exercise and the perception of fatigue during moderate- and heavy-intensity cycling exercises of short duration (12 min). One part of my PhD project was aimed to determine whether, in OB, an acute respiratory muscle unloading during cycling exercise, obtained by switching the inspired gas from AIR to normoxic HeO_2 at exhaustion (AIR+HeO_2) can indeed increase exercise tolerance and prolong the duration of exercise at intensities commonly experienced during daily-living activities.

The other part of my PhD project was aimed to detect whether the implementation of a specific endurance training program for the respiratory muscles (RMET) to a standard multidisciplinary body mass reduction intervention was useful for reducing the O_2 cost of exercise and fatigue perception during walking exercise. In a previous study by our group the addition of RMET on a standard 3-wk body mass reduction program determined a reduction of the O_2 cost of exercise and perceived exertion during cycling exercise at heavy- but not at moderate-intensities. Since the mechanical pattern of walking entails the cyclical elevation and acceleration of body center of mass at every step, and since the muscle mass involved during walking is larger than during cycling, this exercise form can be more challenging for the respiratory system than cycling even at low intensities, thereby increasing the need for a specific RMET intervention.

CHAPTER 2. RESPIRATORY MUSCLE ENDURANCE TRAINING IMPROVES THE O_2 COST OF WALKING AND EXERCISE TOLERANCE IN OBESE ADOLESCENTS

INTRODUCTION

Obese patients have a higher O_2 cost of exercise (51, 86, 102), which negatively affects exercise tolerance (39) and is at least in part attributable to a higher O_2 cost of breathing (50, 87, 88). Obesity has indeed a profound effect on the physiology of breathing (49, 63). In obese subjects resting and exercise tidal breathing occur at low operational lung volumes, thereby increasing the prevalence and severity of expiratory flow limitation and the resistive load on the respiratory system (58). The reduced chest wall compliance, attributable to the excess fat mass on the respiratory wall, and the increased work to be performed against abdominal fat and viscera, further increase the work of breathing (50, 58). In association with respiratory muscle inefficiency, the increased work of breathing determines a substantially higher O_2 cost of breathing (49), contributing to the higher O_2 cost of exercise (86–88, 102). This is exacerbated by the higher pulmonary ventilation at the same work rate observed in obese patients *vs.* normal weight controls (14, 50), possibly leading to exertional dyspnea (89).
The increased O_2 cost of breathing could entail a "competition" between respiratory and locomotor muscles for the finite available O_2 (43), leading to fatigue and premature exhaustion. This would contribute to the inactivity which represents one of the main causes of obesity, impeding the increased level of physical activity which is one of the cornerstones of the treatment of the disease.

In order to interrupt this vicious circle, we recently followed two approaches, attempting to relieve the respiratory limitation in obese adolescents performing cycling exercise. In the first study (88) respiratory muscles were acutely unloaded by normoxic helium-O_2 breathing. Helium [He] has indeed a lower density compared to nitrogen, and thereby HeO_2 breathing requires less respiratory muscle work than air breathing. The intervention reduced the O_2 cost of cycling and the perception of fatigue during moderate- and heavy-intensity constant work rate exercise. In the second study (87) a standardized program of respiratory muscle endurance training (RMET) (82, 92, 94) was superimposed on a standard multidisciplinary body mass reduction program; the intervention slightly decreased perceived exertion and O_2 cost of cycling

during heavy-, but not during moderate-intensity exercise, and improved peak exercise capacity.

The aim of the present study was to evaluate the hypothesis that the RMET effects on the O_2 cost of exercise and exercise tolerance would be more pronounced during walking on a treadmill compared to the effects described during cycling (87), and/or could be identified also during moderate-intensity exercise. Since the mechanical pattern of walking entails the cyclical elevation and acceleration of body center of mass at every step, treadmill exercise is a relatively costly type of locomotion when compared to cycling (51). Obese patients should be more heavily penalized (*vs.* normal weight controls) during weight bearing activities like walking or running compared to cycling. The much larger muscle mass in action during walking or running than during cycling would aggravate the exertional dyspnea and could enhance the competition between respiratory and locomotor muscles for the available O_2, thereby determining a larger "signal" on which to intervene with RMET.

METHODS

Subjects

Sixteen male obese patients (age 15-18 years; Tanner stage 4-5), hospitalized for a multidisciplinary body mass reduction program, were admitted to the study. Patients were randomly assigned to RMET (n = 8; 16.5 ± 0.9 years; body mass 130.5 ± 18.4 kg) or to a control (CTRL) group, (n = 8; 15.5 ± 0.9 years; body mass 124.9 ± 10.0 kg). The RMET group followed a specific program of respiratory muscle endurance training in addition to the standard multidisciplinary body mass reduction program (see below). The CTRL group underwent only the standard body mass reduction program.

Participants' parents provided signed consent statements, after being fully advised about the purposes and testing procedures of the investigation, which were approved by the ethics committee of the Italian Institute for Auxology, Milan, Italy. All procedures were in accordance with the recommendations set forth in the Helsinki Declaration (2000).

Body mass index (BMI) was calculated as body mass divided by height^2, expressed in (kg m^{-2}). The standard deviation score (SDS) of BMI was calculated by applying the LMS method

(based upon the skewness [L], the median [M], and the coefficient of variation [S] of the measurements as a function of age) to Italian reference values for children and adolescents (12). Body composition was determined by bioelectrical impedance (Human-IM Scan, DS-Medigroup, Milan, Italy). Fat mass (FM) and fat free mass (FFM) were expressed as kg and as a percentage of body mass. All examinations were performed by the same investigator before and after the 3-week intervention period (see below).

Inclusion criteria were: 1) BMI > 97th percentile for age and sex, using Italian growth charts (12); 2) no involvement in structured physical activity programs (regular activity more than 120 min week^{-1}) during the 8 months preceding the study; 3) absence of signs or symptoms of diabetes or of any major cardiovascular, respiratory or orthopedic disease contraindicating or significantly interfering with the tests.

Body mass reduction intervention

The patients were admitted as in-patients (Division of Auxology, Italian Institute for Auxology, Piancavallo, Italy) for a 3-week in-hospital multidisciplinary body mass reduction intervention (87), involving the following: a) Moderate energy restriction, with a personalized diet entailing an energy intake ~500 kcal lower than the measured resting energy expenditure. Diet composition was formulated according to the Italian recommended daily allowances (Società Italiana di Nutrizione Umana); the compliance to the diet was monitored daily by a dietician. b) Aerobic exercise training carried out under the guidance of a therapist. The program included two 30-min sessions day^{-1} of cycling, treadmill walking, and stationary rowing, preceded and followed by 5–7-min stretching, for 5 days week^{-1} with heart rate (HR) monitoring and medical supervision. The initial intensity of exercise was set at ~60% of HR_{peak} determined during the incremental exercise test before the intervention and was progressively increased reaching ~80% at the end of the exercise program. While RMET (see below) was performed in the morning, exercise training was administered in the afternoon. c) Psychological and nutritional counselling.

Respiratory muscle endurance training (RMET)

An incremental RMET protocol was performed by using a commercially available device (Spiro Tiger®, Idiag, Fehraltorf, Switzerland), as previously described in a similar population

(82, 87). The device consists of a hand-held unit with a respiratory pouch and a base station. The specific properties of the device allow for personalized respiratory training through maximum inspirations and expirations, without hypocapnia. To avoid hypocapnia despite hyperpnea, the device features a 2-way piston valve to rebreathing bag. As the patient breathes out through the mouthpiece, the rebreathing bag stores part of the expired air, which contain an increased CO_2 partial pressure. Once the rebreathing bag is filled to its capacity, a valve opens allow the rest of expired air to be released to the environment. The valve shuts when expiration finishes, and inspiration starts. Inspiration empties the rebreathing bag first (filled with the exhaled air containing an increased CO_2 partial pressure), then the valve opens, and some fresh outside air is inspired at the end of each inspiration. No symptoms of lightheadedness or malaise were described by any patient during the RMET sessions.

Personal training target values were entered into the base unit and were used to monitor breathing frequency and depth during training. The base station in the hand-held computer monitors the breathing frequency, sets threshold limits for breathing patterns, and displays visual and acoustic feedback to allow the subject to breathe within the threshold values estimated for normocapnia.

The base station stored time and frequency of each exercise sessions, thus allowing the patient and the researcher to retrieve and review the data. The volume of rebreathing in the bag was chosen in order to obtain pulmonary ventilation ($\dot{V}_E$) values corresponding to ~50–60% of maximal voluntary ventilation, as evaluated by spirometry before the training protocol. The duration of each RMET session increased progressively from 12 min (5 min at a respiratory frequency [fR] of 22 breaths min^{-1}, 5 min at 24 breaths min^{-1}, 2 min at 26 breaths min^{-1}) to 18 min (5 min at a fR of 24 breaths min^{-1}, 5 min at 26 breaths min^{-1}, 8 min at 28 breaths min^{-1}). In short, the patients trained for 3 weeks, 5 days $week^{-1}$, 1 session day^{-1}, 12-18 min $session^{-1}$, with a fR of 22-28 breaths min^{-1}, following an incremental protocol described in detail in Rigamonti *et al*. (82).

Spirometry

Before and after (within two days) the interventions (CTRL or RMET) the patients performed standard spirometry tests (forced vital capacity, FVC; forced expiratory volume in 1 second, FEV_1; FEV_1/FVC; forced expiratory flow between 25% and 75% of FVC, $FEF_{25-75\%}$; maximal forced expiratory flow, FEF_{max}) by utilizing a metabolic cart (MedGraphics CPX/D, Medical

Graphics Corp., USA). Pulmonary function testing was performed according to the guidelines of the American Thoracic Society (69). Predicted values were based on Hankinson *et al*. (40).

Exercise protocol

Before and within two days after the three weeks of interventions (CTRL or RMET) exercise tests were conducted during 2 consecutive days under medical supervision; during the tests the subjects were continuously monitored by 12-lead electrocardiography (ECG). A mechanically braked treadmill (TecnoGym, Italy) was utilized. Patients were allowed time to gain familiarity with the researchers and the experimental set-up, were carefully instructed about the procedures and were familiarized with the protocol using short practice walks. Patients were asked to avoid intensive exercise for 24 hours and to refrain from food and caffeine for at least 2 hours before the tests. During the first day the subjects performed an incremental exercise test. After 3minute of resting measurement (subjects in standing position on the treadmill) the incremental exercise began, and the patients walked on the treadmill (0% slope) for 2 minutes at 3.5 km h^{-1}. The velocity was then increased by 0.5 km h^{-1} every minute till 6 km h^{-1}. When the velocity reached 5 km h^{-1} the slope was set at 3% and kept at this level till 6 km h^{-1}; thereafter the slope was increased by 0.5% every minute. When the slope reached 10.5% the velocity was increased to 6.5 km h^{-1} till the subjects reached voluntary exhaustion, defined as the inability to maintain the imposed speed and slope despite vigorous encouragement by the researchers. During the tests the patients could not hold on the handlebars of the treadmill. For all variables (see below), mean values calculated over the last 20-30 seconds of the incremental exercise before reaching voluntary exhaustion were considered “peak” values.

During the second day, the patients performed one repetition of 12-min CWR exercise at ~60% (moderate-intensity) and at ~120% (heavy-intensity) of the gas exchange threshold (GET) (see below), determined during the incremental exercise before each intervention. In order to identify the work rate corresponding to the $\dot{V}O_2$ at GET, the effect of the delayed $\dot{V}O_2$ adjustment to the increased work rate during the incremental test was corrected by shifting the linear $\dot{V}O_2$ *vs.* time (and work rate) relationship to the left, by an amount corresponding to the individual mean response time of the $\dot{V}O_2$ kinetics determined in each subject (105). CWR exercise at ~60% of GET was always carried out before CWR exercise at ~120% of GET.

About one hour of recovery separated the two CWR exercises. Resting $\dot{V}O_2$ (subjects in standing position on the treadmill) was measured before the CWR exercise began.

Measurements

$\dot{V}_E$, tidal volume (V_T), fR, O_2 uptake ($\dot{V}O_2$) and CO_2 output ($\dot{V}CO_2$) were determined on a breath-by-breath basis by means of a metabolic unit (MedGraphics CPX/D, Medical Graphics Corp., USA). Calibration of O_2 and CO_2 analyzers was performed before each experiment by utilizing gas mixtures of known composition. Expiratory flow measurements were performed by a bidirectional pressure differential pneumotachograph, which was calibrated by a 3-liter syringe at varying flow rates. The respiratory gas-exchange ratio (R) was calculated as $\dot{V}CO_2/\dot{V}O_2$. Heart rate (HR) was determined by ECG. GET was determined by the V-slope method; ventilatory equivalents ($\dot{V}_E/\dot{V}O_2$, $\dot{V}_E/\dot{V}CO_2$) were utilized as ancillary signs (7). All the data related to GET were expressed as $\dot{V}O_2$ ($L \cdot min^{-1}$) and as a percentage of $\dot{V}O_{2peak}$. Ratings of perceived exertion (RPE) for respiratory discomfort (RPE_R) and limb effort (RPE_L) were obtained at rest and every minute during exercise by using the Borg's modified CR10 scale (106).

Considering that only one repetition of each CWR exercise could be carried out, a formal $\dot{V}O_2$ kinetics analysis was not performed (52). Mean $\dot{V}O_2$ values were calculated during the last 30 seconds of every minute of CWR exercises. The presence/absence of a steady state in $\dot{V}O_2$ and HR after the first minutes of CWR exercise was evaluated by fitting linear regressions on the data obtained from the 3rd to the last minute of exercise. Whereas the absence of a significant slope of the regression suggests a steady state, a positive slope suggests an increasing O_2 cost of exercise as a function of time during CWR. The O_2 cost of walking (aerobic energy expenditure per unit of covered distance) was calculated as $\Delta\dot{V}O_2$ ($\dot{V}O_2$ determined during the task minus resting $\dot{V}O_2$)/velocity (53, 79). The O_2 cost of walking was expressed as mL O_2 m^{-1} and as mL O_2 kg^{-1} m^{-1}.

Statistical analysis

Results were expressed as means ± standard deviation (x ± SD). Considering the primary outcome of this study, the change of the O_2 cost of walking during moderate- and heavy-

intensity exercise after RMET, a sample size of 8 achieves a 90% power to detect a mean difference of 16% and a standard deviation of differences of 20% with a significance level of 0.03. This difference corresponds to the mean difference previously observed following RMET in obese adolescents during cycling (87). A two-way analysis of variance (ANOVA) with repeated measures (2 groups × 2 times) was used to assess changes in anthropometry, spirometry parameters and exercise tolerance in two groups (RMET vs. CTRL) over the protocol period (pre vs. post). When a statistically significant difference was identified at ANOVA, a Bonferroni *post-hoc* test was applied to locate the difference. Statistical analyses were carried out by utilizing commercially available software packages (Prism 5.0, GraphPad, USA; Statistical Package Social Sciences 15.0, SPSS Inc., USA).

RESULTS

The main anthropometric data are reported in **Table 2.1**. During the 3-week hospitalization period both groups lost BM (~4-5 kg, corresponding to ~3-4% of the baseline BM); BMI and BMI-SDS also decreased significantly after both interventions. No differences between groups at baseline were observed for these variables.

Table 2.1. Age and anthropometric characteristics of the participants in standard body weight reduction intervention (CTRL group) and standard body weight reduction intervention combined with respiratory muscle endurance training (RMET group)

	RMET group (n=8)		CTRL group (n=8)		P Interaction	P group	P time
	PRE	POST	PRE	POST			
Age (years)	16.5 ± 0.9	16.5 ± 0.9	15.5±0.8	15.5±0.8	1.00	0.03	1.00
Height (m)	1.80 ± 0.05	1.80 ± 0.05	1.75±0.05	1.75±0.05	1.00	0.05	1.00
Body mass (kg)	130.5 ± 18.4	125.7 ± 18.0***	124.9±10.0	120.8±9.4***	0.50	0.48	< 0.0001
BMI (kg/m^2)	40.4±5.0	38.6±5.2***	41.0±2.9	39.6±2.8***	0.27	0.71	< 0.0001
BMI-SDS	3.5±0.6	3.3±0.6***	3.7±0.3	3.5±0.3***	0.21	0.50	< 0.0001
FFM (kg)	78.6±9.3	78.7±7.5	76.2±5.5	74.1±4.8	0.10	0.33	0.14
FM (kg)	51.9±10.1	47.0±10.8***	48.7±4.9	46.7±4.8	0.04	0.66	0.0001
FM (% of BM)	39.6±3.1	36.9±3.9**	38.9±1.2	38.6±1.3	0.04	0.69	0.01

BMI-SDS: SD score of body mass index (BMI). Values are expressed as mean±SD.

*** = P<0.001; **=P<0.01; Bonferroni *post-hoc* test to locate the statistically significant differences within groups.

The main spirometry data are reported in **Table 2.2**. No restrictive or obstructive alterations were observed in both groups. FVC was significantly higher after *vs.* before RMET, whereas no significant difference was observed following CTRL. A previous study by our group (60) on a similar population described that three weeks of RMET is enough to reduce abdominal load, recruit lung and chest wall volumes, and as a result increase FVC. No differences between groups at baseline were observed for spirometry variables.

Mean ± SD peak values of the investigated variables obtained during the incremental test are presented in **Table 2.3**. For most variables, no differences were observed after *vs.* before both interventions, with the notable exception of the time to exhaustion and walking slope, which were significantly higher after *vs.* before RMET, whereas no significant differences were observed after *vs.* before CTRL. $\dot{V}O_2$peak values, in absolute values and divided per unit of BM, are similar to those usually obtained in obese adolescents (41, 86–88). GET, expressed as L min^{-1} of $\dot{V}O_2$, was not affected by either intervention (2.31 ± 0.47 and 2.39 ± 0.48 in before and after RMET; 2.14 ± 0.38 and 2.04 ± 0.14 in before and after CTRL). In all conditions GET corresponded to ~70% of $\dot{V}O_2$peak.

Table 2.2. Spirometry data of patients before and after the standard intervention of body mass reduction (CTRL) and the standard intervention combined with RMET

	RMET group (n=8)		CTRL group (n=8)		P Interaction	P Group	P time
	PRE	POST	PRE	POST			
FVC, liters	5.1±0.7	5.6±0.7*	4.4±0.8	4.8±0.6	0.67	0.05	0.03
FVC, % Predicted	97.8±12.8	106.2±9.2	93.4±15	101±17.7	0.89	0.50	0.03
FEV_1, liters	4.3±0.7	4.8±0.7	3.8±0.6	3.9±0.4	0.19	0.06	0.10
FEV_1, % Predicted	96.5±16.4	106.9±13	94.1±10.5	95.8±6.5	0.22	0.32	0.10
FEV_1/FVC, %	83.7±4.8	85.5±4.3	87±6.7	82.6±9.9	0.08	0.95	0.44
$FEF_{25-75\%}$	4.5±0.4	5.3±1.1	4.2±0.8	4±1	0.10	0.09	0.25
$FEF_{25-75\%}$, % Predicted	92.4±9	108.3±23	92.4±10.2	89.1±16.4	0.01	0.23	0.26
PEF, liters/sec	7±1.2	8.5±1.8	6.6±0.4	7.3±0.9	0.49	0.13	0.08
PEF, % Predicted	74.5±15.9	91.2±16.1	78.7±2.3	86.9±8.5	0.47	0.99	0.05

FVC, forced vital capacity; FEV_1, forced expiratory volume in 1 second; $FEF_{25\%-75\%}$, forced expiratory flow between 25 % and 75 % of FVC;
PEF, peak expiratory flow. Values are expressed as mean±SD.
*=P<0.05; Bonferroni *post-hoc* test to locate the statistically significant differences within groups.

All patients completed the 12 min CWR protocols, both for moderate- and heavy-intensity walking. Mean ± SD values of the investigated variables calculated during the last minute of the CWR protocols are reported in **Table 2.4**. During moderate-intensity walking, RMET significantly decreased $\dot{V}O_2$ (expressed in L min^{-1} and divided by BM), whereas no significant differences were observed in after *vs.* before CTRL. When expressed as a percentage of $\dot{V}O_2peak$, $\dot{V}O_2$ values were ~49% *vs.* ~42% in before *vs.* after RMET, and ~49% *vs.* ~47% in before *vs.* after CTRL. The same trends (significant decrease after RMET, no significant difference after CTRL) were observed for $\dot{V}_E$ and $\dot{V}CO_2$. HR significantly (P<0.05) decreased both after RMET and after CTRL. When expressed as a percentage of HRpeak, HR values were ~67% *vs.* ~61% before *vs.* after RMET, and ~68% *vs.* ~65% before *vs.* after CTRL.

Very similar patterns were observed for heavy-intensity walking. RMET significantly decreased $\dot{V}O_2$ (expressed in L min^{-1} and divided by BM), whereas no significant differences for this variable were observed in after *vs.* before CTRL. When expressed as a percentage of $\dot{V}O_2peak$, $\dot{V}O_2$ values were ~92% *vs.* ~81% in before *vs.* after RMET, and ~92% *vs.* ~84% in before *vs.* after CTRL. The same trends (significant decrease after RMET, no significant difference after CTRL) were observed for $\dot{V}E$ and $\dot{V}CO_2$. HR significantly decreased after RMET but not after CTRL. When expressed as a percentage of HRpeak, HR values were ~93% *vs.* ~84% in before *vs.* after RMET, and ~94% *vs.* ~91% in before *vs.* after CTRL. No differences between groups at baseline were observed for these variables.

Table 2.3. Peak values of the main investigated variables, determined at exhaustion during the incremental exercise, before and after the standard intervention of body mass reduction (CTRL group) or the standard intervention combined with the RMET program (RMET group).

	RMET group (n=8)		CTRL group (n=8)		P Interaction	P group	P time
	PRE	POST	PRE	POST			
$\dot{V}O_2$ (L/min)	3.49±0.50	3.63±0.58	2.91±0.53	2.92±0.31$^{\#}$	0.56	0.01	0.50
$\dot{V}O_2$/BM (mL/min/kg)	26.6±3.5	30.1±7.0	23.4±4.2	24.3±3.3$^{\#}$	0.34	0.04	0.11
$\dot{V}CO_2$ (L/min)	3.38±0.60	3.63±0.50	3.00±0.45	2.96±0.33$^{\#}$	0.20	0.03	0.34
fR (breaths/min)	40.2±6.2	42.8±7.9	43.3±10.5	42.8±9.3	0.21	0.72	0.36
V_T BTPS (L)	2.1±0.4	2.2±0.4	2.1±0.3	2.1±0.3	0.53	0.53	0.46
$\dot{V}_E$ BTPS (L/min)	83.6±17.0	92.9±20.3	87.4±22.8	86.2±11.6	0.16	0.87	0.27
R	0.97±0.06	1.01±0.04	1.04±0.11	1.02±0.09	0.16	0.87	0.27
$PETO_2$ (mmHg)	102.5±6.5	103.7±6.2	99.2±7.2	99.3±6.5	0.52	0.26	0.47
$PETCO_2$ (mmHg)	45.5±5.1	45.1±7.5	40.2±6.4	38.8±5.4	0.56	0.07	0.31
$\dot{V}_E / \dot{V}O_2$	24.1±3.4	25.8±3.4	29.6±5.2$^{\#}$	29.0±4.1	0.04	0.04	0.31
$\dot{V}_E / \dot{V}CO_2$	24.8±2.8	25.7±3.5	28.5±3.9	28.6±3.4	0.47	0.07	0.31
HR (beats/min)	172.3±15.8	173.3±8.5	173.1±3.8	171.7±9.2	0.60	0.94	0.92
Waking velocity (km/h)	6.0±0.0	6.1±0.2	6.1±0.2	6.1±0.2	0.09	0.69	0.55
Walking Slope (%)	5.9±2.2	8.6±2.1***	7.9±2.3	8.9±1.5	0.007	0.35	< 0.0001
TE (sec)	690±250	1028±250***	908±300	1020±187	0.004	0.41	< 0.0001

BM, body mass; fR, respiratory rate; HR, heart rate; $PETCO_2$, CO_2 end-tidal pressure; $PETO_2$, O_2 end tidal pressure; R, respiratory gas-exchange ratio; TE, Time to exhaustion; $\dot{V}_E$, pulmonary ventilation; $\dot{V}CO_2$, CO_2 output; $\dot{V}O_2$, O_2 uptake; V_T, tidal volume. Values are expressed as mean±SD.

*** P<0.001; Bonferroni *post-hoc* test to locate the statistically significant differences within groups.
$^{\#}$ P<0.05; Bonferroni *post-hoc* test to locate the statistically significant differences between groups.

Table 2.4. Values of the main investigated variables determined during the last minute of the constant work rate (CWR) exercises carried out at 60%

of the work rate of gas exchange threshold (CWR <GET) and at 120 % of the work rate of GET (CWR >GET), before and after the standard body mass reduction intervention (CTRL group) and the standard intervention combined with RMET (RMET group).

CWR <GET	**RMET group** (n=8)		**CTRL group** (n=8)		**P Interaction**	**P group**	**P time**
	Pre	**Post**	**Pre**	**Post**			
$\dot{V}O_2$ (L/min)	1.69±0.41	1.50±0.33*	1.44±0.43	1.38±0.54	0.17	0.39	0.01
$\dot{V}O_2$/BM (mL/kg/min)	12.8±2.3	11.6±2.3	11.5±2.9	11.4±4.1	0.11	0.61	0.11
$\dot{V}O_{2rest}$ (L/min)	0.54±0.1	0.55±0.09	0.41±0.1	0.40±0.13$^{\#}$	0.68	0.005	0.95
$\dot{V}O_{2rest}$/BM (mL/kg/min)	4.1±0.6	4.3±0.6	3.3±0.8	3.4±1.2	0.77	0.02	0.66
$\dot{V}CO_2$ (L/min)	1.35±0.31	1.21±0.35	1.20±0.35	1.21±0.52	0.09	0.68	0.13
fR (breaths/min)	28.0±5.5	26.5±4.8	30.0±6.5	29.0±9.0	0.90	0.41	0.55
V_T BTPS (L)	1.4±0.4	1.3±0.4	1.1±0.3	1.2±0.4	0.41	0.36	0.69
$\dot{V}_E$ BTPS (L/min)	35.9±8.3	32.6±7.0	33.3±11.4	34.6±15.8	0.10	0.96	0.48
R	0.81±0.03	0.81±0.02	0.84±0.05	0.88±0.06$^{\#\#}$	0.25	0.01	0.16
$PETO_2$ (mmHg)	95.6±2.8	96.4±3.3	89.7±3.8$^{\#}$	92.4±5.2	0.29	0.01	0.06
$PETCO_2$ (mmHg)	43.6±2.2	43.2±1.8	41.8±3.6	40.3±3.9	0.26	0.13	0.06
$\dot{V}_E/VO_2$	21.5±1.6	21.9±1.6	22.5±1.0	24.1±1.8$^{*\#}$	0.21	0.02	0.03
$\dot{V}_E/VCO_2$	26.6±1.7	27.0±1.5	26.8±1.5	27.5±2.1	0.75	0.68	0.24
HR (beats/min)	115±21	105±16**	117±11	111±14	0.36	0.60	0.0008
Walking velocity (km/h)	4.1±0.5	4.1±0.5	4.1±0.6	4.1±0.6	1.00	1.00	1.00
Walking Slope (%)	0.0±0.0	0.0±0.0	0.0±0.0	0.0±0.0	1.00	1.00	1.00

CWR > GET							
$\dot{V}O_2$ (L/min)	3.16±0.56	2.89±0.44**	2.62±0.31#	2.45±0.30	0.37	0.03	0.0008
$\dot{V}O_2$/BM (mL/kg/min)	24.1±3.0	22.6±2.7*	21.1±2.4	20.5±2.8	0.21	0.09	0.02
$\dot{V}O_{2rest}$ (L/min)	0.61.5±0.17	0.57.1±0.12	0.38±0.12##	0.37±0.08##	0.68	0.002	0.34
$\dot{V}O_{2rest}$/BM (mL/kg/min)	4.6±0.9	4.4±0.8	3.1±0.9##	3.1±0.8##	0.62	0.0007	0.70
$\dot{V}CO_2$ (L/min)	2.86±0.61	2.55±0.42	2.54±0.28	2.47±0.45	0.18	0.35	0.05
fR (breaths/min)	42.9±5.2	40.0±6.1	43.7±10.3	41.7±9.4	0.76	0.74	0.06
V_T BTPS (L)	1.9±0.4	1.8±0.5	1.8±0.4	1.8±0.3	0.73	0.69	0.70
$\dot{V}_E$ BTPS (L/min)	79.2±22.8	70.1±16.2*	74.5±12.8	71.3±13.4	0.26	0.83	0.03
R	0.91±0.04	0.88±0.03	0.97±0.09	1.00±0.11##	0.29	0.004	0.79
$PETO_2$ (mmHg)	103.9±6.2	103.1±6.1	98.2±5.7	97.9±6.5	0.81	0.12	0.66
$PETCO_2$ (mmHg)	40.8±4.2	41.0±4.3	39.2±4.7	39.7±5.5	0.78	0.33	0.60
$\dot{V}_E/VO_2$	25.5±3.8	24.7±3.0	27.9±2.6	28.1±2.9#	0.43	0.02	0.70
$\dot{V}_E/VCO_2$	28.1±3.3	27.9±2.9	28.8±2.9	28.2±3.1	0.55	0.43	0.47
HR (beats/min)	160±17	146±18***	163.3±10.6	157.7±7.9	0.03	0.33	< 0.0001
RPE_R	2.7±2.8	0.8±2.1*	4.3±1.8	2.9±1.6	0.69	0.053	0.02
RPE_L	2.6±2.7	1.2±2.2	2.9±2.0	3.8±2.3	0.05	0.21	0.64
Walking velocity (km/h)	5.9±0.2	5.9±0.2	6.0±0.0	6.0±0.0	1.00	0.17	1.00
Walking Slope (%)	4.6±2.2	4.6±2.2	5.3±1.4	5.3±1.4	1.00	0.43	1.00

BM, body mass; fR, respiratory rate; HR, heart rate; $PETCO_2$, CO_2 end-tidal pressure; $PETO_2$, O_2 end tidal pressure; R, respiratory gas-exchange ratio; RPE_L, rate of perceived exertion for leg effort; RPE_R, rate of perceived exertion for respiratory discomfort; TE, Time to exhaustion; $\dot{V}_E$, pulmonary ventilation; $\dot{V}CO_2$, CO_2 output; $\dot{V}O_2$, O_2 uptake; V_T, tidal volume. Values are expressed as mean±SD.

*** = P<0.001, ** = P<0.01, * = P<0.05; Bonferroni *post-hoc* test to locate the statistically significant differences within groups.

= P<0.01, # = P<0.05; Bonferroni *post-hoc* test to locate the statistically significant differences between groups.

Mean (± SD) values of the O_2 cost are presented for moderate-intensity (left panels) and heavy-intensity (right panels) walking in **Figure 2.1**. Data are expressed as mL O_2 m^{-1} (upper panels) and as mL O_2 kg^{-1} m^{-1} (lower panels). In all experimental conditions values calculated during heavy-intensity walking were higher than those obtained during moderate-intensity walking. For both exercise intensities, the O_2 cost of walking decreased following RMET, but not following CTRL. For moderate and heavy-intensity walking, reference values from the literature (28, 67, 78) for a man with a body mass of 75 kg are also shown in the figure (dashed horizontal line). The data of the obese patients from the present study are more than 100% higher than the reference value when expressed as mL O_2 m^{-1}, whereas the difference becomes much smaller (before RMET) or substantially disappears (after RMET) when the O_2 cost of walking is normalized by BM.

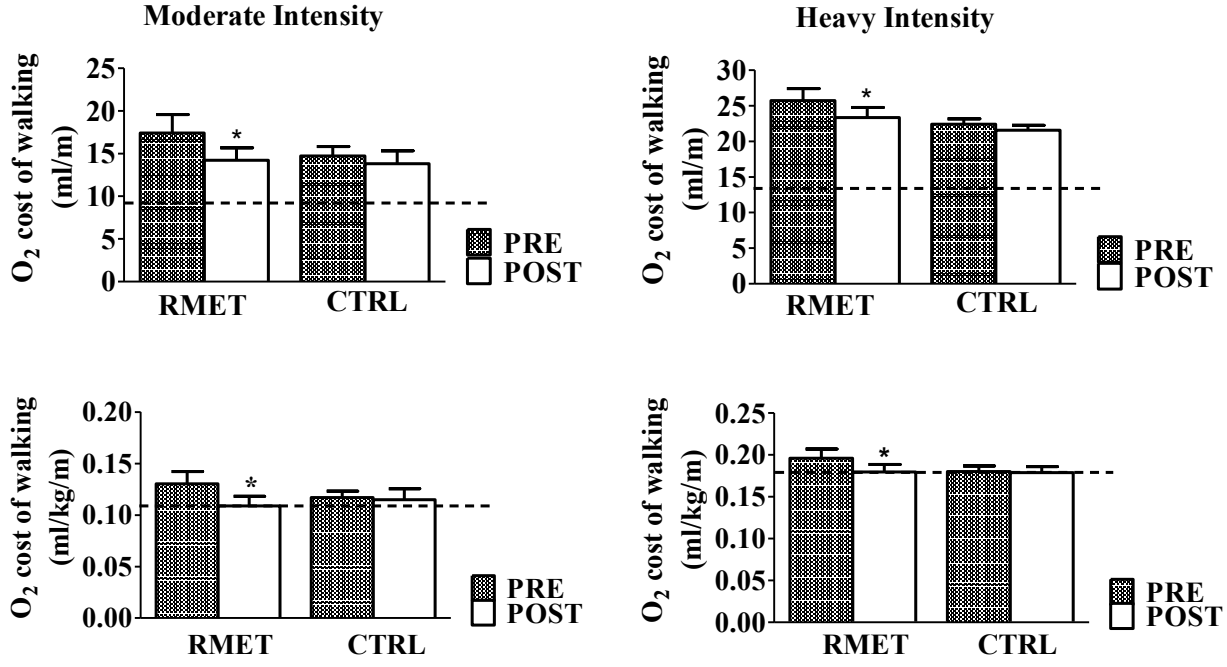

Figure 2.1. Mean (± SD) values of the O_2 cost of walking (oxidative energy expenditure per unit of covered distance, calculated as $\Delta \dot{V} O_2$ velocity^{-1}) during the last minute of CWR exercise at ~60% of GET (moderate-intensity, left panels) and at ~120 % of GET (heavy-intensity, right panels), before and after CTRL and RMET. In the upper panels the O_2 cost of walking is expressed as mL O_2 m^{-1}, whereas in the lower panels the variable is normalized per unit of body mass (mL O_2 kg^{-1} m^{-1}). Dashed horizontal lines are reference values from the literature (28, 67, 78) for a man with a body mass of 75 kg. RMET reduced significantly the O_2 cost of walking.

* = P <0.05. Bonferroni *post-hoc* tests to locate the statistically significant difference (after *vs.* before RMET).

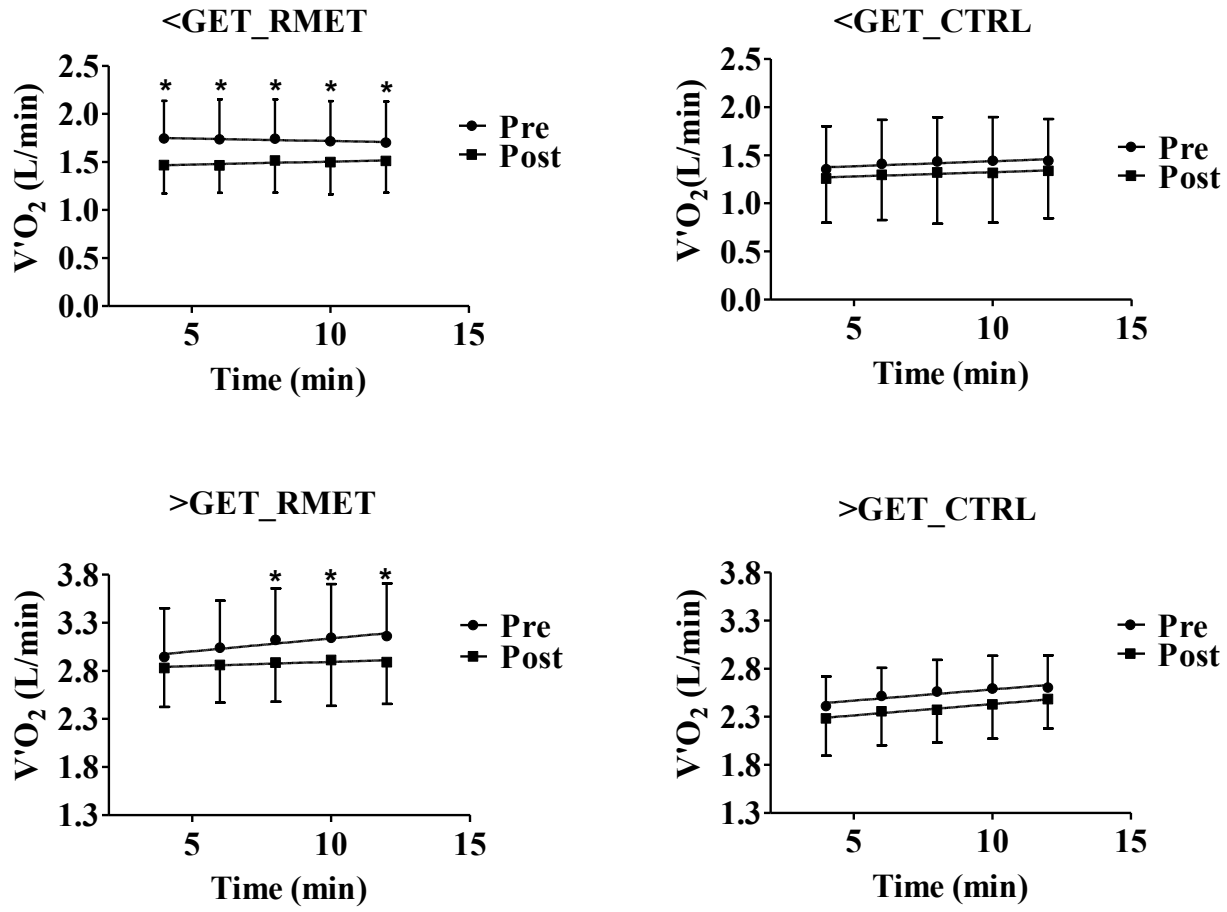

Figure 2.2. Mean (± SD) $\dot{V}O_2$ values calculated every two minutes, from the 3rd to the last minute of CWR walking at ~60% of GET (moderate-intensity, upper panels) and at ~120 % of GET (heavy-intensity, lower panels), before and after RMET and CTRL. During CWR <GET mean values of the individual slopes of the linear regressions of $\dot{V}O_2$ *vs.* time were not significantly different from zero, before and after both interventions. At all-time points $\dot{V}O_2$ values were significantly lower after *vs.* before RMET, whereas no statistically significant differences were observed after *vs.* before CTRL. During CWR >GET the slopes of the linear regressions of $\dot{V}O_2$ *vs.* time were significantly greater than zero before both RMET and CTRL. The mean values of the individual slopes were significantly lower after *vs.* before RMET, but not after *vs.* before CTRL. See text for further details. * = P <0.05.

Mean (± SD) $\dot{V}O_2$ values calculated every 2 minutes, from the 3rd to the 12th minute of exercise, during moderate-intensity walking (upper panels) and heavy-intensity walking (lower panels), are shown in **Figure 2.2**. All data were fitted by linear regression lines, which are shown in the Figure. During moderate-intensity walking the mean values of the individual slopes of the linear regressions of $\dot{V}O_2$ vs. time were not significantly different from zero, before (-0.007 ± 0.010 and 0.010 ± 0.012 L min^{-2} in RMET and CTRL, respectively) and after (0.006 ± 0.010 and 0.009 ± 0.013 L min^{-2}) both interventions. In other words, in all cases $\dot{V}O_2$ was in a condition of steady state. At all-time points, $\dot{V}O_2$ values were significantly lower after *vs.* before RMET, whereas no statistically significant differences were observed after *vs.* before CTRL.

During heavy-intensity walking the slopes of the linear regressions of $\dot{V}O_2$ vs. time were significantly greater than zero before both RMET and CTRL. In other words, before both interventions $\dot{V}O_2$ was not in a condition of steady-state but kept increasing from the 3rd to the last minute of exercise. The mean values of the individual slopes were significantly lower after (0.009 ± 0.015 L min^{-2}) vs. before (0.027 ± 0.011) RMET, but not after (0.024 ± 0.022 mL min^{-2}) vs. before CTRL (0.030 ± 0.014). The amplitude of the $\dot{V}O_2$ (in L min^{-1}) increase between the 3rd and the last minute of exercise was significantly lower after (0.06 ± 0.11) vs. before (0.22 ± 0.08) RMET, but not after (0.20 ± 0.19) vs. before (0.21 ± 0.08) CTRL. The same patterns were described when $\dot{V}O_2$ values were divided by BM (data not shown).

The same analyses carried out for $\dot{V}O_2$ in Figure 2 were carried out for HR in **Figure 2.3**. The results were substantially the same. During moderate-intensity walking (upper panels) the mean values of the individual slopes of the linear regressions of HR vs. time were not different from zero, before (-0.23 ± 0.48 and 0.3 ± 0.4 beats min^{-2} in RMET and CTRL, respectively) and after (0.46 ± 0.45 and 0.59 ± 0.47 beats min^{-2}) both interventions. In other words, HR was in a condition of steady state. At all time-points values after RMET were significantly lower than those before RMET; no significant differences were observed in after *vs.* before CTRL.

During heavy-intensity walking (lower panels) the slopes of the linear regressions of HR *vs.* time were significantly greater than zero before both RMET and CTRL. The mean values of the individual slopes were significantly lower after (0.88 ± 0.61 beats min^{-2}) *vs.* before (1.43 ± 0.56) RMET, but not after (2.10± 1.26 beats min^{-2}) *vs.* before CTRL (2.19 ± 1.33).

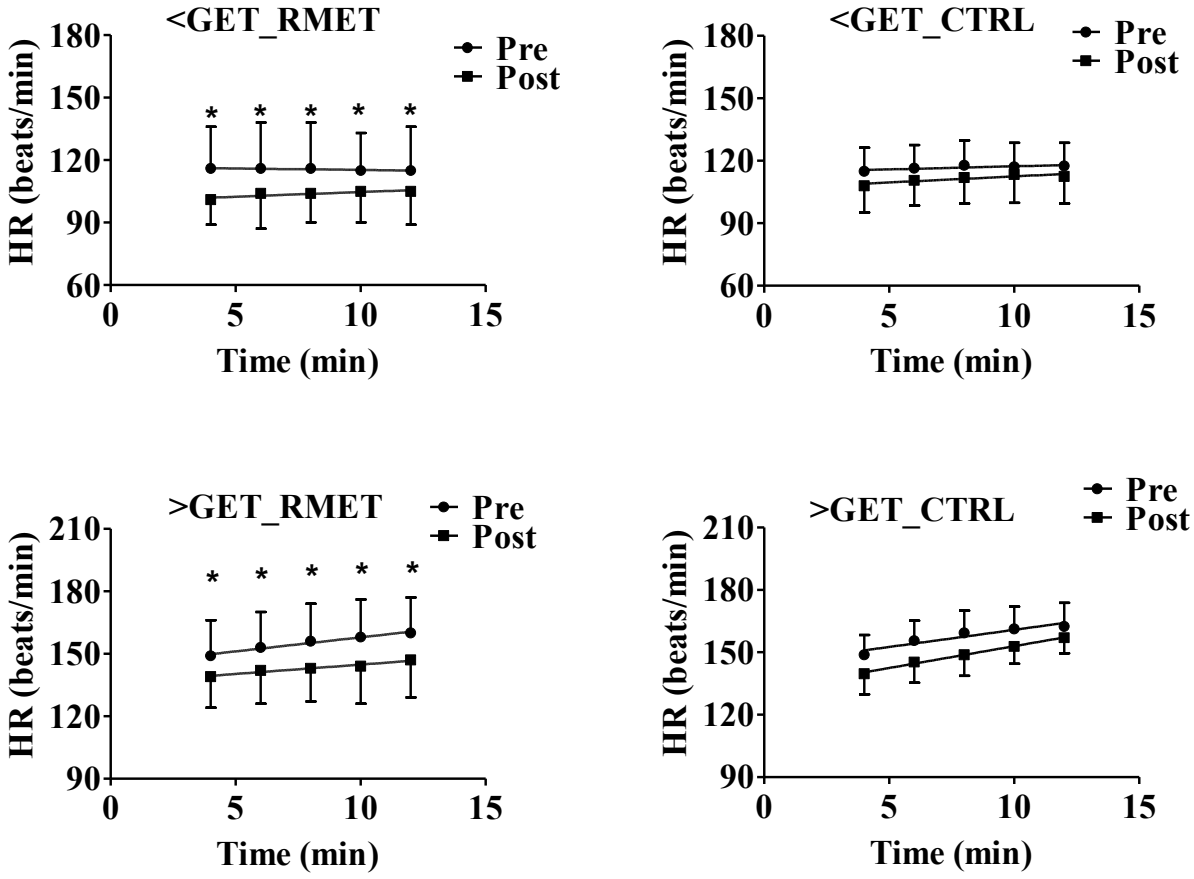

Figure 2.3. Mean (± SD) HR values calculated every two minutes, from the 3rd to the last minute of CWR walking at ~60% of GET (moderate-intensity, upper panels) and at ~120 % of GET (heavy-intensity, lower panels), before and after RMET and CTRL. During CWR <GET (upper panels) the mean values of the individual slopes of the linear regressions of HR *vs.* time were not different from zero, before and after both interventions. At all time-points values after RMET were significantly lower than those before RMET; no significant differences were observed in after *vs.* before CTRL. During CWR >GET (lower panels) the slopes of the linear regressions of HR *vs.* time were significantly greater than zero before both RMET and CTRL. The mean values of the individual slopes were significantly lower after *vs.* before RMET, but not after *vs.* before CTRL. See text for further details. * = P <0.05.

In order to check if the effects of RMET were associated with changes in the ventilatory pattern (the relative contribution of V_T and fR increases to the $\dot{V}_E$ increase), the latter was specifically

investigated by the analysis depicted in **Figure 2.4** (mean values obtained in the different groups during incremental exercise). In the Figure, $\dot{V}_E$ data were plotted as a function of V_T, and iso-fR lines were also drawn. The breathing pattern was not affected by either intervention. The rather small (but statistically significant) $\dot{V}_E$ peak increase following RMET was attributable to an increased fR.

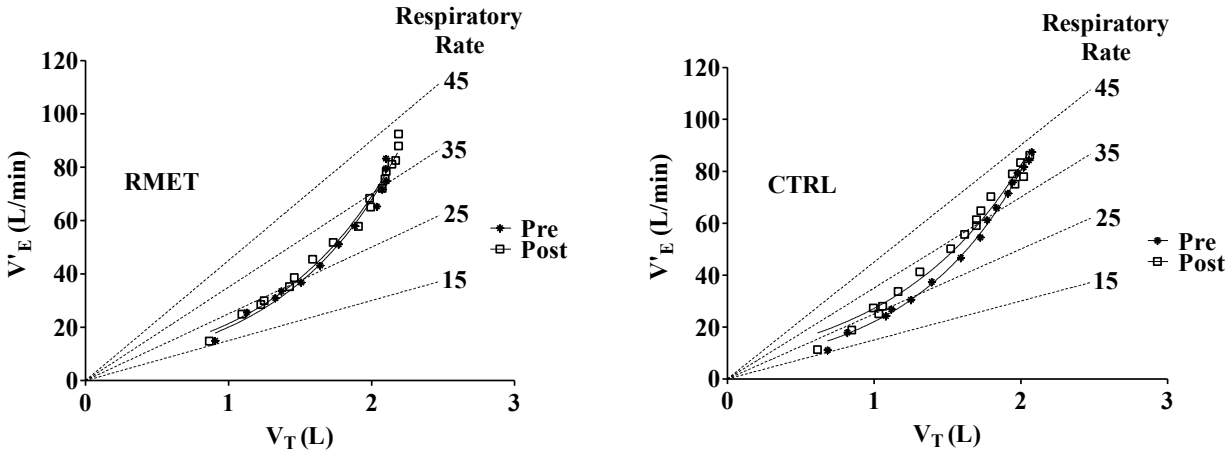

Figure 2.4. Pattern of breathing in two group of subjects during the incremental test. The relationships between mean values of pulmonary ventilation ($\dot{V}_E$) and tidal volume (V_T) for RMET (left panel) and CTRL (right panel) are presented, before and after the interventions. Iso-respiratory frequency (fR) lines (dashed lines, departing from the origin) are also presented. The exponential functions fitting the experimental points are shown. See text for further details.

DISCUSSION

In obese male adolescents, a relatively short (3 weeks) program of RMET (82), superimposed on a standard multidisciplinary body mass reduction intervention (moderate caloric restriction, aerobic exercise training, psychological and nutritional counselling) significantly reduced the O_2 cost of walking and ameliorated signs of exercise tolerance (increased time to exhaustion during an incremental test, lower HR and RPE for the same walking velocity). The improvements were not observed in the control group of patients (CTRL), which underwent only to the multidisciplinary body mass reduction intervention.

Decreased O_2 cost of walking

In the present study the O_2 cost (oxidative energy expenditure per unit of distance) of moderate intensity walking was more than 100% higher in obese adolescents compared to that usually observed in normal controls. This difference is higher than that (about 50%) usually observed for cycling (51, 102). As mentioned in the Introduction, a higher O_2 cost of exercise is inevitably associated with an impaired exercise tolerance (39). It is not surprising, then, that in the present study the decreased O_2 cost of walking observed following RMET improved exercise tolerance. The positive effects of RMET on the O_2 cost of walking were observed both during moderate- and heavy-intensity walking on a treadmill. On the other hand, in a previous study by our group (87), carried out on obese adolescents exercising on a cycle ergometer, the positive effects of RMET on the O_2 cost of exercise were observed only during heavy-intensity CWR exercise. The results suggest that during weight bearing activities like walking or running, in which larger muscle masses are involved compared to cycling, and the patient undergoes cyclical elevations and accelerations of the body's center of mass at every step, obese adolescents are penalized, from the O_2 cost of exercise point of view, also during moderate-intensity exercise.

The reduced O_2 cost of walking following RMET was exemplified by the lower $\dot{V}O_2$ levels (during moderate- and heavy-intensity walking) and by the lower $\dot{V}O_2$ *vs.* time slopes (during heavy-intensity walking) (Figure 2). No formal analyses of the $\dot{V}O_2$ kinetics and its different components (47) was carried out in the present study, since the patients could perform only one repetition of each exercise. Some data, however, allow us to hypothesize, with reasonable confidence, that the reduced O_2 cost during heavy intensity walking was likely attributable to a reduced amplitude or to the disappearance of the "slow component" of the $\dot{V}O_2$ kinetics (47). The slope of the linear increase of the $\dot{V}O_2$ *vs.* time relationship ("excess VO_2", characteristic of the $\dot{V}O_2$ slow component [(39)]), determined from the 3rd to the 1ast minute of exercise, was indeed substantially decreased following RMET, whereas it was not affected by CTRL. A smaller amplitude of the slow component of the $\dot{V}O_2$ kinetics is intrinsically associated with less inefficiency and less fatigue (39, 47).

The lower O_2 cost of walking observed in the present study after RMET could be due to a lower O_2 cost of breathing, to a lower O_2 cost of work by locomotor muscles or to both factors. A

limitation of the present study is represented by the fact that no direct measurements of the work of breathing and of the O_2 cost of breathing were performed. In a previous study carried out by our group in obese adolescents during cycling, however, we observed by optoelectronic plethysmography significant changes of static and dynamic thoraco-abdominal volumes of breathing following a RMET protocol identical to that of the present study (60). More specifically, the patients showed abdominal rib cage hyperinflation as a form of lung recruitment during exercise, with a move to higher operating volumes. Three weeks of RMET were enough to reduce the abdominal load, recruit lung and chest wall volumes, unload respiratory muscles and delay the abdominal rib cage hyperinflation (60). These effects, which were not determined in the present study, resulted in a reduced dyspnea and an enhanced exercise tolerance, and would be presumably associated with reduced work of breathing and O_2 cost of breathing.

In a recent paper, Passoni *et al*. (75) found that in some patients affected by metabolic syndrome, training led to improved efficiency of respiratory activity as suggested by a decrease in respiratory power output as a function of workload. Although in the present study the ventilatory pattern was not affected by RMET, the $\dot{V}_E$ peak increase following RMET was attributable to an increased fR which interpreted as a less costly ventilatory pattern (75).

With some calculations, we tried to partition the relative roles of a reduced O_2 cost of breathing and of a reduced O_2 cost of locomotor muscles on the observed decrease of the O_2 cost of walking. In the present study RMET lowered the $\dot{V}O_2$ by ~190 ml min^{-1} during moderate-intensity exercise and by ~280 mL min^{-1} during heavy-intensity exercise. The effects of CTRL on this variable were, respectively, ~60 and ~180 mL min^{-1}. In order to estimate the $\dot{V}O_2$ of respiratory muscles (RM $\dot{V}O_2$), we utilized the equations proposed by Coast *et al*. (17) for normal subjects, relating $\dot{V}E$ to the work of breathing, and the work of breathing to RM $\dot{V}O_2$. Since the equations proposed by Coast *et al.* (17) were obtained in normal subjects, in order to apply them to the obese population the work of breathing was increased by 70%, as proposed by Koenig (49). After doing so, RMET decreased RM $\dot{V}O_2$ by 7 mL min^{-1} during moderate-intensity exercise, and by 40 mL min^{-1} during heavy-intensity exercise. Substantially no changes were observed following CTRL. The decreases in RM $\dot{V}O_2$ following RMET corresponded to ~4% of the decrease in $\dot{V}O_2$ during moderate-intensity exercise, and to ~14% during heavy-intensity exercise. In other words, a vast majority of the O_2 cost of walking

decrease following RMET can be attributed to the decreased O_2 cost of locomotor muscles, particularly during moderate-intensity exercise. Although the calculations described above are based upon some assumptions and may be somewhat imprecise, the "size" of the phenomenon (85-95% of the reduced O_2 cost of walking likely not directly attributable to a reduced O_2 cost of breathing) should make the concept relatively "safe".

The reduced O_2 cost by locomotor muscles, however, might as well be a consequence of the effects of RMET on respiratory muscles. By improving respiratory muscle function, indeed, RMET could prevent, reduce or delay the development of fatigue within these muscles and the reflex vasoconstriction within the active locomotor muscles (84, 107), allowing for a greater muscle O_2 availability. Above a threshold for respiratory muscle work, accumulation of fatigue-related metabolites in respiratory muscles could stimulate group III and IV afferent fibers going to cardiorespiratory control centers, enhancing effort perception (dyspnea) (1), determining a sympathetically-mediated vasoconstriction of locomotor muscles, leading to decreased efficiency and fatigue (39), and presumably also to an inhibition of central motor output (33). It has been demonstrated that respiratory muscle training increases the intensity of the inspiratory muscle work necessary to activate this reflex (107).

In normal subjects a "competition" between respiratory and locomotor muscle for the finite cardiac output and the finite capacity of cardiovascular O_2 delivery (20) appears to be critical during maximal or near maximal exercise (22), but not during submaximal tasks (104). However, after considering the significantly increased respiratory muscle work and O_2 cost associated with obesity (49), as well as the increased stress on the cardiovascular system imposed by the greater body mass, it appears reasonable to hypothesize that such competition could manifest in obese patients also during submaximal tasks. The problem could be even more significant during treadmill exercise, because of the larger skeletal muscle mass involved in the task and of the weight bearing work. It should also be remembered that, by the same mechanisms, RMET could also positively affect "central" hemodynamics (61, 100) and further enhance O_2 delivery to the locomotor muscles. An increased peripheral O_2 delivery would delay the development of inefficiency and fatigue within these muscles (39, 45, 47) and would reduce the amplitude of the $\dot{V}O_2$ slow component.

The results of the present study and of the previous one (87) should be interpreted in conjunction with another recent study carried by our group in obese adolescents (88), in which acute respiratory muscle unloading, obtained by normoxic helium breathing, reduced the O_2 cost of cycling and the perception of fatigue during moderate- and heavy-intensity CWR exercise. Taken together, these studies point to the respiratory system as a target for interventions aimed at interrupting the vicious cycle between physical inactivity and obesity.

The effectiveness of RMET on 18-50 years-old obese patients had been previously suggested by Frank *et al*. (31), who observed that 7 months of RMET reduced the sensation of breathlessness during exercise and obtained an increase in the distance covered during a 12-min time trial. These authors, however, did not perform a formal evaluation of exercise capacity and tolerance, and could not identify mechanisms potentially responsible for the enhanced performance. These limitations were overcome in our previous study (87) and in the present one, in which several physiological variables related to exercise tolerance were directly determined, allowing mechanistic insights into the factors potentially responsible for the observed changes, such as the effects of RMET on respiratory mechanics (60), the reduced O_2 cost of exercise, the "metaboreflex" concept discussed above. The same concepts apply to another study (27), in which a different type of respiratory muscle training (inspiratory muscle strength training) was utilized.

Enhanced exercise tolerance

RMET increased exercise tolerance, as demonstrated by the increased time to exhaustion during the incremental test, as well as by the lower HR and RPE (during heavy intensity CWR exercise) for the same walking velocity. Reduced RPE following RMET was described also by LoMauro *et al*. (60). Further linking the reduced O_2 cost of walking to an enhanced exercise tolerance, in the present study the effects of RMET on $\dot{V}O_2$ (Figure 2) were substantially identical to those described for HR (Figure 3): lower values of both variables during moderate- and heavy-intensity walking, less pronounced progressive increases of both variables during heavy-intensity walking. Textbook physiology states that, for the same work rate, lower HR corresponds to increased exercise tolerance.

The reduced O_2 cost of exercise is likely responsible for the increased time to exhaustion during the incremental test, despite the absence of changes of $\dot{V}O_2$peak. An increased peak work

capacity, in the presence of an unchanged $\dot{V}O_2$peak, can indeed be explained by an increased efficiency (or decreased inefficiency) of work (53). The lack of effects of RMET on $\dot{V}O_2$peak is consistent with previous observations in healthy normal-weight subjects (26, 30), as well as with the results of our previous study in obese adolescents during cycling (87).

CONCLUSIONS

The present study, carried out on obese adolescents walking on a treadmill, extends the positive effects of a short (3-week) RMET program on the O_2 cost of exercise and on exercise tolerance, previously described by our group in obese adolescents only during heavy-intensity cycling exercise (87), also during moderate-intensity exercise. This appears to be relevant in terms of exercise tolerance and quality of life, since most activities of everyday life are mainly of moderate intensity. As it could be expected, in obese adolescents, respiratory limitations negatively impact on the O_2 cost of walking and on exercise tolerance more markedly when treadmill walking is involved, compared to cycling exercise. By contrasting the vicious circle of obesity → early fatigue → reduced exercise tolerance → reduced physical activity → obesity, the intervention could represent a useful adjunct in the control of obesity. Longer periods of RMET should be investigated.

CHAPTER 3: RESPIRATORY MUSCLE UNLOADING BY NORMOXIC HELIUM-O_2 BREATHING DURING CYCLING EXERCISE DELAYS VOLITIONAL EXHAUSTION IN OBESE ADOLESCENTS

INTRODUCTION

Obesity has a profound effect on the physiology of breathing (49, 63). Obese patients have a higher O_2 cost of exercise (51, 86, 102), which negatively affects exercise tolerance (39) and is at least in part attributable to a higher O_2 cost of breathing (50, 87, 88). Even during quiet breathing morbid obesity is associated with a substantial increase in respiratory muscle $\dot{V}O_2$ (50).

Previous studies that evaluated the effect of respiratory muscle unloading via breathing low density gas (for example normoxic helium-O_2 mixture HeO_2) or by a proportional assist ventilator (PAV) on exercise performance/tolerance in healthy subjects or various patients demonstrated inconsistent results. A recent study by Dominelli et al (22) demonstrated that, in healthy subjects during cycling, respiratory muscle unloading via PAV increased limb (locomotor) blood flow and reduced respiratory muscle blood flow. Whole body $\dot{V}O_2$ during respiratory muscle unloading was also less than in control conditions. Conversely, when the work of breathing (WOB) was increased via resistive load, they observed a reduction in limb blood flow and an increase in blood flow to the respiratory muscles. Similarly, mechanically reducing respiratory muscle work during high-intensity exercise in healthy subjects resulted in increased vascular conductance and blood flow to working limb locomotor muscles and in significant increases in endurance-exercise performance (5). Respiratory muscle unloading via normoxic HeO_2 extended exercise duration in patients with heart failure (66), increased lower limbs muscle oxygen delivery during exercise in COPD patients (15, 62). Other investigators have also demonstrated that normoxic HeO_2 breathing during exercise increased ventilation and peak $\dot{V}O_2$ in young healthy subjects (10), whereas others have not found any improvement in peak exercise performance (3). In a previous study by our group (88) acute respiratory muscle unloading via normoxic HeO_2 breathing determined in a group of obese adolescents (OB) a lower O_2 cost of exercise and perceived exertion during moderate- and heavy-intensity short-duration exercises on a cycle ergometer. The purpose of the present study was then to determine

whether, in OB, acute respiratory muscle unloading can indeed extend the duration of exercise at intensities proxy to those actually experienced during daily-living activities. Respiratory muscle unloading was acutely induced during cycling exercise by switching the inspired gas from ambient air (AIR) to normoxic HeO_2 at exhaustion (AIR+HeO_2) in OB versus normal-weight controls (CTRL).

METHODS

Subjects

We studied ten male OB [age: 16 ± 2.0 years (mean ± SD)], Tanner stage 4–5 (i.e., late puberty), who were admitted as in-patients (Division of Auxology, Italian Institute for Auxology, Piancavallo, Italy) for a multidisciplinary body weight reduction program and ten age- and sex-matched controls (CTRL) [age: 17 ± 0.9 years (mean ± SD)]. Anthropometric characteristics of the subjects are shown in Table 3.1. Inclusion criteria were: (1) BMI > 97^{th} centile [OB] and < 50^{th} centile [CTRL] for age and sex, using the Italian growth charts (12); (2) no involvement in structured physical activity programs (regular activity more than 120 min/week) during the 8 months preceding the study; (3) absence of overt uncompensated diabetes; (4) absence of signs or symptoms referable to any major cardiovascular, respiratory or orthopedic disease contraindicating or significantly interfering with the tests. The standard deviation score (SDS) of BMI was calculated by applying the LMS method (based upon the skewness (L), the median (M), and the coefficient of variation (S) of the measurements as a function of age to Italian reference values for children and adolescents (12). Fat-free mass (FFM) was assessed by bioelectric impedance analysis (64). Whole body resistance to an applied current (50 kHz, 0.8 mA) was measured with a tetrapolar device (Human IM, Dietosystem, Italy). Fat mass (FM) was calculated as the difference between total body mass (BM) and FFM.

Participants agreed to be enrolled in the study. Participants' parents provided signed consent statements, after being fully advised about the purposes and testing procedures of the investigation, which were approved by the ethics committee of the Italian Institute for Auxology, Piancavallo, Italy, where the experiments were carried out. All procedures were performed in agreement with the recommendations set forth in the Helsinki Declaration (2000).

Before the exercise protocols, the OB and CTRL subjects performed pulmonary function testing while breathing room air (Med-Graphics CPX/D, Medical Graphics Corp., USA; Quark CPET, COSMED Srl - Italy). Tests were performed according to the guidelines of the American Thoracic Society (69). Forced vital capacity (FVC), forced expiratory volume in 1 s (FEV_1), FEV_1/FCV and peak expiratory flow rate (PEFR) were determined. Predicted values were based on Hankinson *et al*. (40).

Exercise protocol

Experiments were conducted with the participants inspiring AIR for the entire pedaling duration or with the inspired gas switched to normoxic HeO_2 (a 21% O_2–79% helium mixture) [AIR+HeO_2] when the patients were reaching volitional exhaustion. Each study participant was seen five times on separate days. All tests were conducted under medical supervision, and study participants were continuously monitored by 12-lead electrocardiography (ECG). A mechanically braked cycle ergometer (Monark Ergomedic 839E) was utilized. Pedaling frequency was digitally displayed to the participants, who were asked to keep a constant cadence throughout the tests between 60 and 70 rpm. Each participant had chosen his preferred cadence during practice trials; the resistance of the pedals was calculated to obtain the desired work rate.

Participants were allowed time to gain familiarity with the investigators and experimental set up and were familiarized with the exercise protocols by means of short preliminary practice runs. During the first day, the participants performed an incremental exercise test with AIR. After 3 minutes resting measurement (subjects were positioned on the cycle ergometer) the incremental exercise began with a 2 min warm-up at 20 W; the work rate was then increased by 20 W every two minute until the subjects could no longer maintain the imposed work rate at the required frequency despite verbal encouragement. For all variables, values determined at exhaustion were considered “peak” values.

During the second and third days, participants performed two bouts of constant work rate exercise (CWR), in AIR or AIR+HeO_2. Work rates were selected to be in the moderate (below the gas exchange threshold, <GET, corresponding to ~80% of the GET) and heavy (above the gas exchange threshold, >GET, corresponding to 50% of the difference between GET and peak

$\dot{V}O_2$) intensity domains. The moderate-intensity CWR exercises was carried out for 40 min or to voluntary exhaustion; whereas heavy-intensity CWR exercises were carried out to voluntary exhaustion. About one hour of recovery separated the two CWR exercises. In one of the two CWR exercises patients switched from AIR to HeO_2 when they were facing exhaustion. The inspired gas switched to HeO_2 as HR reached 85% or 95% of peak HR in moderate and heavy intensity cycling, respectively, or as subjects rated RPE_R or RPE_L 7 or higher. Moderate intensity CWR exercise was always carried out before heavy intensity CWR exercise. The sequence of conditions (AIR and AIR+HeO_2) was randomized.

Measurements

$\dot{V}_E$, V_T, fR, $\dot{V}O_2$ and $\dot{V}CO_2$ were determined on a breath-by-breath basis by means of a metabolic unit in AIR (MedGraphics CPD, Medical Graphics Corp., USA; Quark CPET, COSMED Srl - Italy). Calibration of O_2 and CO_2 analyzers was performed before each experiment by utilizing gas mixtures of known composition (Air Liquide, Milan, Italy). Expiratory flow measurements were performed by a bidirectional pressure differential pneumotachograph, which was calibrated by a 3 L syringe at different flow rates. A two-way non-rebreathing valve (Hans Rudolph Inc., USA) was attached immediately distal to the turbine. The inspiratory port of the breathing valve was connected, via a three-way stopcock, to a 180 L Douglas bag (continuously primed with gas) containing HeO_2 or AIR. Care was taken to ensure that layering in the gas cylinders due to density differences between He and O_2 did not occur. Heart rate (HR) was determined by ECG. Ratings of perceived exertion (RPE) for respiratory discomfort (RPE_R) and limb effort (RPE_L) were obtained at rest and every minute during exercise by using the Borg's modified CR10 scale (106). GET was determined by the V-slope method; ventilatory equivalents ($\dot{V}E/\dot{V}O_2$, $\dot{V}E/\dot{V}CO_2$) were utilized as ancillary signs (7). The gas exchange ratio (R) was calculated as $\dot{V}CO_2/\dot{V}O_2$.

Kinetics analysis. Average $\dot{V}O_2$ and HR values every 10 s were calculated and utilized for kinetics analysis, which was carried out during the transition from rest to CWR. $\dot{V}O_2$ kinetics analysis dealt with the phase 2 of the response (fundamental component), which should more closely reflect gas exchange kinetics occurring at the skeletal muscle level (38), as well as with

the slow component (37). To mathematically evaluate the $\dot{V}O_2$ kinetics, data were first fitted by a monoexponential function of the type

$$y(t) = y\text{BAS} + \text{Af} \cdot (1 - \exp^{-(t\text{-TDf})/\tau\text{f}} \qquad (1)$$

where yBAS indicates the $\dot{V}O_2$ value at baseline; Af the amplitude of $\dot{V}O_2$ calculated between the baseline value and the steady-state value for the fundamental component; TDf is the time delay, and τf the time constant of the function for the fundamental component. To check the presence of a slow component of the kinetics, data were also fitted by a double exponential function of the type

$$y(t) = y\text{BAS} + \text{Af} \cdot (1 - \exp^{-(t\text{-TDf})/\tau\text{f}} + \text{As} \cdot (1 - \exp^{-(t\text{-TDs})/\tau\text{s}} \qquad (2)$$

where As, TDs, and τs indicate, respectively, the amplitude, the time delay, and the time constant of the slow component of the kinetics. Sometimes, after the first exponential rise, $\dot{V}O_2$ increased linearly without reaching a steady-state value. In this case, Eq. 2 did not provide a good fit of data. Thus, a third equation was also utilized, with an exponential function for the fundamental component and a linear function for the slow component (exponential + linear fitting) (23)

$$y(t) = y\text{BAS} + \text{Af} \cdot (1 - \exp^{-(t\text{-TDf})/\tau\text{f}} + \text{S} \cdot (\text{t} - \text{TDs}) \qquad (3)$$

where S (slope) is the angular coefficient of the linear regression of $\dot{V}O_2$ vs. time.

The equation that best fit the experimental data was determined by the F-test. That is to say, when Eq. 2 or Eq. 3 provided a better fit of the data, a slow component of $\dot{V}O_2$ kinetics was present, superimposed on the fundamental component. The actual amplitude of the slow component (As) was estimated as the difference between the average $\dot{V}O_2$ value obtained during the last 20–30 s of CLE and the asymptotic value of the fundamental component (37). The percentage contribution of the slow component to the total amplitude of the response (As/Atot) was also calculated. HR kinetics was similarly analyzed. In HR analyses the phase one was included.

Statistical analysis

Results were expressed as mean ± standard deviation (SD). Statistical significance of differences between AIR+HeO_2 and AIR was checked by two-tailed Student's t test for paired data. Data fitting by exponential functions were performed by the least-squared residuals method. Comparisons between fitting with different models were carried out by the F-test. The level of significance was set at $P < 0.05$. Statistical analyses were carried out with a commercially available software package (Prism 5.0, GraphPad).

RESULTS

The main anthropometric data are reported in **Table 3.1.** A statistically significant difference between OB and CTRL was observed for all anthropometry features (except for height).

Table 3.1. Age and anthropometric characteristics of the participants.

	OB	CTRL
N	10	10
Age (years)	16±2.0	17±0.9
BM (kg)	117.5±21.3	68.4±10**
Height (m)	1.7±0.1	1.8±0.1
BMI (Kg/m^2)	38.9±6.1	21.4±2.7**
BMI-SDS	3.3±0.3	-0.2±0.9***
FFM (Kg)	71.7±10.5	53.5±6.2**
FM (Kg)	45.8±11.3	14.9±4.6**
FM (% of BM)	38.7±2.9	21.5±3.6**

BM, Body mass; BMI-SDS: SD score of body mass index (BMI); FFM, Fat free mass; FM, Fat mass; TBW: Total Body Water. Values are expressed as mean±SD. *** = P<0.001; **=P<0.01

The main spirometry data are reported in **Table 3.2**. OB had slightly lower FVC and FEV_1 values compared with their age and sex matched controls. A 5% statistically significant difference in FEV_1/FVC observed between the two groups.

Table 3.2. Spirometry data of obese patients and control subjects.

	OB	CTRL
FVC, liters	5±0.7	5.6±1.1
FVC, % Predicted	107.1±10.7	108.4±19
FEV_1, liters	4.3±0.8	4.9±0.9
FEV_1, % Predicted	105.5±16.2	112.4±21.6
FEV_1/FVC, %	84.7±5.8	89.7±4.6*
$FEF_{25-75\%}$	4.6±1.3	5.4±1.2
$FEF_{25-75\%}$, % Predicted	102.7±28.3	94.3±19.5
PEF, liters/sec	8±1.3	8.3±2.4
PEF, % Predicted	95.8±6.5	100.1±23.4

FVC, forced vital capacity; FEV_1, forced expiratory volume in 1 second; $FEF_{25\%-75\%}$, forced expiratory flow between 25 % and 75 % of FVC; PEF, peak expiratory flow. Values are expressed as mean±SD. *=$P<0.05$

The peak values of the main investigated variables obtained during the incremental exercise are reported in **Table 3.3.** Peak values of work rate, HR, $\dot{V}_E$ and other ventilatory variables, $\dot{V}O_2$, were significantly different between these two groups. On the other hand, GET values, when described as percentage of peak work rate (72.1±6 [OB] vs. 71.9±9.9 [CTRL]) and percentage of $\dot{V}O_2$peak (73±6 [OB] vs. 76.3±7.3 [CTRL]) were not significantly different.

Table 3.3. Peak values of incremental exercise test.

	OB	CTRL
Exe. Duration, min	16.2±3.2	20.4±4.1*
HR, beats/min	170.6±9	189.1±4.5***
RPE_R (0-10)	6.3±3.1	8.3±2.1
RPE_L (0-10)	8±2.1	9.2±1
$\dot{V}O_2$, l/min	2.5±0.5	3±0.6*
$\dot{V}O_2$/kg, ml/min/kg	21.2±4	44.6±9.9***
$\dot{V}O_2$/FFM, ml/min/kg	35.1±17.2	57±12.5***
$\dot{V}CO_2$, l/min	2.6±0.6	3.3±0.7*
$\dot{V}E/VO_2$	32.5±4.4	38.7±6.8*
$\dot{V}E/VCO_2$	31.1±3.3	35.4±5.7
$\dot{V}E$, l/min	86.4±25.4	115.5±24.2*
R	1.04±0.05	1.09±0.04
$PETO_2$, mmHg	94.6±3.9	116.4±5.1***
$PETCO_2$, mmHg	34.2±3.4	33.4±5.7
fR, breaths/min	37.9±5.7	49.2±10.6**
VT, l/breath	2.3±0.5	2.4±0.4
WR_{peak}, watt	164±32.4	206±40.1*
SPO_2	97.4±1.6	96.3±2.1

fR, respiratory rate; HR, heart rate; $PETCO_2$, CO_2 end-tidal pressure; $PETO_2$, O_2 end tidal pressure; R, respiratory gas-exchange ratio; RPE_L, rate of perceived exertion for leg effort; RPE_R, rate of perceived exertion for respiratory discomfort; SPO_2, oxygen saturation; $\dot{V}_E$, pulmonary ventilation; $\dot{V}CO_2$, CO_2 output; $\dot{V}O_2$, O_2 uptake; V_T, tidal volume; WR_{peak}, peak work rate. Values are expressed as mean±SD. ***=P<0.001; **=P<0.01; *=P<0.05

The results of metabolic and ventilatory measurements for the OB and CTRL at the end of moderate (<GET) and heavy intensity (>GET) CWR exercise are shown in **Table 3.4.** During CWR<GET CTRL completed the 40 min exercise duration, whereas OB reached exhaustion before reaching 40 minutes.

Table 3.4. Metabolic and ventilatory measurements for the OB and CTRL at the end of moderate (<GET) and heavy intensity (>GET) CWR exercise in AIR.

	MODERATE INTENSITY		HEAVY INTENSITY	
	OB	CTRL	OB	CTRL
Exe. Duration, min	21.8±6.8	40±0***	6.8±2.5	9.8±4.2
Work rate, watt	97±23.3	116.8±23.9	142.5±30.5	176±33.4*
Work rate, %peak	58.7±5.3	57.1±7.6	86.6±3.2	85.7±4.7
HR, beats/min	146.9±13.4	163.2±15*	160.1±11.4	183.9±5.5***
HR, %peak	86.1±5	86.3±8	93.8±3	97.3±3.6*
RPE_R	4.1±3.3	4.8±3.5	4.5±3.1	8.1±1.8**
RPE_L	8.1±2.3	7.3±2.5	8.8±1.8	9.7±0.5
$\dot{V}O_2$, l/min	1.83±0.4	2.3±0.3*	2.3±0.5	3±0.5**
$\dot{V}O_2$, %peak	73.6±6.9	77±9.6	92.8±5.6	99.7±6.4*
$\dot{V}O_2$/kg, ml/min/kg	15.5±2.5	33.9±4.8***	19.6±3.3	44.5±8.3***
$\dot{V}CO_2$, l/min	1.68±0.4	2.02±0.26*	2.31±0.53	2.99±0.49**
Bf, 1/min	32.6±5	34.5±5.8	38.5±6	48.8±10.4*
$\dot{V}E$, l/min	55.3±17.2	63.4±7	78.2±23	111.3±18.7**
$\dot{V}E/VO_2$	27.8±4	27.8±3.2	31.6±4.4	37.5±6.1*
$\dot{V}E/VCO_2$	30.4±3.5	31.6±3.3	31.7±3.2	37.5±5.5**
R	0.91±0.05	0.88±0.03	0.99±0.05	1±0.05
$PETO_2$, mmHg	91.5±4	106±5.1***	94.9±3.9	114.7±3.7***
$PETCO_2$, mmHg	34.1±3.2	37.6±5.3	33.2±2.9	31.4±4.2

fR, respiratory rate; HR, heart rate; $PETCO_2$, CO_2 end-tidal pressure; $PETO_2$, O_2 end tidal pressure; R, respiratory gas-exchange ratio; RPE_L, rate of perceived exertion for leg effort; RPE_R, rate of perceived exertion for respiratory discomfort; $\dot{V}_E$, pulmonary ventilation; $\dot{V}CO_2$, CO_2 output; $\dot{V}O_2$, O_2 uptake; V_T, tidal volume. Values are expressed as mean±SD.

*** P<0.001; **P<0.01; *P<0.05 student t-test to detect the statistically significant differences between groups for each intensity.

Table 3.5 shows the end-exercise values of exercise time, HR and RPE during moderate- and heavy- intensity CWR for OB and CTRL in the two conditions (AIR vs AIR+HeO_2). In OB time to exhaustion was ~15% longer ($p<0.05$) in AIR+HeO_2 (1524 ± 480 sec) vs. AIR (1308 ± 408), whereas end-exercise heart rate (HR) was not significantly different (148 ± 16 vs. 147 ± 13 b min^{-1}) in the two conditions, despite the longer exercise duration in AIR+HeO_2. During

CWR>GET in OB time to exhaustion was ~40% longer ($p<0.05$) in AIR+HeO_2 (570 ± 306) vs. AIR (408 ± 150 s), also in this case HR was not significantly different from AIR. No significant difference was observed for time to exhaustion (582 ± 348 vs. 588 ± 252 s) and HR (183.9±5.5 vs. 182.8±5.6) in CTRL.

Table 3.5. End exercise values during constant work rate (CWR) exercise for Obese and CTRL subjects

	MODERATE INTENSITY			HEAVY INTENSITY			
	OBESE		CTRL	OBESE		CTRL	
	AIR	AIR+HELIOX	AIR	AIR	AIR+HELIOX	AIR	AIR+HELIOX
Exe. Duration, min	21.8±6.8	25.4±8*	40±0	6.8±2.5	9.5±5.1*	9.8±4.2	9.7±5.8
Work rate, watt	97±23.3	97±23.3	116.8±23.9	142.5±30.5	142.5±30.5	176±33.4	176±33.4
Work rate, %peak	58.7±5.3	58.7±5.3	57.1±7.6	86.6±3.2	86.6±3.2	85.7±4.7	85.7±4.7
HR, beats/min	146.9±13.4	148.2±15.5	163.2±15	160.1±11.4	165.4±12.2	183.9±5.5	182.8±5.6
HR, %peak	86.1±5	86.7±6.2	86.3±8	93.8±3	96.9±2.7	97.3±3.6	96.7±3.1
RPE_R	4.1±3.3	3.3±3.4	4.8±3.5	4.5±3.1	3.8±3.5	8.1±1.8	6.6±2.6*
RPE_L	8.1±2.3	6.4±2.9*	7.3±2.5	8.8±1.8	8±2.6	9.7±0.5	9.8±0.4

HR, heart rate; RPE_L, rate of perceived exertion for leg effort; RPE_R, rate of perceived exertion for respiratory discomfort. Values are expressed as mean±SD. *P<0.05 student t-test to detect the statistically significant differences between two conditions (AIR vs. AIR+HeO_2) for each group.

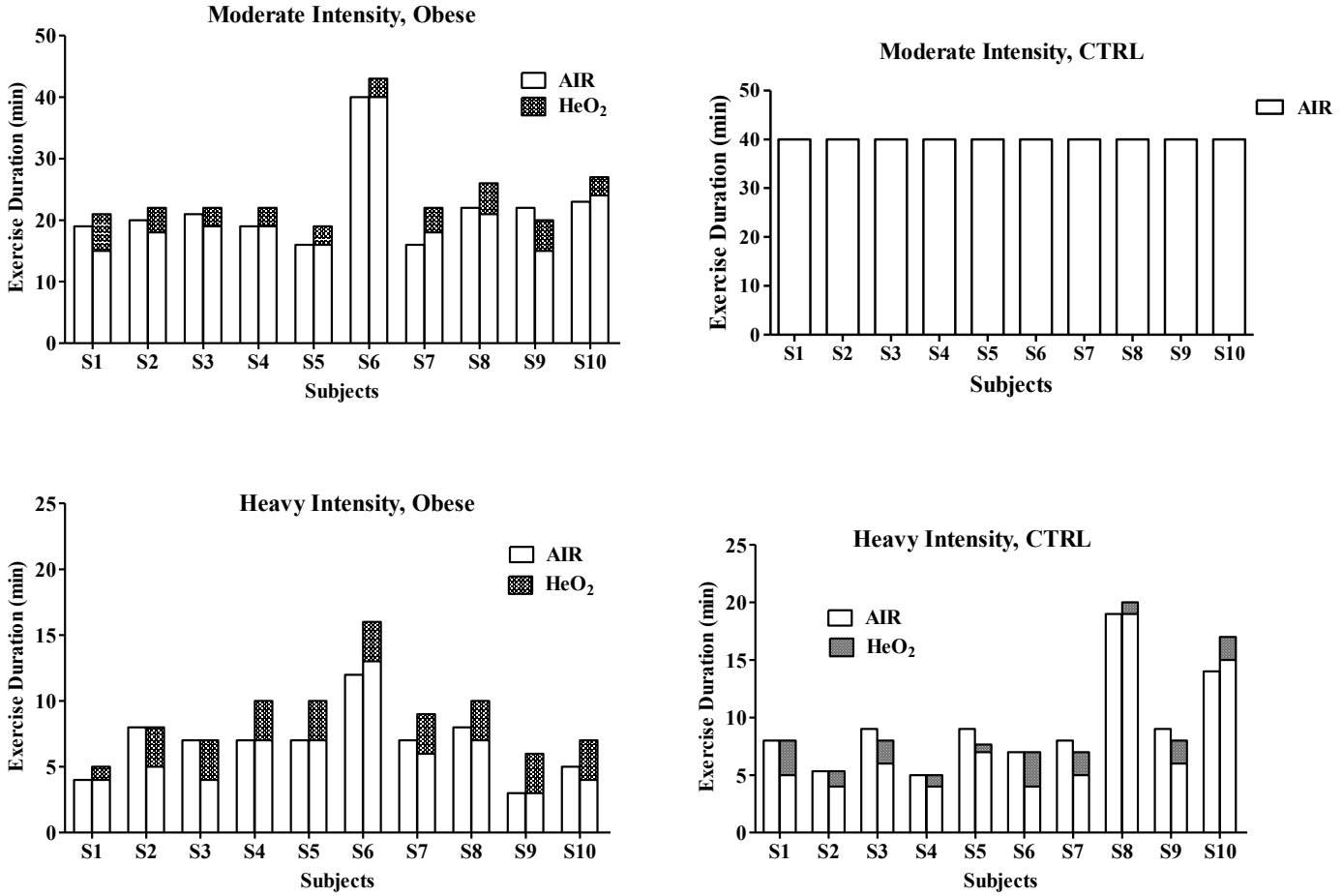

Figure 3.1. Exercise duration (min) for individual Obese patients (upper panels) and control subjects (lower panel). Figure showed that respiratory muscle unloading, obtained by switching the inspired gas from AIR to HeO_2, prolonged cycling duration in OB both during moderate- and heavy-intensity exercise but not in CTRL. Note that during CWR<GET all CTRL completed the 40 min exercise duration and thus no AIR+HeO_2 repetition was performed.

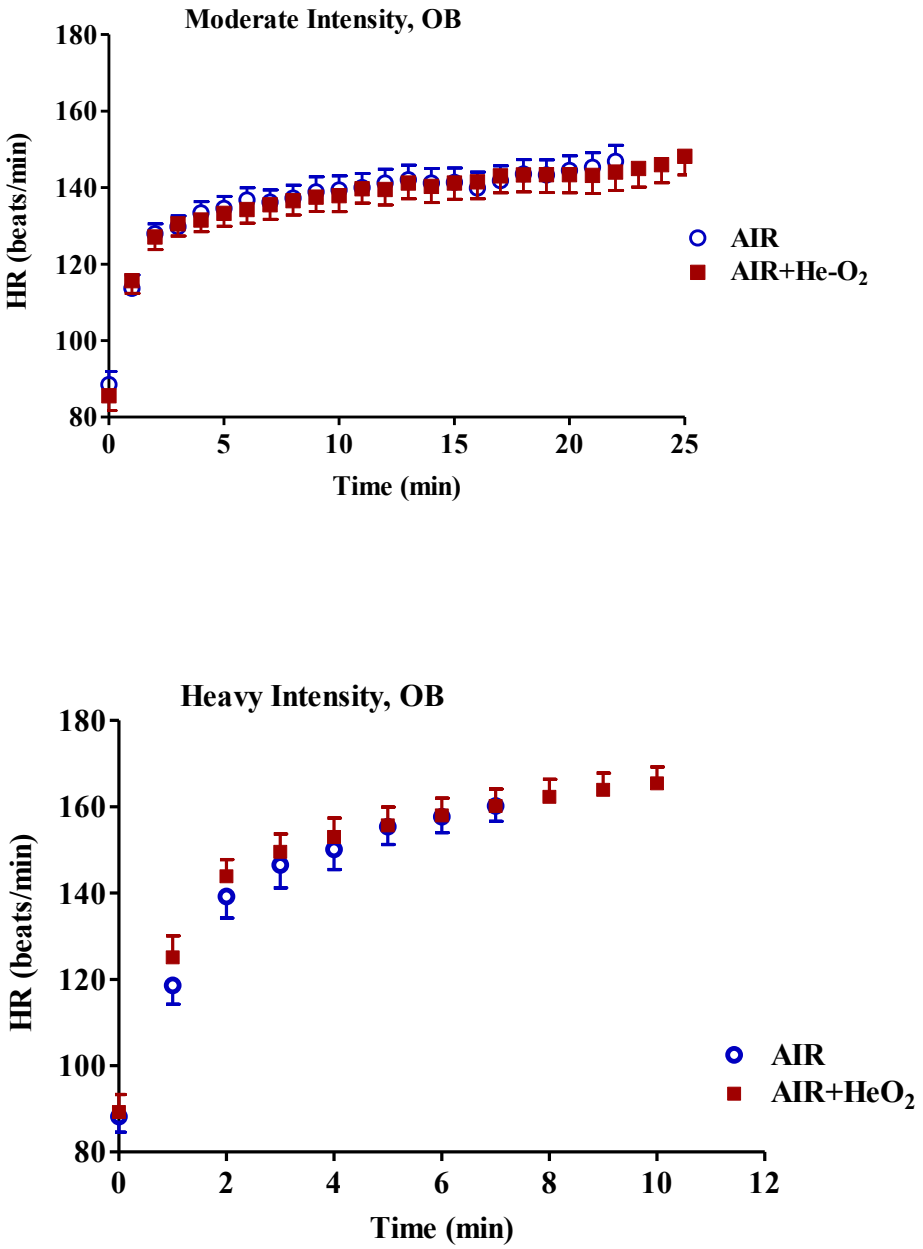

Figure 3.2. Mean ± SD HR values calculated every minute in OB during moderate intensity (upper panel) and heavy intensity (lower panel) CWR cycling from the start to voluntary exhaustion. The switch of the inspired gas from AIR to HeO_2 at exhaustion (AIR+HeO_2) prolonged exercise duration without altering the values and the pattern of HR.

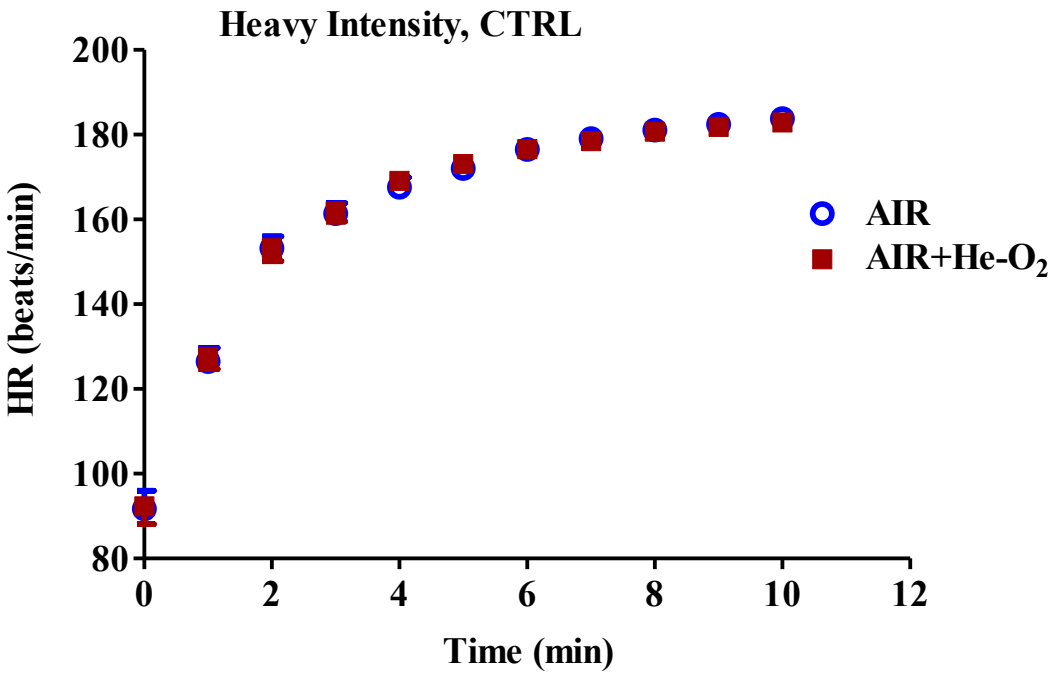

Figure 3.3. Mean ± SD HR values calculated every minute in CTRL from the start to voluntary exhaustion during heavy intensity CWR cycling. HeO_2 did not alter the exercise duration nor the HR values measured during the exercise.

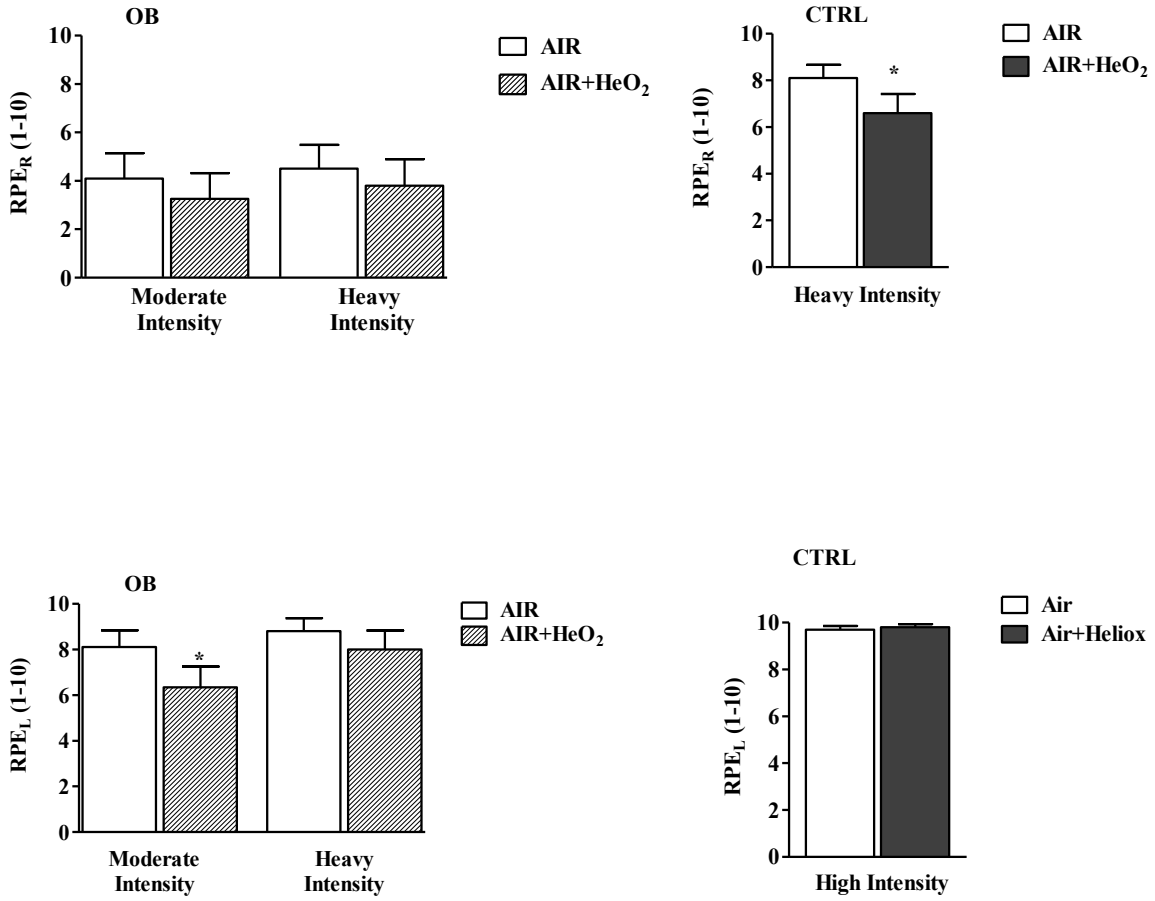

Figure 3.4. Rate of perceived exertion (Borg's modified CR10 scale) at exhaustion for respiratory fatigue (RPE_R; upper panels) and leg effort (RPE_L; lower panels) in OB (during moderate and heavy intensity CWR) and CTRL (during heavy intensity CWR).

* $p<0.05$ t-test between AIR and AIR+HeO_2

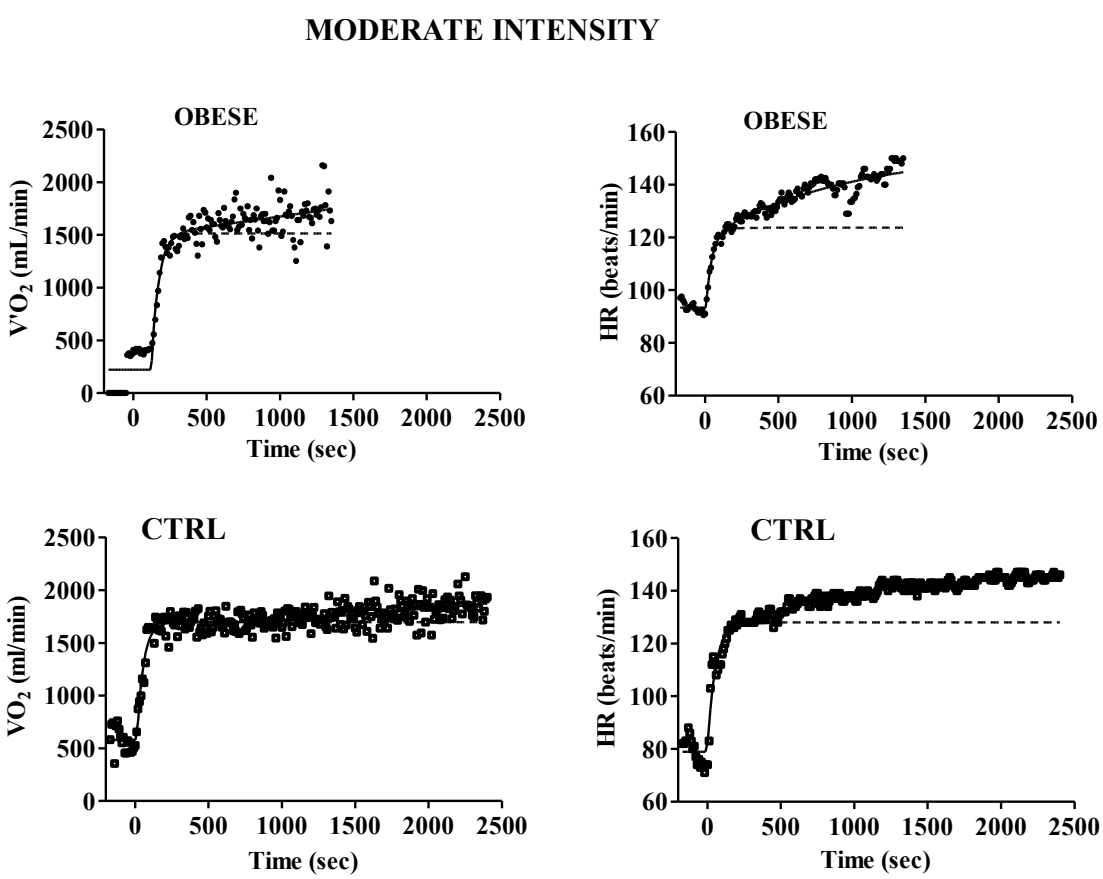

Figure 3.5. Pulmonary O_2 uptake ($\dot{V}O_2$) and heart rate (HR) kinetics for representative OB (upper panels) and CTRL (lower panels) subjects during moderate intensity CWR exercise.

We can note that the relative amplitude of the HR slow component (HR_{SC}) was greater than the relative amplitude of the $\dot{V}O_2$ slow component ($\dot{V}O_{2SC}$) in both groups of subjects (see figure 3.5). During moderate intensity CWR exercise in OB the mean amplitude of $\dot{V}O_{2SC}$ (expressed in % of the amplitude of the overall response) was 9% while the mean amplitude of HR_{SC} was 28%. Similarly, in CTRL the mean amplitude of $\dot{V}O_{2SC}$ was 12% and the mean amplitude of HR_{SC} was 33%.

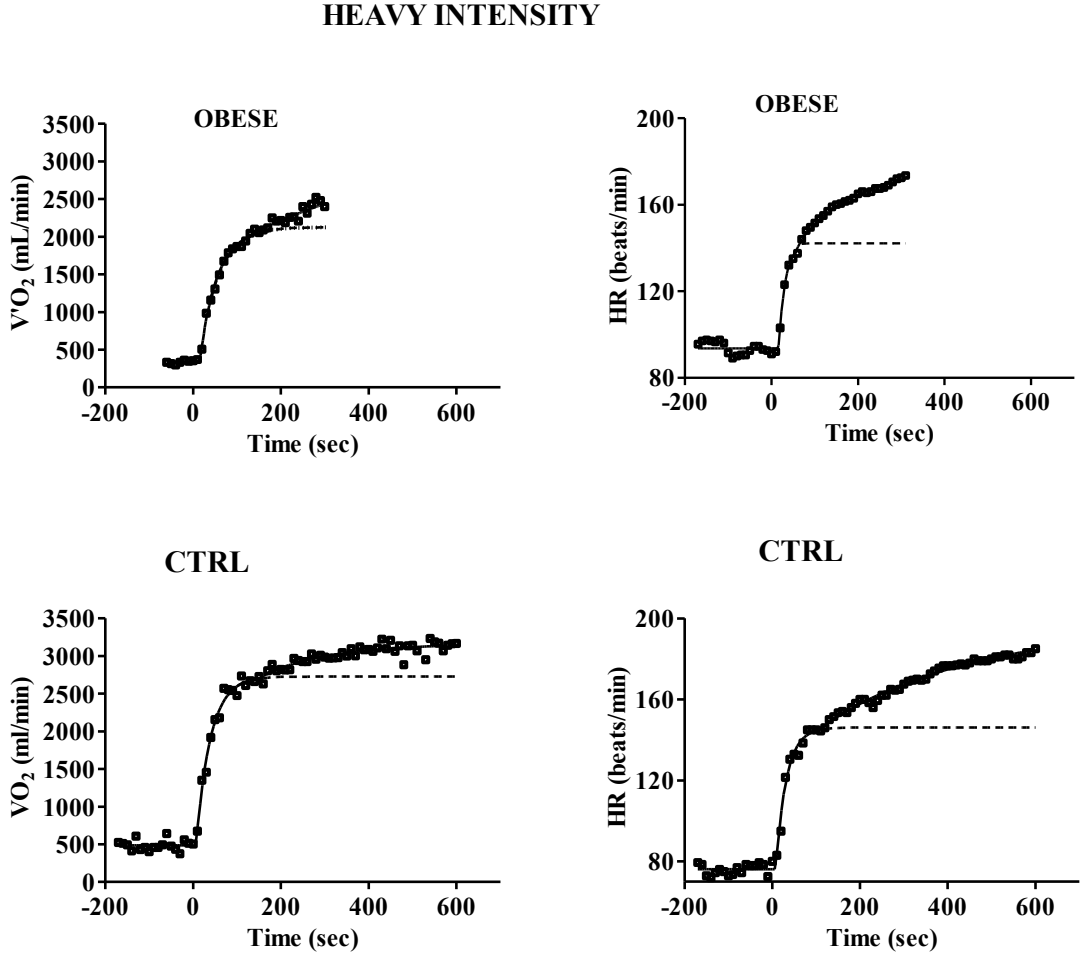

Figure 3.6. Pulmonary O_2 uptake ($\dot{V}O_2$) and heart rate (HR) kinetics for representative OB (upper panels) and CTRL (lower panels) subjects during heavy intensity CWR exercise.

Also, at heavy intensity we can note that the mean amplitude of HR_{SC} is greater than the mean amplitude of $\dot{V}O_{2SC}$ in either group of subjects. In OB $\dot{V}O_{2SC}$ (expressed in % of the total $\dot{V}O_2$ response) was on average 6% and HR_{SC} on average 26%. Similarly, in CTRL the amplitude of $\dot{V}O_{2SC}$ was 10% and the amplitude of HR_{SC} was 28%.

DISCUSSION

In the present study, we demonstrated that in CTRL, acute unloading of the respiratory muscles by switching the inspired gas from AIR to normoxic HeO_2 minimally affected exercise tolerance. In contrast, in OB there was a significant increase in exercise tolerance during both

CWR < GET or >GET. Prior investigators have examined exercise performance of healthy subjects or patients while breathing a normoxic helium mixture. Mancini et al (66) observed that in patients with heart failure the metabolic cost of breathing affected exercise performance. During exercise performed while breathing normoxic helium mixture, during which the work of breathing is reduced, patients could delay the exhaustion (66). Some other investigators demonstrated an increase in exercise ventilation and peak $\dot{V}O_2$ in young healthy subjects (10), whereas others did not find any improvement in exercise performance (3). In a previous study by our group (88) acute respiratory muscle unloading via normoxic helium–O_2 breathing was applied to a group of obese adolescents. In this study OB performed, on a cycle ergometer, an incremental exercise, 12 min CWR exercises at 70 % of GET (<GET) and 120 % of GET (>GET) breathing either AIR or a 21% O_2–79% helium mixture (HeO_2). $\dot{V}O_2$ peak was not different in the two conditions. From the 3rd to the 12th minute of exercise (both during CWR < GET and CWR > GET), $\dot{V}O_2$ was lower in HeO_2 vs. AIR. During CWR > GET in AIR, $\dot{V}O_2$ linearly increased from the 3rd to the 12th minute of exercise, whereas no substantial increase was observed in HeO_2. The O_2 cost of cycling was ~10 % (<GET) and ~15 % (>GET) lower in HeO_2 vs. AIR. Heart rate and ratings of perceived exertion for dyspnea/respiratory discomfort (RPE_R) and leg effort (RPE_L) were lower in HeO_2.

In the present study, participants performed CWR exercises of longer duration (40 min or voluntary exhaustion instead of 12 min), and respiratory muscles were acutely unloaded by switching the inspired gas from AIR to normoxic HeO_2 when participants faced exhaustion. All CTRL subjects were able to complete the 40min moderate- intensity task, therefore no switch to HeO_2 was applied. In the same CTRL subjects, the unloading of the respiratory muscles by switching the inspired gas from AIR to a normoxic HeO_2 did not affect exercise performance during heavy intensity cycling (see figure 3.1). These findings would support the central-cardiovascular limitation to exercise in healthy CTRL subjects (figure 3.3). In contrast, in OB there was a significant increase in exercise duration during AIR+HeO_2 breathing either in CWR < GET (by ~ 3min) and >GET (by ~ 3min) despite minimal changes in peak HR (see Figure 3.2). Therefore, in OB, pulmonary factors appear to contribute to reduce exercise tolerance in either moderate or heavy intensity CWR exercises. At the end of heavy intensity exercise CTRL perceived less exertion for RPE_R in AIR+HeO_2 than AIR, but their perception for RPE_L was the same in the two conditions (see figure 3.4). So most likely this group of subjects ceased pedaling because of leg fatigue, in other words lower limb locomotor muscles were not

benefited from respiratory muscle unloading. In OB even though the exercise duration was longer in AIR+HeO_2 at both intensities the scores of RPE_R in the two conditions (in AIR and AIR+HeO_2) were not statistically significantly different. RPE_L scores were significantly lower in AIR+HeO_2 vs. AIR during moderate intensity exercise (figure 3.4).

The possible explanations for the generally improved exercise tolerance achieved by AIR+HeO_2 in obese patients could involve complex interactions between respiratory and locomotor muscles in relation to O_2 delivery. Previous investigations demonstrated that altering the work of breathing (WOB) during near-maximal whole-body exercise influences both respiratory and quadriceps muscle blood flow (22). According to this finding, when the WOB decreased (via proportional assist ventilator), respiratory muscle blood flow decreased, while quadriceps blood flow increased. Conversely, when the WOB was increased (via resistors), respiratory muscle blood flow increased, while quadriceps blood flow decreased. Collectively, these findings supported the notion of a competitive relationship between the respiratory and quadriceps muscles for blood flow during intense exercise. When the respiratory demand for blood flow is reduced, additional blood can be directed towards active musculature, meaning that the high respiratory muscle work, normally incurred during heavy and maximal exercises, can attenuate blood flow to the locomotor muscles.

In this demanding condition a respiratory muscle unloading could prevent respiratory muscle fatigue and the reflex vasoconstriction within the active locomotor muscles and can ultimately preserve limb blood flow (5, 15, 42, 83). Although in normal subjects, this phenomenon may not happen during submaximal exercise (104), it could occur in obese patient population characterized by a substantially higher work of breathing and increased metabolic demand. Other study by Harms et al (44) demonstrated a significant effect of respiratory muscle unloading on stroke volume (SV) and cardiac output (CO) during maximal exercise in the healthy, trained human. The authors found that a reduction of the WOB by a proportional-assist ventilation during maximal exercise caused a significant decrease of $\dot{V}O_2$ and CO, due primarily to reduced SV, whereas increasing the WOB during maximal exercise had no effect on CO or $\dot{V}O_2$. In the present study, peak HR measured in OB at the end of both CWR exercises in the two conditions (AIR and AIR+HeO_2) was not statistically different although the exercise duration was extended by ∼3min in AIR+HeO_2 in either intensity. Our findings support the concept of blood flow redistribution between respiratory and locomotor muscles

during respiratory muscle unloading. When the inspired gas switched from AIR to normoxic HeO_2 there may no change in CO but patient extended pedaling for 3 more minutes most likely because of blood flow redistribution which resulted from delayed respiratory muscle fatigue and the reflex vasoconstriction within active locomotor muscles and increased limb blood flow as described above (5, 15, 42, 83). Indeed, previous studies in COPD patients (62, 100) demonstrated a reduced expiratory muscle activity during HeO_2 breathing, with consequent improvements in CO and "central" hemodynamics and further increases in peripheral muscle O_2 delivery.

Improvements in locomotor muscle O_2 delivery would delay/reduce the development of peripheral muscle fatigue (45, 83), preserve the metabolic stability in these muscles (109), prevent the recruitment of additional muscle fibers (83) and the loss of muscle efficiency (16), thereby explaining the increased exercise duration and improved exercise tolerance in AIR+HeO_2.

The main result of our kinetics analysis was that the amplitude of the slow component of HR kinetics was much greater than the amplitude of the slow component of $\dot{V}O_2$ kinetics during either moderate or heavy intensity CWR exercises in both groups of subjects. The results of this study are in agreement with a recent study by Zuccarelli *et al* (110) that indicated the ''slow component'' of the HR kinetics occurs at a lower work rate than the slow component of the $\dot{V}O_2$ kinetics and that, at the same absolute work rate, the relative amplitude of the HR slow component is greater than the relative amplitude of the $\dot{V}O_2$ slow component.

CONCLUSIONS

In OB, the O_2 cost of breathing affects exercise performance. We found that with an acute unloading of the respiratory muscles obtained by switching the inspired gas from AIR to normoxic HeO_2 as patients faced fatigue OB could prolong the duration of exercise during both moderate and heavy intensity CWR exercises. This improvement was not observed in CTRL. Thus, in these patients respiratory limitations can impair exercise tolerance also during moderate- intensity daily-living activities. Most likely, with a reduced work of breathing, more blood flow may be distributed to the active limb muscles and more work can be performed at

the same oxygen cost. These findings would confirm the need for implementing therapeutic approaches specifically aimed to improve strength and endurance of respiratory muscles and subsequently to enhance exercise tolerance in these patients.

Findings obtained from the analyses of HR and $\dot{V}O_2$ patterns should also be taken into account in the exercise prescription. The data suggest that the ‘‘translation’’ of work rates, or of percentages of $\dot{V}O_2$peak associated with variables such as the GET or critical power, into HR values is not straightforward. Because of the occurrence of a HR drift throughout the exercise, even at low intensities, exercises performed at target HR values, when carried out for periods longer than a few minutes, could lead to premature fatigue and to exercise termination. Further studies are needed to clarify this critical issue and better understand the mechanistic bases of these phenomena.

CHAPTER 4: RESPIRATORY MUSCLE UNLOADING BY NORMOXIC HELIUM-O_2 BREATHING DURING HIGH INTENSITY TREADMILL WALKING REDUCES HEART RATE AND IMPROVES EXERCISE TOLERANCE IN OBESE ADOLESCENTS

INTRODUCTION

Overweight and obese subjects often perceive increased breathlessness during minor exertion and therefore avoid exercise (31). In these patients, pulmonary factors, including respiratory muscle work and airflow resistances may contribute to limit exercise performance and affect exercise tolerance (66). Substituting the low density gas helium for nitrogen in the inhaled gas lowers the density of breathed air by 39% and its kinematic viscosity by 35% (101). The reduced turbulence resulting from the low-density gas inhalation would allow higher flow with unchanged ventilatory drive. This effect is evident in the rapid and abrupt increase of $\dot{V}E$ during heavy intensity steady-state work rate observed after switching to normoxic helium breathing (101).

Concerning the effects of loaded and unloaded breathing on ventilatory responses and exercise capacity, studies have produced varied results. It is known that an increase or decrease in gas mixtures density does not significantly affect the respiratory system at rest (21, 101), but during exercise this factor may be essential, since the dependence of the non-elastic resistance from density gas mixtures increases with the rise of respiratory flow rates in accordance with Rohrer's equation (90). In a previous study by our group (88) respiratory muscle unloading via normoxic HeO_2 breathing determined in a group of OB lower O_2 cost of exercise and perceived exertion during moderate- and heavy-intensity short-duration exercises on a cycle ergometer. Correspondingly, we demonstrated that in OB, acute unloading of the respiratory muscles by switching the inspired gas from AIR to a normoxic HeO_2 when the subjects were facing exhaustion significantly increased exercise tolerance in either moderate- (CWR < GET) or heavy- (CWR > GET) cycling. The purpose of the present study was then to determine whether, in OB, respiratory muscle unloading can indeed extend the duration of exercise during heavy intensity treadmill walking. We hypothesize that the effects of the respiratory muscle unloading on exercise tolerance would be more pronounced during walking compared to cycling because

the mechanical pattern of walking entails the cyclical elevation and acceleration of body center of mass at every step, treadmill exercise is a relatively costly type of locomotion when compared to cycling (51). Respiratory muscle unloading was induced by using normoxic HeO_2 breathing gas mixtures.

METHODS

Subjects

Eight male obese patients (age 17±2.9 years; Tanner stage 4-5; body mass 120.4±18.7, height 1.8±0.1m; BMI 39.5±6.1kg/m^2), hospitalized for a multidisciplinary body mass reduction program, were admitted to the study.

Participants/Participants' parents provided signed consent statements, after being fully advised about the purposes and testing procedures of the investigation, which were approved by the ethics committee of the Italian Institute for Auxology, Milan, Italy. All procedures were in accordance with the recommendations set forth in the Helsinki Declaration (2000).
Body mass index (BMI) was calculated as body mass divided by height^2, expressed in (kg m^{-2}). Body composition was determined by bioelectrical impedance (Human-IM Scan, DS-Medigroup, Milan, Italy). Fat mass (FM) and fat free mass (FFM) were expressed as kg and as a percentage of body mass
Inclusion criteria were: 1) BMI > 97th percentile for age and sex, using Italian growth charts (12); 2) no involvement in structured physical activity programs (regular activity more than 120 min $week^{-1}$) during the 8 months preceding the study; 3) absence of signs or symptoms of diabetes or of any major cardiovascular, respiratory or orthopedic disease contraindicating or significantly interfering with the tests.

Spirometry

Patients performed standard spirometry tests (forced vital capacity, FVC; forced expiratory volume in 1 second, FEV_1; FEV_1/FVC; forced expiratory flow between 25% and 75% of FVC, $FEF_{25-75\%}$; maximal forced expiratory flow, FEF_{max}) by utilizing a metabolic cart (MedGraphics CPX/D, Medical Graphics Corp., USA). Pulmonary function testing was performed according

to the guidelines of the American Thoracic Society (69). Predicted values were based on Hankinson *et al*. (40).

Exercise protocol

Exercise tests were conducted during 3 consecutive days under medical supervision; during the tests the subjects were continuously monitored by 12-lead electrocardiography (ECG). A mechanically braked treadmill (TecnoGym, Italy) was utilized. Patients were allowed time to gain familiarity with the researchers and the experimental set-up, were carefully instructed about the procedures and were familiarized with the protocol using short practice walks. Patients were asked to avoid intensive exercise for 24 hours and to refrain from food and caffeine for at least 2 hours before the tests. During the first day the subjects performed an incremental exercise test. After 3minute of resting measurement (subjects in standing position on the treadmill) the incremental exercise began, and the patients walked on the treadmill (0% slope) for 2 minutes at 4 km h^{-1}. The velocity was then increased by 0.5 km h^{-1} every minute till 6 km h^{-1}. Once the patient walked at a velocity of 6 km h^{-1} for a minute, the slope was set at 3%; thereafter the slope was increased by 1% every minute. When the slope reached 15% the velocity was increased to 6.5 km h^{-1} till the subjects reached voluntary exhaustion, defined as the inability to maintain the imposed speed and slope despite vigorous encouragement by the researchers. During the tests the patients could not hold on the handlebars of the treadmill. For all variables (see below), mean values calculated over the last 20-30 seconds of the incremental exercise before reaching voluntary exhaustion were considered “peak” values.

During the second and third days, two bouts of CWR exercise in AIR or HeO_2 at ~120% of the GET were carried out till voluntary exhaustion. The sequence of conditions (AIR and HeO_2) was randomized. Resting $\dot{V}O_2$ (subjects in standing position on the treadmill) was measured before the CWR exercise began.

Measurements

Heart rate (HR) was determined by ECG. GET was determined by the V-slope method (7). Ratings of perceived exertion (RPE) for respiratory discomfort (RPE_R) and limb effort (RPE_L) were obtained at rest and every minute during exercise by using the Borg's modified CR10 scale (106). $\dot{V}_E$, tidal volume (V_T), fR, O_2 uptake ($\dot{V}O_2$) and CO_2 output ($\dot{V}CO_2$) were determined on a breath-by-breath basis by means of a metabolic unit in AIR (MedGraphics CPX/D, Medical Graphics Corp., USA). Calibration of O_2 and CO_2 analyzers was performed before each experiment by utilizing gas mixtures of known composition. Expiratory flow measurements were performed by a bidirectional pressure differential pneumotachograph, which was calibrated by a 3-liter syringe at varying flow rates. The respiratory gas-exchange ratio (R) was calculated as $\dot{V}CO_2/\dot{V}O_2$. HR, RPE_R, RPE_L and SPO_2 in iso-time between the two conditions (AIR Vs HeO_2) were compared.

Statistical analysis

Results were expressed as mean ± standard deviation (SD). Statistical significance of differences between two conditions (HeO_2 Vs AIR) was checked by two-tailed Student's t test for paired data. The level of significance was set at $P < 0.05$. Statistical analyses were carried out with a commercially available software package (Prism 5.0, GraphPad).

RESULTS

The main anthropometric data are reported in **Table 1**.

Table 4.1. Age and anthropometric characteristics of the patients.

N	8
Age (years)	17±2.9
Body Mass (kg)	120.4±18.7
Height (m)	1.8±0.1
BMI (Kg/m^2)	39.5±6.1
FFM (Kg)	69.2±9.7
FFM (%)	57.6±2.6
FAT (Kg)	51.2±9.8
FAT (%)	42.4±2.6

The main spirometry data are reported in **Table 4.2**. As the % predicted values are in normal range (96) no restrictive or obstructive alterations were observed in the patients.

Table 4.2. Spirometry data of patients.

N	8
FVC, liters	4.7±0.8
FVC, % Predicted	97.8±15.1
FEV_1, liters	4.3±0.7
FEV_1, % Predicted	104.8±17.7
FEV_1/FVC, %	0.9±0.1
$FEF_{25-75\%}$	5±1.4
$FEF_{25-75\%}$, % Predicted	111.3±36.7
PEF, liters/sec	8±2
PEF, % Predicted	93±24.1

FVC, forced vital capacity; FEV_1, forced expiratory volume in 1 second; $FEF_{25\%-75\%}$, forced expiratory flow between 25 % and 75 % of FVC; PEF, peak expiratory flow. Values are expressed as mean±SD.

Mean ± SD values of the investigated variables determined at exhaustion during the incremental (peak values) and CWR tests in AIR are presented in **Table 4.3**.

Table 4.3 Values of the main investigated variables determined at exhaustion during the incremental exercise (peak values), and CWR (120% of GET) exercise in AIR.

	Incremental	CWR
N	8	8
Exe. Duration, min	12.5±3.5	14.3±6.7
HR, beats/min	173.6±11	166.5±5.6
RPE_R (0-10)	7.8±1.7	4.9±3
RPE_L (0-10)	7.4±2.4	6.7±3.4
SPO_2	93.2±2.4	95.8±1.7
$\dot{V}O_2$, l/min	2.4±0.8	2.4±0.5
$\dot{V}O_2$/kg, ml/min/kg	19.6±4.8	19.5±2.4
$\dot{V}O_2$/FFM, ml/min/kg	34.9±8	34.9±4
$\dot{V}CO_2$, l/min	2.5±0.7	2.4±0.5
$\dot{V}E/\dot{V}O_2$	31.7±4.1	32.6±3.5
$\dot{V}E/\dot{V}CO_2$	30.2±2.6	33±1.7
$\dot{V}_E$, l/min	79.9±16	83.9±16.9
fR, breaths/min	41.1±7.8	44.8±11.2
$\dot{V}_T$, l/breath	2±0.6	1.9±0.4
R	1.05±0.07	0.99±0.06
$PETO_2$, mmHg	94±4.6	95.2±3.5
$PETCO_2$, mmHg	34±4.6	31.7±2.1
Velocity (km/hr)	6±0	6±0
Slope (%)	8.4±3.6	6.4±2.6

fR, respiratory rate; HR, heart rate; $PETCO_2$, CO_2 end-tidal pressure; $PETO_2$, O_2 end tidal pressure; R, respiratory gas-exchange ratio; RPE_L, rate of perceived exertion for leg effort; RPE_R, rate of perceived exertion for respiratory discomfort; SPO_2, arterial blood oxygen saturation; $\dot{V}_E$, pulmonary ventilation; $\dot{V}CO_2$, CO_2 output; $\dot{V}O_2$, O_2 uptake; V_T, tidal volume; WR_{peak}, peak work rate. Values are expressed as mean±SD.

Comparison of HR, SPO_2 and RPE_R and RPE_L determined during CWR test in the two conditions (AIR Vs HeO_2) at iso time (the highest equivalent exercise time achieved during CWR tests in AIR [14.25 min]) is presented in **Table 4.4.** As shown in the table HR was

significantly less when patients inspired HeO_2 than AIR. SPO_2 was significantly greater when patients inspired HeO_2 than AIR. Although not statistically significant patients scored less for RPE_R and RPE_L in HeO_2 than AIR.

Table 4.4. Heart rate, arterial blood oxygen saturation by pulse oximetry (SpO_2) and rate of perceived exertion (for respiratory fatigue, RPE_R and leg effort, RPE_L) at iso time in the two conditions (AIR Vs HeO_2).

	HR		SPO_2		RPE_R		RPE_L	
SUBJECT	AIR	HeO_2	AIR	HeO_2	AIR	HeO_2	AIR	HeO_2
1	161	154	96	98	3	4	10	10
2	163	167	98	99	3	0	4	2
3	167	162	97	97	6	5	6	5
4	160	142	97	97	10	10	10	10
5	168	165	96	97	4	4	5	4
6	169	160	93	96	0.5	1	0.5	1
7	178	176	95	96	8	2	9	8
8	166	157	94	98	5	5	9	5
MEAN	166.5	160.4*	95.8	97.3*	4.9	3.9	6.7	5.6
SD	5.7	10.0	1.7	1.0	3.0	3.1	3.4	3.4

*$P<0.05$ student t-test to detect the statistically significant differences between two conditions (AIR vs. HeO_2) for each variable.

Exercise duration for each patient during CWR test in the two conditions (AIR and HeO_2) is shown in **figure 4.1**. Time to exhaustion was longer ($p=0.01$) in HeO_2 (983±370) vs. AIR (855±399 sec), whereas end exercise heart rate was not different ($p=0.11$) in HeO_2 (162 ± 10) vs. AIR (167 ± 6 b min^{-1}), which are 96 and 94 % of the peak HR respectively (see **figure 4.2**), despite the longer exercise duration in HeO_2.

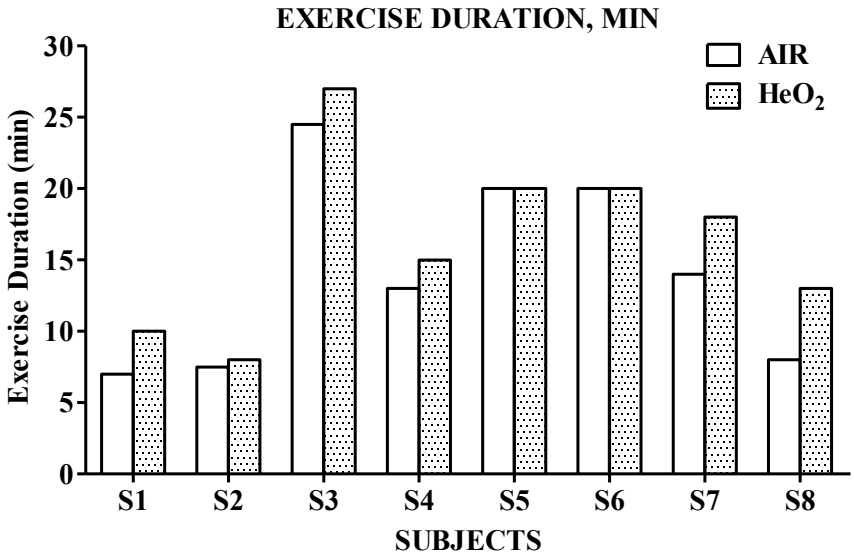

Figure 4.1. Exercise duration (min) for individual patients during CWR test with AIR and HeO_2. Figure showed respiratory muscle unloading obtained by breathing normoxic HeO_2, prolonged the duration of walking.

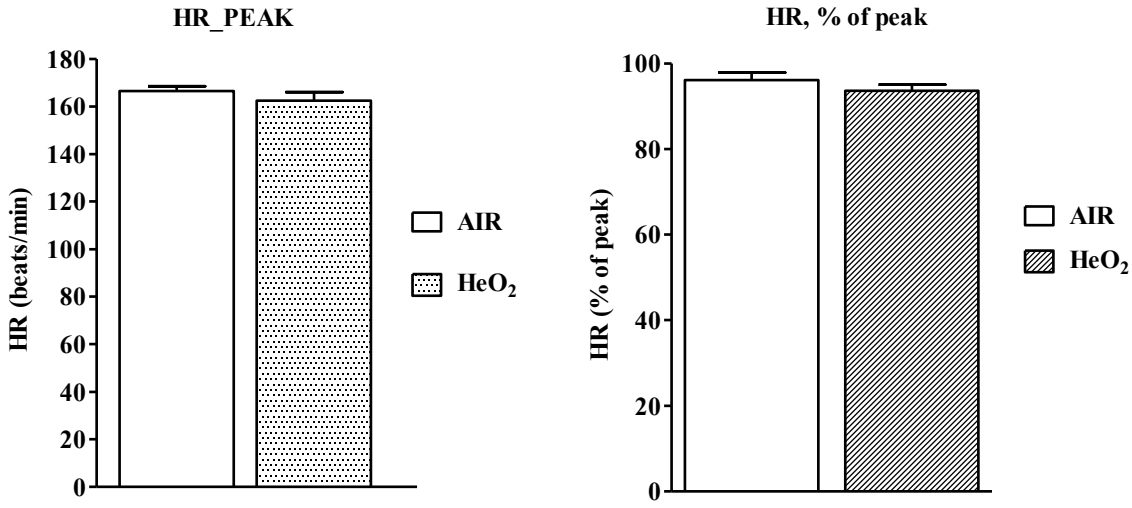

Figure 4.2. Mean ± SD of HR value calculated at exhaustion during CWR test in the two conditions, AIR vs. HeO_2 (left panel) and % of the peak HR proportionated to HR measured during incremental tests (right panel). End exercise heart rate was not different in AIR vs. HeO_2, being 96 and 94 % of the peak HR respectively.

DISCUSSION

These data support the concept that, in obese adolescents, a respiratory muscle unloading, obtained by breathing a normoxic HeO_2 gas mixture, results in an increase of exercise tolerance during heavy intensity walking. Indeed, 6 out of 8 patients walked longer while breathing HeO_2, and 5 out of 8 patients increased the duration of exercise by more than 2 minutes. Despite the longer exercise duration, end-exercise HR was not significantly different in HeO_2 compared to AIR. These findings suggest that in OB the respiratory system may limit exercise tolerance. At iso-time during exercise in HeO_2 (Table 4.4), HR was significantly lower ($P = 0.03$) compared to AIR. Textbook physiology states that, for the same work rate, a lower HR is a sign of increased exercise tolerance. Similarly, at the 14.25 min of exercise SpO_2 was higher ($P = 0.04$) in HeO_2 compared to AIR (Table 4.4). This may be interpreted as an indication of increased systemic oxygen delivery with HeO_2 compared with AIR. This improved SPO_2 can be explained in two ways: firstly, breathing HeO_2 may reduce the work and the O_2 cost of the respiratory muscle. A similar finding was reported by Mancini *et al* (66) in patients with heart failure. In these patients breathing normoxic HeO_2 decreased accessory respiratory muscle fractional oxygen extraction. Secondly, we cannot rule out that the improvement in O_2 delivery with HeO_2 may have selectively decreased the activation of less efficient type II fibers and reduced the O_2 cost of walking (44). In the current study, at iso-time there was also a tendency for RPE_R and RPE_L to be lower in HeO_2, thus suggesting that the occurrence of respiratory and limb muscle fatigue may be delayed once the respiratory load is reduced.

In conclusion these data may provide indication that strategies aimed to reduce the mechanical burden of breathing in obese patients can improve peripheral O_2 delivery and utilization during heavy intensity exercise and this should lead to an improved exercise capacity in this patient population.

CHAPTER 5: RECOMMENDATION AND FUTURE PERSPECTIVES

The major findings of my PhD research project have emphasized the importance of the respiratory system in determining exercise tolerance and performance in obese adolescents. Obesity is usually associated with a reduced exercise tolerance which impede increase of physical activity which in turn represents one of the cornerstones for the treatment of the disease. In order to interrupt this vicious circle, we followed two approaches, attempting to relieve the respiratory limitation in obese adolescents performing cycling and walking exercises. In the first approach, respiratory muscles were unloaded by breathing normoxic-HeO_2. This unloading lowered the O_2 cost of exercise and perceived exertion, and ultimately increased the duration of exercise performed at moderate and heavy- intensities, either cycling or walking exercises. In the second approach, a standardized program of RMET was superimposed on a standard multidisciplinary body mass reduction program; RMET decreased the O_2 cost of exercise and the perceived exertion, which represent clear signs of improved exercise tolerance. Since a short period of training (3 weeks) was utilized in the present study, more prolonged periods will have to be tested. In this respect, RMET offers the advantages of the relatively low cost of the instrumentation, and the fact that the procedure is simple and can be easily utilized, after some training, by the patient itself, making home-based training feasible. The effects observed after prolonged training could be more pronounced than those described in the present study.

In the future, we propose to measure, in a similar population of obese patients, the work of breathing and the consequent oxygen consumption of the respiratory muscles during rest, exercise of different intensities and isocapnic hyperpnea, and to detect its specific contribution in determining exercise performance and tolerance.

Moreover, we recommend further studies towards strategies that aim to reduce the mechanical burden of breathing in obese patients.

REFERENCES

1. **Amann M**, **Blain GM**, **Proctor LT**, **Sebranek JJ**, **Pegelow DF**, **Dempsey JA**. Group III and IV muscle afferents contribute to ventilatory and cardiovascular response to rhythmic exercise in humans. *J Appl Physiol* 109: 966–976, 2010.

2. **Ansley L**, **Petersen D**, **Thomas A**, **St Clair Gibson A**, **Robson-Ansley P**, **Noakes TD**. The effect of breathing an ambient low-density, hyperoxic gas on the perceived effort of breathing and maximal performance of exercise in well-trained athletes. *Br J Sports Med* 41: 2–7, 2007.

3. **BABB TG**. Breathing He-O_2 Increases Ventilation but Does Not Decrease the Work of Breathing during Exercise. *Am J Respir Crit Care Med* 163: 1128–1134, 2001.

4. **Babb TG**, **Wyrick BL**, **DeLorey DS**, **Chase PJ**, **Feng MY**. Fat distribution and end-expiratory lung volume in lean and obese men and women. *Chest* 134: 704–711, 2008.

5. **Babcock MA**, **Pegelow DF**, **Harms CA**, **Dempsey JA**. Effects of respiratory muscle unloading on exercise-induced diaphragm fatigue. *J Appl Physiol* 93: 201–206, 2002.

6. **Banner M**. Respiratory Muscle Loading and The Work of Breathing. *J Cardtothoracic Vasc Anesth* 9: 192–204, 1995.

7. **Beaver WL**, **Wasserman K**, **Whipp BJ**. A new method for detecting anaerobic threshold by gas exchange. *J Appl Physiol* 60: 2020–2027, 1986.

8. **Bernardi E**, **Melloni E**, **Mandolesi G**, **Uliari S**, **Grazzi G**, **Cogo A**. Respiratory Muscle Endurance Training Improves Breathing Pattern in Triathletes. *Ann Sport Med Res* 1: 1–7, 2014.

9. **Brazzale DAJ**, **Pretto JEJ**, **Schachter LIM**. Optimizing respiratory function assessments to elucidate the impact of obesity on respiratory health. *Respirology* 20: 715–721, 2015.

10. **Brice AG**, **Welch HG**. Metabolic and cardiorespiratory responses to He-O_2 breathing during exercise [Online]. *JApplPhysiol* 54: 387–392, 1983. pm:6833035.

11. **Burwell CS**, **Robin ED**, **Whaley RD**, **Bickelmann AG**. Extreme obesity associated

with alveolar hypoventilation - A Pickwickian Syndrome. *Am J Med* 21: 811–818, 1956.

12. **Cacciari E**, **Milani S**, **Balsamo A**, **Spada E**, **Bona G**, **Cavallo L**, **Cerutti F**, **Gargantini L**, **Greggio N**, **Tonini G**, **Cicognani A**. Italian Cross Sectional Growth Charts for Height Weight and BMI(2 To 20Yr). *J Endocrinol Invest* 29: 581–593, 2006.

13. **CARO CG**, **BUTLER J**, **DUBOIS AB**. Some effects of restriction of chest cage expansion on pulmonary function in man: an experimental study. *J Clin Invest* 39: 573–583, 1960.

14. **Cherniack RM**. Respiratory Effects of Obesity. *Can Med Assoc J* 80: 613–616, 1959.

15. **Chiappa GR**, **Queiroga F**, **Meda E**, **Ferreira LF**, **Diefenthaeler F**, **Nunes M**, **Vaz MA**, **Machado MCL**, **Nery LE**, **Neder JA**. Heliox improves oxygen delivery and utilization during dynamic exercise in patients with chronic obstructive pulmonary disease. *Am J Respir Crit Care Med* 179: 1004–1010, 2009.

16. **Cleland SM**, **Murias JM**, **Kowalchuk JM**, **Paterson DH**. Effects of prior heavy-intensity exercise on oxygen uptake and muscle deoxygenation kinetics of a subsequent heavy-intensity cycling and knee-extension exercise. *Appl Physiol Nutr Metab* 37: 138–148, 2012.

17. **Coast JR**, **Rasmussen SA**, **Krause KM**, **O'Kroy JA**, **Loy RA**, **Rhodes J**. Ventilatory work and oxygen consumption during exercise and hyperventilation. *J Appl Physiol* 74: 793–798, 1993.

18. **Collins LC**, **Hoberty PD**, **Walker JF**, **Fletcher EC**, **Peiris AN**. The effect of body fat distribution on pulmonary function tests. *Chest* 107: 1298–1302, 1995.

19. **Cross TJ**, **Sabapathy S**, **Schneider DA**, **Haseler LJ**. Breathing He – O_2 attenuates the slow component of O 2 uptake kinetics during exercise performed above the respiratory compensation threshold. *Exp Physiol* 95: 172–183, 2010.

20. **Dempsey JA**, **Romer L**, **Rodman J**, **Miller J**, **Smith C**. Consequences of exercise-induced respiratory muscle work. *Respir Physiol Neurobiol* 151: 242–250, 2006.

21. **DeWeese EL**, **Sullivan TY**, **Yu PL**. Ventilatory and occlusion pressure responses to helium breathing. *J Appl Physiol* 54: 1525–1531, 1983.

22. **Dominelli PB**, **Archiza B**, **Ramsook AH**, **Mitchell RA**, **Peters CM**, **Molgat-Seon Y**, **Henderson WR**, **Koehle MS**, **Boushel R**, **Sheel AW**. Effects of respiratory muscle work on respiratory and locomotor blood flow during exercise. *Exp Physiol* 11: 1535–1547, 2017.

23. **Dominelli PB**, **Render JN**, **Molgat-Seon Y**, **Foster GE**, **Romer LM**, **Sheel AW**. Oxygen cost of exercise hyperpnoea is greater in women compared with men. *J Physiol* 593: 1965–1979, 2015.

24. **Driller M**, **Paton C**. The Effects of Respiratory Muscle Training in Highly-Trained Rowers. *J Exerc Physiol Online* 15: 93–102, 2012.

25. **Ebbeling CB**, **Pawlak DB**, **Lugwig DS**. Childhood obesity: public health crisis, common sense cure. *Lancet* 360: 473–482, 2002.

26. **Edwards AM**, **Cooke CB**. Oxygen uptake kinetics and maximal aerobic power are unaffected by inspiratory muscle training in healthy subjects where time to exhaustion is extended. *Eur J Appl Physiol* 93: 139–144, 2004.

27. **Edwards AM**, **Graham D**, **Bloxham S**, **Maguire GP**. Efficacy of inspiratory muscle training as a practical and minimally intrusive technique to aid functional fitness among adults with obesity. *Respir Physiol Neurobiol* 234: 85–88, 2016.

28. **Ekelund U**, **Franks PW**, **Wareham NJ**, **Åman J**. Oxygen uptakes adjusted for body composition in normal-weight and obese adolescents. *Obes Res* 12: 513–520, 2004.

29. **Esposito F**, **Ferretti G**. The effects of breathing He-O_2 mixtures on maximal oxygen consumption in normoxic and hypoxic men. *J Physiol* 503: 215–221, 1997.

30. **Esposito F**, **Limonta E**, **Alberti G**, **Veicsteinas A**, **Ferretti G**. Effect of respiratory muscle training on maximum aerobic power in normoxia and hypoxia. *Respir Physiol Neurobiol* 170: 268–272, 2010.

31. **Frank I**, **Briggs R**, **Spengler CM**. Respiratory muscles, exercise performance, and health in overweight and obese subjects. *Med Sci Sports Exerc* 43: 714–727, 2011.

32. **Fretzayas A**, **Moustaki M**, **Loukou I**, **Douros K**. Is obesity related to the lung function of non-asthmatic children? *World J Clin Pediatr* 7: 67–74, 2018.

33. **Gandevia SC**. Spinal and supraspinal factors in human muscle fatigue. *Physiol Rev* 81: 1725–1789, 2001.

34. **Gething AD**, **Passfield L**, **Davies B**. The effects of different inspiratory muscle training intensities on exercising heart rate and perceived exertion. *Eur J Appl Physiol* 92: 50–55, 2004.

35. **Gibson GJ**. Obesity, respiratory function and breathlessness. *Thorax* 55 Suppl 1: S41–S44, 2000.

36. **Gigliotti F**, **Binazzi B**, **Scano G**. Does training of respiratory muscles affect exercise performance in healthy subjects? *Respir Med* 100: 1117–1120, 2006.

37. **Grassi B**, **Pogliaghi S**, **Rampichini S**, **Quaresima V**, **Ferrari M**, **Marconi C**, **Cerretelli P**. Muscle oxygenation and pulmonary gas exchange kinetics during cycling exercise on-transitions in humans. *J Appl Physiol* 95: 149–158, 2003.

38. **Grassi B**, **Poole DC**, **Richardson RS**, **Knight DR**, **Erickson BK**, **Wagner PD**. Muscle 02 uptake kinetics in humans: implications for metabolic control. *J Appl Physiol* 80: 988–998, 1996.

39. **Grassi B**, **Rossiter HB**, **Zoladz JA**. Skeletal Muscle Fatigue and Decreased Efficiency:Two Sides of the Same Coin? *Exerc Sport Sci Rev* 42: 75–83, 2015.

40. **Hankinson IL**, **Odencrantz JR**, **Fedan KB**. Spirometrie Reference Values from a Sample of the General U . S . Population. *Am J Respir Crit Care Med* 159: 179–187, 1999.

41. **Hansen D**, **Marinus N**, **Remans M**, **Courtois I**, **Cools F**, **Calsius J**, **Massa G**, **Takken T**. Exercise tolerance in obese vs. lean adolescents: A systematic review and meta-analysis. *Obes Rev* 15: 894–904, 2014.

42. **Harms CA**, **Babcock MA**, **McClaran SR**, **Pegelow DF**, **Nickele GA**, **Nelson WB**, **Dempsey JA**. Respiratory muscle work compromises leg blood flow during maximal exercise. *J Appl Physiol* 82: 1573–1583, 1997.

43. **Harms CA**, **Wetter TJ**, **Croix CMS**, **Pegelow DF**, **Dempsey JA**. Effects of respiratory muscle work on exercise performance. *J Appl Physiol* 89: 131–138, 2000.

44. **Harms CA**, **Wetter TJ**, **McClaran SR**, **Pegelow DF**, **Nickele GA**, **Nelson WB**, **Hanson P**, **Dempsey JA**. Effects of respiratory muscle work on cardiac output and its distribution during maximal exercise. *J Appl Physiol* 85: 609–618, 1998.

45. **Hogan MC**, **Richardson RS**, **Haseler LJ**. Human muscle performance and PCr hydrolysis with varied inspired oxygen fractions: a ^{31}P-MRS study. *J Appl Physiol* 86: 1367–1373, 1999.

46. **Holm P**, **Sattler A**, **Fregosi RF**. Endurance training of respiratory muscles improves cycling performance in fit young cyclists. *BMC Physiol* 4: 9, 2004.

47. **Jones AM**, **Grassi B**, **Christensen PM**, **Krustrup P**, **Bangsbo J**, **Poole DC**. Slow component of VO2 kinetics: Mechanistic bases and practical applications. *Med Sci Sports Exerc* 43: 2046–2062, 2011.

48. **KAUFMAN BJ**, **FERGUSON MH**, **CHERNIACK RM**. HYPOVENTILATION IN OBESITY. *J Clin investigtion* 38: 500–507, 1959.

49. **Koenig SM**. Pulmonary complications of obesity. *Am J Med Sci* 321: 249–279, 2001.

50. **Kress JP**, **Pohlman AS**, **Alverdy J**, **Hall JB**. The impact of morbid obesity on oxygen cost of breathing (VO2RESP) at rest. *Am J Respir Crit Care Med* 160: 883–886, 1999.

51. **Lafortuna CL**, **Agosti F**, **Galli R**, **Busti C**, **Lazzer S**, **Sartorio A**. The energetic and cardiovascular response to treadmill walking and cycle ergometer exercise in obese women. *Eur J Appl Physiol* 103: 707–717, 2008.

52. **Lamarra N**, **Whipp BJ**, **Ward SA**, **Wasserman K**. Effect of interbreath fluctuations on characterizing exercise gas exchange kinetics. *J Appl Physiol* 62: 2003–12, 1987.

53. **Lazzer S**, **Taboga P**, **Salvadego D**, **Rejc E**, **Simunic B**, **Narici M V**, **Buglione A**, **Giovanelli N**, **Antonutto G**, **Grassi B**, **Pisot R**, **di Prampero PE**. Factors affecting metabolic cost of transport during a multi-stage running race. *J Exp Biol* 217: 787–95, 2014.

54. **Lazzeri G**, **Giacchi MV**, **Spinelli A**, **Pammolli A**, **Dalmasso P**, **Nardone P**,

Lamberti A, **Cavallo F**. Overweight among students aged 11-15 years and its relationship with breakfast, area of residence and parents' education: Results from the Italian HBSC 2010 cross-sectional study. *Nutr J* 13: 1–10, 2014.

55. **Lemaitre F**, **Coquart JB**, **Chavallard F**, **Castres I**, **Mucci P**, **Costalat G**, **Chollet D**. Effect of additional respiratory muscle endurance training in young well-trained swimmers. *J Sports Sci Med* 12: 630–8, 2013.

56. **Leone N**, **Courbon D**, **Thomas F**, **Bean K**, **Jégo B**, **Leynaert B**, **Guize L**, **Zureik M**. Lung function impairment and metabolic syndrome the critical role of abdominal obesity. *Am J Respir Crit Care Med* 179: 509–516, 2009.

57. **Lin CK**, **Lin CC**. Work of breathing and respiratory drive in obesity. *Respirology* 17: 402–411, 2012.

58. **Littleton SW**. Impact of obesity on respiratory function. *Respirology* 17: 43–49, 2012.

59. **Lobstein T**, **Frelut M-L**. Prevalence of overweight among children in Europe. *Obes Rev* 4: 195–200, 2003.

60. **LoMauro A**, **Cesareo A**, **Agosti F**, **Tringali G**, **Salvadego D**, **Grassi B**, **Sartorio A**, **Aliverti A**. Effects of a multidisciplinary body weight reduction program on static and dynamic thoraco-abdominal volumes in obese adolescents. *Appl Physiol Nutr Metab* 41: 649–658, 2016.

61. **Louvaris Z**, **Vogiatzis I**, **Aliverti A**, **Habazettl H**, **Wagner H**, **Wagner P**, **Zakynthinos S**. Blood flow does not redistribute from respiratory to leg muscles during exercise breathing heliox or oxygen in COPD. *J Appl Physiol* 117: 267–76, 2014.

62. **Louvaris Z**, **Zakynthinos S**, **Aliverti A**, **Habazettl H**, **Vasilopoulou M**, **Andrianopoulos V**, **Wagner H**, **Wagner P**, **Vogiatzis I**. Heliox increases quadriceps muscle oxygen delivery during exercise in COPD patients with and without dynamic hyperinflation. *J Appl Physiol* 113: 1012–1023, 2012.

63. **Luce JM**. Respiratory Complications of Obesity. *Chest* 78: 626–631, 1980.

64. **Lukaski HC**, **Bolonchuk WW**, **Hall CB**, **Siders WA**. Validation of tetrapolar

bioelectrical impedance method to assess human body composition. *J Appl Physiol* 60: 1327–1332, 1986.

65. **Mador MJ**, **Deniz O**, **Deniz O**, **Aggarwal A**, **Shaffer M**, **Kufel TJ**, **Spengler CM**. Effect of respiratory muscle endurance training in patients with COPD undergoing pulmonary rehabilitation. *Chest* 128: 1216–24, 2005.

66. **Mancini D**, **Donchez L**, **Levine S**. Acute Unloading of the Work of Breathing Extends Exercise Duration in Patients With Heart Failure. *J Am Coll Cardiol* 29: 590–596, 1997.

67. **Margaria R**, **Cerretelli P**, **Aghemo P**, **Sassi G**. Energy cost of running. *J Appl Physiol* 18: 367–370, 1963.

68. **Milic-emili J**, **Orzalesi MM**. Mechanical work of breathing during maximal voluntary ventilation. *J Appl Physiol* 85: 254–258, 1998.

69. **Miller MR**, **Hankinson J**, **Brusasco V**, **Burgos F**, **Casaburi R**, **Coates A**, **Crapo R**, **Enright P**, **van der Grinten CPM**, **Gustafsson P**, **Jensen R**, **Johnson DC**, **MacIntrye N**, **McKay R**, **Navajas D**, **Pedersen OF**, **Pellegrino R**, **Viegi G**, **Wagner J**. Standardisation of spirometry. *Eur Respir J* 26: 319–338, 2005.

70. **Naimark A**, **Cherniack RM**. Compliance of the respiratory system and its components in health and obesity. *J Appl Physiol* 15: 377 LP-382, 1960.

71. **O'Donnell DE**, **O'Donnell CDJ**, **Webb KA**, **Guenette JA**. Respiratory consequences of mild-to-moderate obesity: Impact on exercise performance in health and in chronic obstructive pulmonary disease. *Pulm Med* 2012, 2012.

72. **OGILVIE CM**, **FORSTER RE**, **BLAKEMORE WS**, **MORTON JW**. A standardized breath holding technique for the clinical measurement of the diffusing capacity of the lung for carbon monoxide. *J Clin Invest* 36: 1–17, 1957.

73. **Orlando A**, **Cazzaniga E**, **Giussani M**, **Palestini P**, **Genovesi S**. Hypertension in Children: Role of Obesity, Simple Carbohydrates, and Uric Acid. *Front Public Heal* 6: 1–7, 2018.

74. **Parameswaran K**, **Todd DC**, **Soth M**. Altered respiratory physiology in obesity. *Can*

Respir J 13: 203–210, 2006.

75. **Passoni E**, **Lania A**, **Adamo S**, **Grasso GS**, **Noè D**, **Miserocchi G**, **Beretta E**. Mild training program in metabolic syndrome improves the efficiency of the oxygen pathway. *Respir Physiol Neurobiol* 208: 8–14, 2015.

76. **Pelosi P**, **Croci M**, **Ravagnan I**, **Vicardi P**, **Gattinoni L**. Total Respiratory System, Lung, and Chest Wall Mechanics in Sedated-Paralyzed Postoperative Morbidly Obese Patients. *Chest* 109: 144–151, 1996.

77. **Powers S**, **Jacques M**, **Richard R**, **Beadle R**. Effects of Breathing a Normoxic He-O 2 Gas Mixture on Exercise Tolerance and V̇O2 max. *Int J Sports Med* 07: 217–221, 1986.

78. **Di Prampero PE**. The energy cost of human locomotion on land and in water. *Int. J. Sports Med.* 7: 55–72, 1986.

79. **di Prampero PE**, **Salvadego D**, **Fusi S**, **Grassi B**. A simple method for assessing the energy cost of running during incremental tests. *J Appl Physiol* 107: 1068–1075, 2009.

80. **Rassler B**, **Marx G**, **Hallebach S**, **Kalischewski P**, **Baumann I**. Long-term respiratory muscle endurance training in patients with myasthenia gravis: first results after four months of training. *Autoimmune Dis* 2011: 808607, 2011.

81. **Rastogi D**, **Bhalani K**, **Hall CB**, **Isasi CR**. Association of pulmonary function with adiposity and metabolic abnormalities in Urban minority adolescents. *Ann Am Thorac Soc* 11: 744–752, 2014.

82. **Rigamonti AE**, **Agosti F**, **Patrizi A**, **Tringali G**, **Fessehatsion R**, **Cella SG**, **Sartorio A**. GH Responsiveness before and after a 3-Week Multidisciplinary Body Weight Reduction Program Associated with an Incremental Respiratory Muscle Endurance Training in Obese Adolescents. *Horm Metab Res* 46: 59–64, 2014.

83. **Romer LM**, **Lovering AT**, **Haverkamp HC**, **Pegelow DF**, **Dempsey JA**. Effect of inspiratory muscle work on peripheral fatigue of locomotor muscles in healthy humans. *J Physiol* 571: 425–439, 2006.

84. **Romer LM**, **Polkey MI**. Exercise-induced respiratory muscle fatigue: implications for

performance. *J Appl Physiol* 104: 879–888, 2008.

85. **Roussos C**, **Macklem P**. The Respiratory Muscles. *N Engl J Med* 307: 786–797, 1982.

86. **Salvadego D**, **Lazzer S**, **Busti C**, **Galli R**, **Agosti F**, **Lafortuna C**, **Sartorio A**, **Grassi B**. Gas exchange kinetics in obese adolescents. Inferences on exercise tolerance and prescription. *Am J Physiol Regul Integr Comp Physiol* 299: R1298–R1305, 2010.

87. **Salvadego D**, **Sartorio A**, **Agosti F**, **Tringali G**, **Patrizi A**, **Isola M**, **LoMauro A**, **Aliverti A**, **Grassi B**. Respiratory muscle endurance training reduces the O2 cost of cycling and perceived exertion in obese adolescents. *Am J Physiol - Regul Integr Comp Physiol* 313: 487–95, 2017.

88. **Salvadego D**, **Sartorio A**, **Agosti F**, **Tringali G**, **Patrizi A**, **Lo Mauro A**, **Aliverti A**, **Grassi B**. Acute respiratory muscle unloading by normoxic helium – O 2 breathing reduces the O 2 cost of cycling and perceived exertion in obese adolescents. *Eur J Appl Physiol* 115: 99–109, 2015.

89. **Scano G**, **Stendardi L**, **Bruni GI**. The respiratory muscles in eucapnic obesity: Their role in dyspnea. *Respir Med* 103: 1276–1285, 2009.

90. **Segizbaeva M**. Loading and Unloading Breeathing during Exercise: Responses and Compensatory Mechanisms. *Eur J Med Res* 15: 157–163, 2010.

91. **Sharp JT**, **Henry JP**, **Sweany SK**, **Meadows WR**, **Pietras RJ**. The Total Work of Breathing in Normal and Obese Men. *J Clin investigtion* 43: 728–739, 1964.

92. **Sheel AW**. Respiratory Muscle Training in Healthy Individuals: Physiological Rationale and Implications for Exercise Performance. *Sport Med* 32: 567–581, 2002.

93. **Speiser PW**, **Rudolf MCJ**, **Anhalt H**, **Camacho-Hubner C**, **Chiarelli F**, **Eliakim A**, **Freemark M**, **Gruters A**, **Hershkovitz E**, **Iughetti L**, **Krude H**, **Latzer Y**, **Lustig RH**, **Pescovitz OH**, **Pinhas-Hamiel O**, **Rogol AD**, **Shalitin S**, **Sultan C**, **Stein D**, **Vardi P**, **Werther GA**, **Zadik Z**, **Zuckerman-Levin N**, **Hochberg Z**. Childhood Obesity. *J Clin Endocrinol Metab* 90: 1871–1887, 2005.

94. **Spengler CM**, **Boutellier U**. Breathless Legs? Consider Training Your Respiration. [Online]. *News Physiol Sci* 15: 101–105, 2000.

http://www.ncbi.nlm.nih.gov/pubmed/11390888.

95. **Suratt PM**, **Wilhoit SC**, **Hsiao HS**, **Atkinson RL**, **Rochester DF**. Compliance of chest wall in obese subjects. [Online]. *J Appl Physiol* 57: 403–7, 1984. http://www.ncbi.nlm.nih.gov/pubmed/6469810.

96. **Tian J**, **Zhou Y**, **Cui J**, **Wang D**, **Wang X**, **Hu G**, **Tian Y**, **Jiang Y**, **Zheng J**, **Wang J**, **Zhong N**, **Ran P**. Peak expiratory flow as a screening tool to detect airflow obstruction in a primary health care setting. *Int J Tuberc Lung Dis* 16: 674–680, 2012.

97. **Vella CA**, **Marks D**, **Robergs RA**. Oxygen cost of ventilation during incremental exercise to VO2 max. *Respirology* 11: 175–181, 2006.

98. **Verges S**, **Boutellier U**, **Spengler CM**. Effect of respiratory muscle endurance training on respiratory sensations, respiratory control and exercise performance. A 15-year experience. *Respir Physiol Neurobiol* 161: 16–22, 2008.

99. **Villiot-Danger J-C**, **Villiot-Danger E**, **Borel J-C**, **Pépin J-L**, **Wuyam B**, **Vergès S**. Respiratory muscle endurance training in obese patients. *Int J Obes (Lond)* 35: 692–699, 2011.

100. **Vogiatzis I**, **Habazettl H**, **Aliverti A**, **Athanasopoulos D**, **Louvaris Z**, **LoMauro A**, **Wagner H**, **Roussos C**, **Wagner PD**, **Zakynthinos S**. Effect of helium breathing on intercostal and quadriceps muscle blood flow during exercise in COPD patients. *Am J Physiol Regul Integr Comp Physiol* 300: R1549–R1559, 2011.

101. **WARD SA**, **WHIPP BJ**, **POON C-S**. DENSITY-DEPENDENT AIRFLOW AND VENTILATORY CONTROL DURING EXERCISE. *Respir Physiol* 49: 267–277, 1982.

102. **Wasserman K**, **Whipp BJ**. Exercise Physiology in Health and Disease. *Am Rev Respir Dis* 112: 219–249, 1975.

103. **Watson RA**, **Pride NB**, **Thomas EL**, **Fitzpatrick J**, **Durighel G**, **McCarthy J**, **Morin SX**, **Ind PW**, **Bell JD**. Reduction of total lung capacity in obese men: comparison of total intrathoracic and gas volumes. *J Appl Physiol* 108: 1605–12, 2010.

104. **Wetter TJ**, **Harms CA**, **Nelson WB**, **Pegelow DF**, **Dempsey JA**. Influence of

respiratory muscle work on V and leg blood flow during submaximal exercise. *J Appl Physiol* 2: 643–651, 1999.

105. **Whipp BJ**, **Davis JA**, **Torres F**, **Wasserman K**. A test to determine parameters of aerobic function during exercise. [Online]. *J Appl Physiol* 50: 217–21, 1981. http://www.ncbi.nlm.nih.gov/pubmed/6782055.

106. **Wilson RC**, **Jones PW**. Long-term reproducibility of Borg scale estimates of breathlessness during exercise. *Clin Sci* 80: 309–312, 1991.

107. **Witt JD**, **Guenette JA**, **Rupert JL**, **McKenzie DC**, **Sheel AW**. Inspiratory muscle training attenuates the human respiratory muscle metaboreflex. *J Physiol* 584: 1019–28, 2007.

108. **Young-Hyman D, Schlundt D, Herman L, De Luca F CD**. Evaluation of the Insulin Resistance Syndrome in 5- to 10-Year-Old Overweight/Obese African-American Children. *Diabetes Care* 24: 1359–1364, 2001.

109. **Zoladz JA**, **Gladden LB**, **Hogan MC**, **Nieckarz Z**, **Grassi B**. Progressive recruitment of muscle fibers is not necessary for the slow component of V̇ <scp>o</scp> $_2$ kinetics. *J Appl Physiol* 105: 575–580, 2008.

110. **Zuccarelli L**, **Porcelli S**, **Rasica L**, **Marzorati M**, **Grassi B**. Comparison between slow components of HR and VO2 kinetics: Functional significance. *Med Sci Sports Exerc* 50: 1649–1657, 2018.

ACKNOWLEDGEMENTS

I would like to express my gratitude to all who have supported me during my studies through their advice, guidance, encouragement and example, in particular my supervisors, Prof. Bruno Grassi, and Dr. Desy Salvadego. I would like to thank my fellow PhD students and researchers for their invaluable peer support: Prof. Stefano Lazzer, Dr. Nicola Giovanelli, Dr. Lea Biasutti, Dr. Mirco Floreani, Dr. Fillippo Vaccari, Dr. Lucrezia Zuccarelli, Dr. Alessio del Torto, Dr. Davide Anchisi and many others. I would also like to thank collaborators in Istituto Auxologico Italiano, IRCCS, in particular Prof. Alessandro Sartorio and his research team at Experimental Laboratory for Auxo-endocrinological research in Piancavallo (VB), whose support contributed to making my research work little bit easier.

I owe my deepest gratitude to the subjects who participated in my studies, they were generous in giving some of their time, energy and focus to this research.

Lastly, I would like to thank my families, who have supported me throughout this academic endeavor – I could not have done it without you.

PUBLICATIONS

Respiratory Physiology & Neurobiology 246 (2017) 53–58

Contents lists available at ScienceDirect

Respiratory Physiology & Neurobiology

journal homepage: www.elsevier.com/locate/resphysiol

Air blood barrier phenotype correlates with alveolo-capillary O_2 equilibration in hypobaric hypoxia

Egidio Beretta[a,*], Francesca Lanfranconi[a], Gabriele Simone Grasso[a], Manuela Bartesaghi[a], Hailu Kinfu Alemayehu[b], Lorenza Pratali[c], Bruna Catuzzo[d], Guido Giardini[d], Giuseppe Miserocchi[a]

[a] Ambulatorio di Fisiologia Clinica e dello Sport, Scuola di Specializzazione in Medicina dello Sport, Università di Milano-Bicocca. Via Cadore, 48 20900 Monza, Italy
[b] Dipartimento di Scienze Mediche e Biologiche, Università degli Studi di Udine, Piazzale M. Kolbe 4, 33100 Udine, Italy
[c] Istituto di Fisiologia Clinica – CNR, Via Moruzzi 1 Pisa, Italy
[d] Centro di Medicina di Montagna, Ospedale Regionale "U. Parini", Aosta, Italy

ARTICLE INFO

Keywords:
High altitude pulmonary edema
DLCO
Diffusion subcomponents
Lung interstitial edema
Diffusion limitation
oxygen diffusion-transport

ABSTRACT

The O_2 diffusion limitation across the air blood barrier (DO_2 and subcomponents *Dm* and *Vc*) was evaluated in 17 healthy participants exposed to hypobaric hypoxia (HA, 3840m, P_IO_2 ~90 mmHg). A 10% decrease in alveolar volume (*VA*) in all participants suggested the development of sub-clinical interstitial lung edema. In > 80% of participants DO_2/VA increased, reflecting an individual strategy to cope with the hypoxia stimulus by re-modulating *Vc* or *Dm*. Opposite changes in *Dm*/*Vc* ratio were observed and participants decreasing *Vc* showed reduced alveolar blood capillary transit time. The interplay between diffusion and perfusion (cardiac output) was estimated in order to investigate the individual adaptive response to hypoxia. It appears remarkable that despite individual differences in the adaptive response to HA, diffusion limitation did not exceed ~11% of the alveolar-venous PO_2 gradient, revealing an admirable functional design of the air-blood barrier to defend the O_2 diffusion/perfusion function when facing hypobaric hypoxia corresponding to 50 mmHg decreased P_AO_2.

1. Introduction

Exposure to hypobaric hypoxia on reaching high altitudes leaves as open question the potential role of diffusion limitation to affect the alveolar-capillary PO_2 gradient. A new impetus to answer this question was given by the development of an individual-based method allowing to effectively compare the lung diffusion capacity at sea level and at high altitude, as in the latter condition lung diffusion is known to be affected by the greater hemoglobin affinity of CO (the tracer gas used to estimate lung diffusion capacity) (Beretta et al., 2017). The present paper is aimed at providing new knowledge concerning the adaptive responses of the air-blood barrier (ABB) to hypobaric hypoxia (3840m), that is known to represent a strong edemagenic condition (Miserocchi et al., 2001) that *per se* may affect the lung diffusion capacity (Bartesaghi et al., 2014). We attempted to characterize the adaptive hypoxia response based on the individual ABB phenotype, as defined by its diffusive/perfusive properties namely *Dm*, the air-blood membrane diffusion, and *Vc*, an estimate of the extension of the alveolar capillary network. The impact of diffusion limitation was estimated by correlating the individual diffusive/perfusive properties with the overall diffusive/perfusive capacity ratio of ABB based on the non-invasive model of Piiper and Scheid (1981) allowing to define the kinetics of the alveolo-venous equilibration process.

2. Material and Methods

2.1. Participants

Data were obtained from 17 healthy participants (12 males, 5 females), average age 36.4 ± 8.2, who regularly practiced mountaineering and/or mountain hiking. All participants were no smokers or mild smokers (less than 4 cigarettes/day) and their spirometric parameters were above 90% of predicted values. The research project was approved by the ethical committee of University of Milano Bicocca and was conducted in accordance with the Helsinki Declaration on human to assure ethical standards were being met. Participants were instructed about the experimental procedure and related discomfort, as well as of the risks of acute exposure to hypoxia, and signed an informed consent.

All measurements were performed at sea level (SL, Monza Italy, 170m, P_IO_2 157 mmHg) and at high altitude (HA, Aiguille du Midi,

* Corresponding author. Beretta Egidio, Dipartimento di Medicina e Chirurgia, Università di Milano Bicocca, Via Cadore, 48 20900 Monza, Italy.
E-mail address: egidio.beretta@unimib.it (E. Beretta).

http://dx.doi.org/10.1016/j.resp.2017.08.006
Received 6 June 2017; Received in revised form 2 August 2017; Accepted 4 August 2017
Available online 08 August 2017
1569-9048/

3840m, P_IO_2 90 mmHg). Participants spent the night of the eve at SL; the following morning they reached the laboratory at HA by cable car (about 30 minutes) and measurements were done after 4 hours from reaching the laboratory at HA.

2.2. Diffusion measurement

Measurement of *DLCO* and subcomponents were performed at SL and at HA according to standardized procedures at rest, in sitting position at total lung capacity (TLC) by single breath method (QUARK PFT, Cosmed, Roma, Italy). Participants inspired 3 gas mixtures containing 0.3% CH_4 (tracer to measure lung volume, *VA*), 0.3% CO and 20, 40 and 60% O_2, respectively. Each maneuver was performed at least 6 min after the previous one. *Dm* and *Vc* were determined from the experimentally derived linear regression as defined by (Roughton and Forster, 1957):

$$\frac{1}{DLCO} = \frac{1}{Dm} + \frac{1}{\theta \cdot [\mathrm{Hb}] \cdot Vc} \quad (1)$$

where θ is the binding rate of CO with Hb, [Hb] is the ratio between individual hemoglobin concentrations over reference values of hemoglobin concentration for men and women, $\frac{1}{Vc}$ is the slope of the relationship and $\frac{1}{Dm}$ the intercept. We chose a $1/\theta$ value as defined (Forster, 1987) according to the equation:

$$\frac{1}{\theta} = 0.75 + (0.0057 \cdot P_A O_2) \quad (2)$$

where P_AO_2 is assumed equal to the measured end tidal O_2 pressure ($PetO_2$).

DLCO values measured at HA were adjusted according to a recently developed method that accounts for the inter-individual differences of the effect of hypoxia exposure on diffusion subcomponents (Beretta et al., 2017); this approach allows maintaining on numerical basis the validity of Eq. (1). Blood samples were taken in resting conditions at SL to determine Hb concentration and hematocrit. Data were standardized to Hb concentration of 14.6 g/dl in men and 13.4 g/dl in women. DO_2 was derived as 1.23·*DLCO* measured with 20% O_2.

2.3. Echocardiography

Standard 2D echocardiography was performed at rest in supine position using a portable echo machine with a 2.5-3.5 MHz cardiac probe (Vivid I, General Electric Healthcare Clinical System) by a single experienced cardiologist, both at SL and HA. Care was taken to ensure that the position of the participants and the transducer were similar in all examinations. Stroke volume was obtained from apical 4 chamber view. Cardiac output ($\dot{Q}$) was measured multiplying left ventricle outflow tract time-velocity integral, measured using pulse wave Doppler, by its cross-sectional area and heart rate (Lang et al., 2015). Systolic pulmonary arterial pressure (*PAPs*) was estimated from the peak velocity of the tricuspid regurgitation jet by continuous flow Doppler and the systolic right atrium (RA) pressure estimated from the inferior vena cava diameter and its respiratory excursion (0–15 mmHg) using the formula: PAPs = 4 V^2 + RA pressure (Yock and Popp, 1984). Pulmonary vascular resistance (*PVR*) was estimated from the ratio of peak tricuspidal velocity (m/s) to the right ventricular outflow tract velocity-time integral, obtained by placing a 1–2 mm pulsed wave Doppler sample volume in the proximal right ventricular outflow tract, just within the pulmonary valve in the para-sternal short-axis view (Wood unit, Abbas et al., 2003). This relationship was considered valid for *PVR* Wood units < 8 (Rajagopalan et al., 2009).

2.4. Ventilatory and physiologic parameters

Pulmonary ventilation ($\dot{V}E$, in BTPS) and end tidal O_2 and CO_2 partial pressure ($PetO_2$, $PetCO_2$), were determined by a portable metabolic cart (K4b2, Cosmed, Roma, Italy). Heart rate (HR) was determined from a 12-lead electrocardiographic signal interfaced to Sensor Medics metabolic cart. Arterial blood O_2 saturation ($\%SatO_2$) was monitored continuously through oximetry at the finger (RAD 9 Signal Extraction Pulse Oximeter: Masimo Corporation, Irvine − California, USA) and only valid signals were considered checking the quality of the pulse wave signal. The environmental temperature was kept at 18 °C using an air-conditioning system and the current barometric pressure was recorded.

2.5. Estimate of diffusion limitation

Based on the mass conservation principle, Piiper and Scheid (1981) developed a theoretical model considering the equality of the diffusive and convective flux of O_2 when blood flows along the alveolar gas-exchanging unit. According to the model, the degree of diffusion limitation (*Ldiff*) resulting from the alveolar-capillary equilibration at the arterial end of the capillary can be defined as:

$$Ldiff = \frac{P_A - P_a}{P_A - P_{\bar{v}}} = e^{-\frac{DO_2}{\beta \dot{Q}}} \quad (3)$$

being P_A, P_a and $P_{\bar{v}}$ the O_2 partial pressures in the alveolar compartment, in the arterialized blood leaving the capillary and in the mixed venous blood reaching the alveoli, respectively; DO_2 is the O_2 diffusive capacity, $\dot{Q}$ is the cardiac output and β is the Hb binding capacity for O_2 (we assumed β values of 0.83 and 2.5 ml L^{-1} $mmHg^{-1}$ for SL and HA, respectively). The ratio $\frac{DO_2}{\beta \dot{Q}}$, defined as "equilibration index", is a pure number as the numerator and denominator have the units of ml min^{-1} $mmHg^{-1}$ and *Ldiff* varies from 0 (perfect equilibration) to 1 (no equilibration, as in case of arteriovenous shunt). By defining the average pulmonary blood capillary transit time (*Tt*) as $Tt = \frac{Vc}{\dot{Q}}$, one can reformulate diffusion limitation as

$$Ldiff = e^{-\frac{DO_2}{\beta} \cdot \frac{Tt}{Vc}}$$

2.6. Statistical analysis

Values were expressed in Tables as median and Interquartile Range (IQR 25th-75th percentile). Other values are reported as mean ± SD. The statistical significance of the difference for paired samples was estimated with Wilcoxon test. Regression and correlation analyses were performed using the least squared residuals method. All statistical analyses were performed by utilizing a commercially available software package (Origin, Origin Lab Corporation).

3. Results

Fig. 1A shows the relationship between *DLCO* measured at HA (adjusted according to Beretta et al., 2017) vs the corresponding SL values. It appears that data essentially scattered around the identity line, with a tendency to decrease at HA only for subjects having the highest value of *DLCO* at SL. Fig. 1B shows that *DLCO/VA* values increased on exposure to HA in 65% of the participants, did not change in 23% and clearly decreased only in 1 participant, the same showing the highest decrease in *DLCO* (Fig. 1A).

Fig. 2 shows the inverse relationship between the relative changes in *Vc* and *Dm* in HA normalized to SL value.

Fig. 3A shows an important difference when considering the relationship between the changes in *Dm/Vc* on exposure to HA *vs* the corresponding changes in $PetO_2$: in group identified as G1 (n = 5, closed circles), the *Dm/Vc* ratio significantly decreased, while the opposite occurred for the other group, identified as G2 (n = 12, open circles). B shows that values of *Dm/Vc* and of $\frac{DO_2}{\beta \dot{Q}}$ have opposite trends in the 2 groups at SL and at HA.

Table 1 reports the average values for *DLCO*, *VA*, *Dm/Vc*, *Vc/VA* and

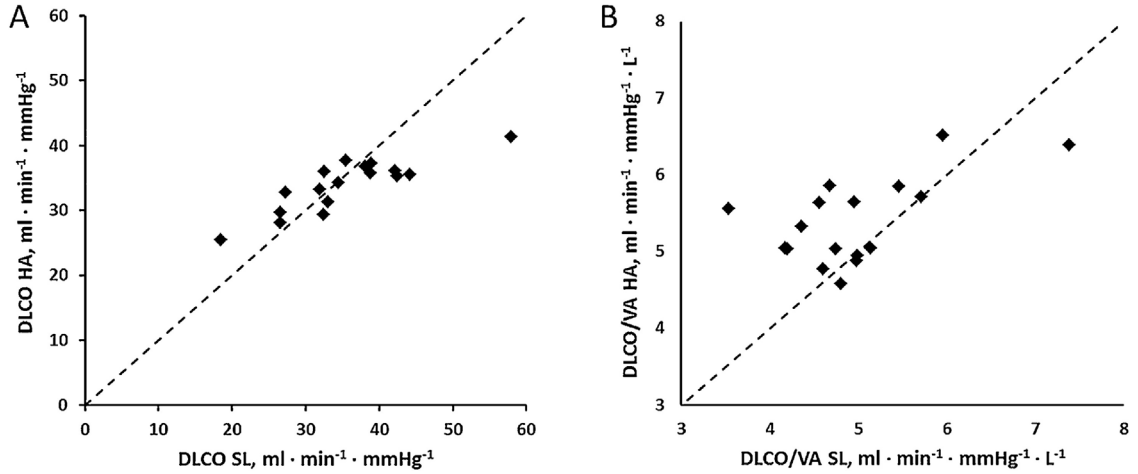

Fig. 1. Changes in lung diffusive capacity (*DLCO*) induced by hypoxia exposure.
Panel A: plot of the individual-based adjusted *DLCO* values measured in hypoxia (HA, adjusted according to Beretta et al., 2017) vs the corresponding sea level (SL) values, for all participants. Panel B: plot of individual *DLCO* values measured at HA and SL, normalized to the corresponding alveolar volume (*DLCO/VA*). Both panels report identity line (dashed lines).

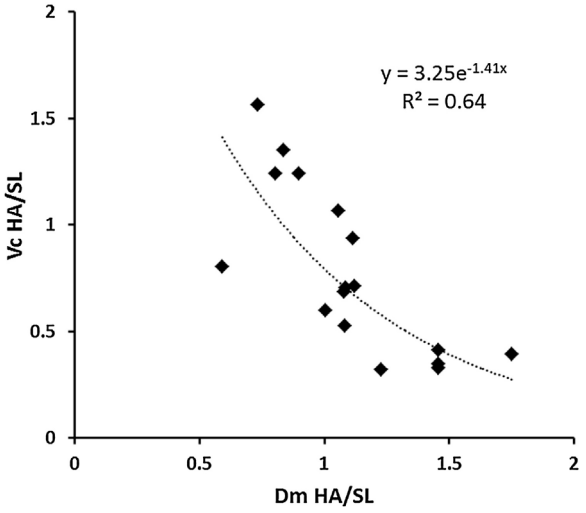

Fig. 2. Relative changes in diffusive subcomponents (*Dm* and *Vc*) induced by hypoxia exposure.
Correlation between hypoxia-induced changes of capillary lung volume (*Vc*) and membrane diffusive capacity (*Dm*), normalized to sea level values (HA/SL).

Dm/VA at SL and HA for the 2 groups.

Table 2 reports for the 2 groups the average values of cardiac output ($\dot{Q}$), Pulmonary Vascular Resistance (*PVR*), Pulmonary Artery Systolic Pressure (*PAPs*), pulmonary capillary transit time (*Tt*) and the diffusion-perfusion equilibration index ($DO_2/\beta\dot{Q}$).

Pulmonary ventilation remained essentially unchanged in G1 (mean value 180 ± 62 and 184 ± 42 $ml \cdot Kg^{-1} \cdot min^{-1}$ at SL and HA, respectively), conversely it increased by ~20 $ml \cdot Kg^{-1} \cdot min^{-1}$ in G2 in HA (averaging 210 ± 27 and 230 ± 61 $ml \cdot Kg^{-1} \cdot min^{-1}$ at SL and HA, respectively). $PetO_2$, $PetCO_2$ and $\%SatO_2$ decreased in HA both in G1 (51.2 ± 2.8 mmHg, 33.1 ± 0.3 mmHg and 88.2 ± 3%, respectively) and in G2 (54 ± 1 mmHg, 30.6 ± 0.4 mmHg and 86.9 ± 4 respectively).

Fig. 4A shows the transit times (*Tt*) vs *Ldiff* in the 2 groups: for G2 a significant ($p < 0.01$) negative correlation could be found. B shows the correlation between *Ldiff* and $PetO_2$ in the 2 groups HA. Lake Louise Score averaged 4.4 ± 0.89 and 4.8 ± 2.44 in G1 and G2 respectively.

4. Discussion

4.1. Grouping of participants based on the adaptive response to HA

We defined *a posteriori* as Group 1 (G1) participants decreasing *Dm/*

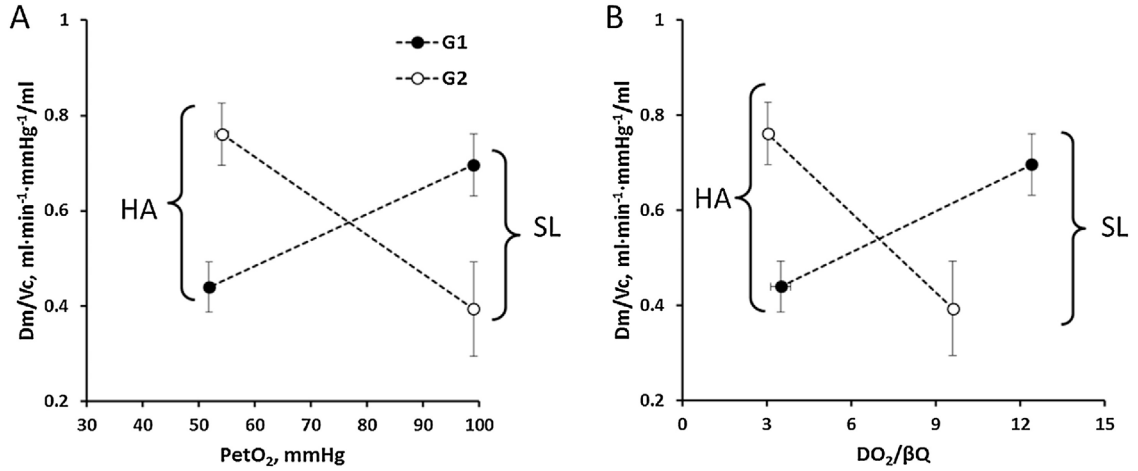

Fig. 3. Correlation between *Dm/Vc* ratio with $PetO_2$ and equilibration index ($DO_2/\beta\dot{Q}$).
Panel A: Figure allows to identify two groups of participants (G1, closed circles and G2, open circles) based on the opposite changes in *Dm/Vc* ratio plotted as a function of the decrease in $PetO_2$ from sea level (SL) to hypoxia (HA). Panel B: correlation between *Dm/Vc* ratio vs $DO_2/\beta\dot{Q}$ for G1 and G2 at SL and HA.

Table 1
Medians (IQR 25-75) of DLCO, VA, Dm/Vc, Vc/VA and Dm/VA on exposure to hypobaric hypoxia (HA) compared to sea level (SL) for the 2 groups.

	DLCO (ml min^{-1} mmHg^{-1})		**VA** (L)		**Dm/Vc** (ml min^{-1} mmHg^{-1}/ml)		**Vc/VA** (ml L^{-1})		**Dm/VA** (ml min^{-1} mmHg^{-1} L^{-1})	
	SL	**HA**	**SL**	**HA**	**SL**	**HA**	**SL**	**HA**	**SL**	**HA**
G1	38.1 (30.5–48.4)	36.8 (31.1–39.3)	7.41 (6.6–7.6)	6.4* (5.8–7.2)	0.57 (0.51–0.93)	0.39* (0.33–0.56)	15.7 (12.9–17.5)	19.3* (18.4–22.7)	9.7 (8.0–13.4)	8.4* (7.2–10.4)
G2	32.7 (28.4–41.2)	34.2 (30.1–35.9)	7.4 (5.8–8.0)	6.3** (5.4–7.1)	0.31 (0.2–0.56)	0.71** (0.55–0.91)	22.2 (15.9–28.3)	13.8** (10.5–16.7)	7.0 (5.9–8.4)	9.6** (8.5–10.9)

* HA vs SL $p < 0.05$.
** HA vs SL $p < 0.01$.

Table 2
Medians (IQR 25-75) of cardiac output ($\dot{Q}$), Pulmonary Vascular resistance (*PVR*), Pulmonary Artery Systolic Pressure (*PAPs*), pulmonary capillary transit time (*Tt*) and diffusion-perfusion equilibration index ($DO_2/\beta\dot{Q}$) on exposure to hypobaric hypoxia (HA) compared to sea level (SL) for the 2 groups.

	$\dot{Q}$ (L min^{-1})		*PVR* (Wood Units)		*PAPs* (mmHg)		*Tt*[a] (sec)		$DO_2/\beta\dot{Q}$[b]	
	SL	HA	SL	HA	SL	HA	SL	HA	SL	HA
G1	3.9 (2.9-4.5)	4.9* (4.1-6.2)	2.2 (2.1-2.3)	3.8* (1.9-3.9)	23 (19-28)	39* (30-57)	1.8 (1.5-2.0)	1.5 (1.4-1.7)	11.7 (10.2-14.8)	3.8** (2.8-4.0)
G2	4.1 (3.8-4.8)	5.2* (4.8-7.2)	1.5 (1.2-1.9)	2.3* (2.0-2.6)	20 (19-21)	36** (30-41)	2.4 (1.5-3.0)	0.8** (0.6-1.0)	9.9 (7.4-12.4)	3.0** (2.4-3.2)

[a] transit time (Tt) calculated as $Vc/\dot{Q}$.
[b] absolute number; DO_2 was calculated as 1.23**DLCO*; β is the Hb binding capacity for O_2, 0.83 and 2.5 ml L^{-1} mmHg^{-1} for SL and HA, respectively.
* HA vs SL $p < 0.05$.
** HA vs SL $p < 0.01$.

Vc in HA, while Group 2 (G2) included participants showing an opposite response (Fig. 2B). This grouping was in line with the one adopted in a previous report (Bartesaghi et al., 2014) referring to a lower altitude exposure (3269 m, P_IO_2 = 107 mmHg).

4.2. The decrease of VA at HA

The decrease in distribution volume for methane reveals a decrease in *VA* in both groups at HA (Table 1). As a possible interpretation for this finding, one may invoke the existence of interstitial edema occluding the more distal airways due to an increase in pulmonary interstitial pressure (Miserocchi et al., 2001). This interpretation is also compatible with the reported decrease in lung compliance at altitude (Pellegrino et al., 2010; Gautier et al., 1982). Furthermore, it is in line with a reported increase in pulmonary reactance measured by Impulse Oscillometry System (IOS) in humans exposed to 3269 m (Bartesaghi et al., 2014), a sensible technique that allows to detect an increase of lung extravascular water not exceeding 10% (Dellacà et al., 2008) corresponding to the condition of interstitial lung edema.

4.3. Air blood barrier diffusive/perfusive properties

DLCO data in HA (Fig. 1A) were corrected based on a new method (Beretta et al., 2017), allowing an individual adjustment accounting for increased binding of CO to Hb. In fact, the standard method previously proposed by the American Thoracic Society (1995), and the European Respiratory Society (MacIntyre et al., 2005) invalidates Eq. (1) on numerical basis by neglecting individual differences in 1/*Vc* and 1/*Dm* when moving from SL to HA (Bartesaghi et al., 2014). Further, a comparison of the two adjustment methods reveals that the old one essentially overestimates the increased binding capacity of CO to Hb, resulting in a larger reduction of the *DLCO* values measured at HA. The increase in *DLCO/VA* reported in most of the participants in HA (Fig. 1B) represents a new interesting notion appearing functionally

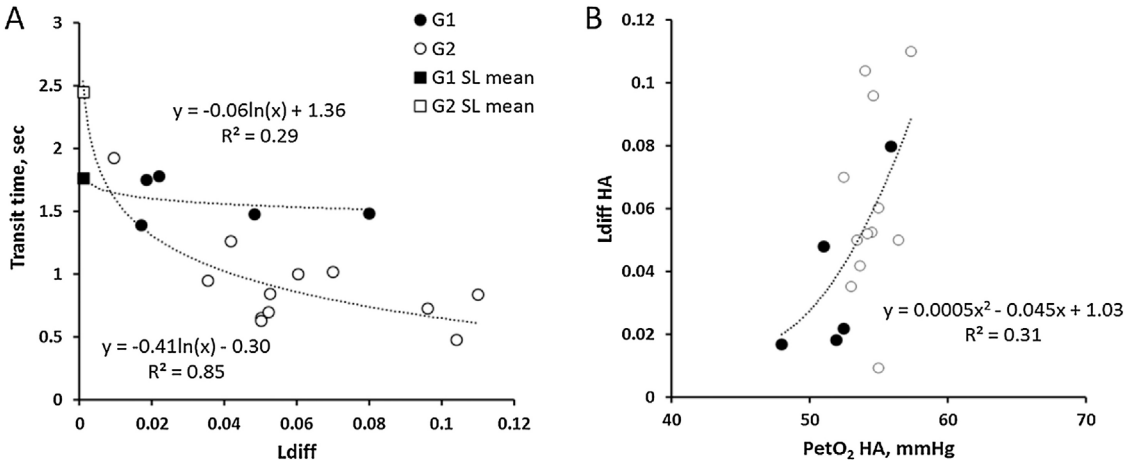

Fig. 4. Relationships between transit time *vs Ldiff* and of *Ldiff vs* $PetO_2$ on exposure to hypoxia.
Panel A: relationships between lung capillary transit time and diffusion limitation (*Ldiff*) in G1 (closed circles) and G2 (open circles) in HA. Figure also reports SL mean value for G1 and G2 (closed and open squares, respectively). Panel B: correlation between *Ldiff vs* $PetO_2$ in both groups in HA.

justified to match the decrease in overall O_2 diffusion pressure gradient. We shall now discuss how the increase in *DLCO/VA* reflects changes in *DLCO* subcomponents. We attempt an interpretation of changes in *Dm* based on morphological modification of the air-blood barrier considering that *Dm* is $\propto \frac{Salv}{\tau}$, being *Salv* and τ the surface and the thickness of ABB, respectively; further we consider *Vc* as an index of extension of the alveolar capillary network (Miserocchi et al., 2008). No specific changes would be expected for *DLCO* and subcomponents, normalized to *VA*, in case their changes in HA were proportional to the decrease in *VA*. Conversely, an interpretation is required when changes were observed (Fig. 2A). In G1 *Dm/VA* decreased in HA (Table 1) likely reflecting an increase in thickness of ABB due to interstitial edema; this however did not impact on *DLCO/VA* that actually increased due to a significant increase of *Vc/VA* (Table 1) suggesting recruitment of the alveolar capillary network. Accordingly, the decrease of *Dm/Vc* in G1 essentially reveals that the response to HA is characterized by a decrease of the ratio between diffusive/perfusive properties of ABB. Considering now G2, the increase in *DLCO/VA* correlates with the increase in *Dm/VA* (Table 1). In this case, a decrease in τ could be invoked. This effect could possibly be explained by recalling morphologic data from experimental models of interstitial lung edema (Conforti et al., 2002; Palestini et al., 2002; Weibel and Knight, 1964). These data showed that a non-homogeneous distribution of extravascular water in the air-blood barrier, such as fluid accumulation in few localized endothelial cellular blebs with remarkable thinning for the rest of the barrier, results in a decrease of the harmonic mean value of τ (Weibel and Knight, 1964; Weibel et al., 1993). In fact, the harmonic mean increases the relative weight of the thinner portions by mitigating the impact of the few large outliers (the blebs). This peculiar adaptive response would provide an advantage for diffusion as suggested by a time-based understanding model recently developed by Kang and Sapoval (2016) suggesting an inverse relationship between diffusion time and τ. Next, the decrease in *Vc/VA* (Table 1) in G2 on exposure to HA suggests a remarkable de-recruitment of the alveolar capillary network that could be explained by two mechanisms: (1) pre-capillary vasoconstriction in lung regions developing interstitial edema (Rivolta et al., 2011) and (2) compression of the alveolar capillary network caused by the increase in interstitial pressure induced by edema (Mazzuca et al., 2016).

One can discuss the changes in *PVR* in the 2 groups based on the changes in Vc. *PVR* was higher in G1 at SL (Table 2) due to a less extended alveolar capillary network (lower *Vc*); in both groups hypoxia caused an increase in *PAPs*, but the increase in *PVR* was larger in G2 due to the de-recruitment of the alveolar capillary network (Table 2). In summary, the *Dm/Vc* ratio, at variance with G1, increased in G2, suggesting an increase of the diffusion/perfusion property of the ABB in HA.

4.4. Overall lung diffusion/perfusion capacitance and diffusion limitation

It is generally considered that unequal distribution of $\dot{V}_A/\dot{Q}$ ratio within the lung represents an obvious cause of inefficiency of gas exchange function. Yet, in absence of regional $\dot{V}_A/\dot{Q}$ distribution data, we wish now to discuss how the inter-individual differences in the adaptive response of ABB on exposure to HA affect the interplay between diffusion and perfusion of ABB to attain the alveolar-capillary O_2 equilibration. We attempt to relate the morpho-functional phenotype of ABB, as defined by the diffusion/perfusion property (*Dm/Vc*), to the overall lung diffusion/perfusion capacitance, as defined by the equilibration index $\frac{DO_2}{\beta\dot{Q}}$ as well as to the diffusion limitation (*Ldiff*) as defined by Eq.3.

One shall note that the 2 groups differ in terms of ABB phenotype: in G1 a relatively higher value of *Dm* (Table 1) can be explained on morpho-functional ground by a high number of alveoli and/or a low thickness ABB phenotype (Miserocchi et al., 2008). Conversely, in G2 the greater value of *Vc* at SL (Table 1) reveals an inborn more extended alveolar capillary network (Miserocchi et al., 2008). In both groups, HA exposure led to a decrease of the equilibration index down to a similar value (Table 2) and therefore to a similar increase in *Ldiff* (Eq. (3)): yet, in G1, the decrease of $\frac{DO_2}{\beta\dot{Q}}$ was remarkably larger (about 3.5 fold) starting from a high value (~12) at SL. Note that the impact of the increase in β, reflecting the greater slope of Hb dissociation curve in the hypoxic PO_2 range of values, is equal in both groups. It is noteworthy that the values of *Dm/Vc* and of $\frac{DO_2}{\beta\dot{Q}}$ are opposite in the 2 groups at SL and HA (Fig. 3B). It looks like in G1 at HA the overall diffusion/perfusion capacitance ($\frac{DO_2}{\beta\dot{Q}}$) results in blunting of the phenotype character being prevalent at SL (high *Dm*) to favor the less prevalent character (low *Vc*), the opposite being observed in G2. On the average, a similar increase in *Ldiff* occurred in HA for both groups. Considering now transit time (*Tt*), one can appreciate in Fig. 4A that the increase in *Ldiff* in G1 does not correlate with any change in *Tt*. Conversely, in G2 the increase in *Ldiff* reflects the shortening of *Tt* (Fig. 4A), due to the increase in $\dot{Q}$ and a corresponding decrease in *Vc*.

Oxygen equilibration further depends on the interplay between diffusive-perfusive conductance and alveolar ventilation. The significantly higher $PetO_2$ in G2 participants (Fig. 4B) can be explained by an increase in ventilation (on the average 20 ml/kg/min) that can be regarded as compensatory to favor O_2 transport in presence of diffusion limitation due to shortening of *Tt*. In G1 no such increase in ventilation was observed in HA. Overall, the arterial O_2 saturation was similarly decreased in both groups in HA. On the whole, in both groups *Ldiff* did not exceed 11% of the initial O_2 partial pressure gradient acting at the venous end of the alveolar capillary ($P_A - P_{\bar{v}}$). At similar simulated altitude, experimental measurements of arterial and mixed venous blood (Swan-Ganz catheter) led to an estimated P_A-P_a not exceeding 2 mmHg (Torre-Bueno et al., 1985).

4.5. Correlation between diffusive-perfusive function and microvascular fluid exchanges in hypoxia

Despite the opposite features of the adaptive responses one may hypothesize that they should be aimed at a more efficient response to assure the need for increased O_2 transport on one side and, to protect against the risk of developing lung edema in an edemagenic condition such as hypoxia exposure (Andersson and Tracey, 2011) as suggested by the decrease of *VA* in both groups. The present data refer to an adaptive phase to HA that does not imply a severe condition of lung edema that would obviously result in a remarkable decrease in *DLCO*. It is relevant that G1 participants recruit alveolar capillary network, that represents *per se* a further edemagenic factor: one is therefore tempted to hypothesize that these subjects better tolerate and resist to lung edema formation. In G2, the adaptive response to hypoxia is rather more complex: in this group, the microvascular filtration coefficient is quite high at SL due the extended surface of the capillary network (Bartesaghi et al., 2014). Accordingly, de-recruitment may be interpreted as being protective against the development of edema. The paradoxical increase in *Dm* might be regarded as the effect of remarkable decrease of blood capillary pressure in the underperfused regions favoring fluid reabsorption from the extravascular space. Despite the fact that Lake Louise Score was not significantly different between the two groups, the coefficient of variation of the Score in G2 amounting to 50% of the mean suggests remarkable variability in neurological disturbance elicited by hypoxia. Yet, the severity of neurological symptoms poorly correlates with loss of pulmonary function.

We ignore so far whether mechanisms of control of vascular perfusion are set in place in order to control the volume of extra-vascular water in the ABB when edemagenic conditions develop. It is tempting to consider such control mechanism as being reflex in nature, recalling a possible role of interstitial vagal “J” (juxta-capillary) receptors whose afferent discharge was found to increase on exposure to edemagenic factors (Paintal, 1969). Despite the large inter-individual functional adaptive responses to HA, it is noteworthy to remark the admirable

functional assembly and design of the lung allowing to keep diffusion limitation minimal when challenging a decrease in in P_AO_2 from 100 down to about 50 mmHg.

Conflict of interest

The authors declare that they have no conflict of interest.

Acknowledgments

Financial support by project Alcotra n°114 Resamont 2. Facilities and equipment provided by the University of Milano Bicocca, Sports Medicine School. We acknowledge the organizational and logistical support of the Foundation "Montagna Sicura" – Courmayeur in the person of Dr. Micole Trucco. The authors thank Giovanni Corna, Luca Pollastri, MD, for providing experimental support.

References

Abbas, A.E., Fortuin, F.D., Shiller, N.B., Appleton, C.P., Moreno, C.A., Lester, S.J., 2003. A simple method for noninvasive estimation of pulmonary vascular resistance. J. Am. Coll. Cardiol. 41, 1021–1027. http://dx.doi.org/10.1016/S0735-1097(02)02973-X.

American Thoracic Society, 1995. Single-breath carbon monoxide diffusing capacity (transfer factor) Recommendations for a standard technique–1995 update. Am. J. Respir Crit. Care Med. 152, 2185–2198. http://dx.doi.org/10.1164/ajrccm.152.6.8520796.

Andersson, U., Tracey, K.J., 2011. HMGB1 is a therapeutic target for sterile inflammation and infection. Annu. Rev. Immunol. 29, 139–162. http://dx.doi.org/10.1146/annurev-immunol-030409-101323.

Bartesaghi, M., Beretta, E., Pollastri, L., Scotti, V., Mandolesi, G., Lanfranconi, F., Miserocchi, G., 2014. Inter-individual differences in control of alveolar capillary blood volume in exercise and hypoxia. Respir. Physiol. Neurobiol. 190, 96—104. http://dx.doi.org/10.1016/j.resp.2013.08.021.

Beretta, E., Lanfranconi, F., Grasso, G.S., Bartesaghi, M., Alemayehu, H.K., Miserocchi, G., 2017. Reappraisal of DLCO adjustment to interpret the adaptive response of the air-blood barrier to hypoxia. Respir. Physiol. Neurobiol. 238, 59–65. http://dx.doi.org/10.1016/j.resp.2016.08.009.

Conforti, E., Fenoglio, C., Bernocchi, G., Bruschi, O., Miserocchi, G., 2002. Morpho-functional analysis of lung tissue in mild interstitial edema. Am. J. Physiol. Lung. Cell Mol. Physiol. 282, 766–774. http://dx.doi.org/10.1152/ajplung.00313.2001.

Dellacà, R.L., Zannin, E., Sancini, G., Rivolta, I., Leone, B.E., Pedotti, A., Miserocchi, G., 2008. Changes in the mechanical properties of the respiratory system during the development of interstitial lung edema. Respir. Res. 9, 51. http://dx.doi.org/10.1186/1465-9921-9-51.

Forster, R.E., 1987. Diffusion of gases across the alveolar membrane. In: Fishman, A.P., Fahri, L.E., Tenney, S.M., Geiger, S.R. (Eds.), Handbook of Physiology. Section 3: The Respiratory System. Vol IV: Gas Exchange. American Physiological Society, Washington DC, pp. 71–88 Chapt 5.

Gautier, H., Peslin, R., Grassino, A., Milic-Emili, J., Hannhart, B., Powell, E., Miserocchi, G., Bonora, M., Fischer, J.T., 1982. Mechanical properties of the lungs during acclimatization to altitude. J. Appl. Physiol. Respir. Environ. Exerc. Physiol. 52, 1407–1415.

Kang, M.Y., Sapoval, B., 2016. Time-based understanding of DLCO and DLNO. Respir. Physiol. Neurobiol. 225, 48–59. http://dx.doi.org/10.1016/j.resp.2016.01.008.

Lang, R.M., Badano, L.P., Mor-Avi, V., Afilalo, J., Armstrong, A., Ernande, L., Flachskampf, F.A., Foster, E., Goldstein, S.A., Kuznetsova, T., Lancellotti, P., Muraru, D., Picard, M.H., Rietzschel, E.R., Rudski, L., Spencer, K.T., Tsang, W., Voigt, J.U., 2015. Recommendations for cardiac chamber quantification by echocardiography in adults: an update from the American Society of Echocardiography and the European Association of Cardiovascular Imaging. Eur. Heart J. Cardiovasc. Imaging 16, 233—270. http://dx.doi.org/10.1093/ehjci/jev014.

MacIntyre, N., Crapo, R.O., Viegi, G., Johnson, D.C., van der Grinten, C.P.M., Brusasco, V., Burgos, F., Casaburi, R., Coates, A., Enright, P., Gustafsson, P., Hankinson, J., Jensen, R., McKay, R., Miller, M.R., Navajas, D., Pedersen, O.F., Pellegrino, R., Wanger, J., 2005. Standardization of the single breath determination of carbon monoxide uptake. Eur. Respir. J. 26, 720–735. http://dx.doi.org/10.1183/09031936.05.00034905.

Mazzuca, E., Aliverti, A., Miserocchi, G., 2016. Computational micro-scale model of control of extravascular water and capillary perfusion in the air blood barrier. J. Theor. Biol. 400, 42—51. http://dx.doi.org/10.1016/j.jtbi.2016.03.036.

Miserocchi, G., Passi, A., Negrini, D., Del Fabbro, M., De Luca, G., 2001. Pulmonary interstitial pressure and tissue matrix structure in acute hypoxia. Am. J. Physiol. Lung Cell. Mol. Physiol. 280, 881–887.

Miserocchi, G., Messinesi, G., Tana, F., Passoni, E., Adamo, S., Romano, R., Beretta, E., 2008. Mechanisms behind inter-individual differences in lung diffusing capacity. Eur. J. Appl. Physiol. 102, 561–568. http://dx.doi.org/10.1007/s00421-007-0625-2.

Paintal, A.S., 1969. Mechanism of stimulation of type J pulmonary receptors. J. Physiol. 203, 511–532. http://dx.doi.org/10.1113/jphysiol.1969.sp008877.

Palestini, P., Calvi, C., Conforti, E., Botto, L., Fenoglio, C., Miserocchi, G., 2002. Composition, biophysical properties, and morphometry of plasma membranes in pulmonary interstitial edema. Am. J. Physiol. Lung. Cell Mol. Physiol. 282, L1382–1390. http://dx.doi.org/10.1152/ajplung.00447.2001.

Pellegrino, R., Pompilio, P., Quaranta, M., Aliverti, A., Kayser, B., Miserocchi, G., Fasano, V., Cogo, A., Milanese, M., Cornara, G., Brusasco, V., Dellacà, R., 2010. Airway responses to methacholine and exercise at high altitude in healthy lowlanders. J. Appl. Physiol. 108, 256–265. http://dx.doi.org/10.1152/japplphysiol.00677.2009.

Piiper, J., Scheid, P., 1981. Model for capillary-alveolar equilibration with special reference to O2 uptake in hypoxia. Respir. Physiol. 46, 193–208.

Rajagopalan, N., Simon, M.A., Suffoletto, M.S., Shah, H., Edelman, K., Mathier, M.A., López-Candales, A., 2009. Noninvasive estimation of pulmonary vascular resistance in pulmonary hypertension. Echocardiography 26, 489–494. http://dx.doi.org/10.1111/j.1540-8175.2008.00837.x.

Rivolta, I., Lucchini, V., Rocchetti, M., Kolar, F., Palazzo, F., Zaza, A., Miserocchi, G., 2011. Interstitial pressure and lung oedema in chronic hypoxia. Eur. Respir. J. 37, 943–949. http://dx.doi.org/10.1183/09031936.00066710.

Roughton, F., Forster, R.E., 1957. Relative importance of diffusion and chemical reaction rates in determining rate of exchange of gases in the human lung with special reference to true diffusing capacity of pulmonary membrane and volume of blood in the lung capillaries. J. Appl. Physiol. 11, 290–302.

Torre-Bueno, J.R., Wagner, P.D., Saltzman, H.A., Gale, G.E., Moon, R.E., 1985. Diffusion limitation in normal humans during exercise at sea level and simulated altitude. J. Appl. Physiol. 58, 989–995.

Weibel, E.R., Knight, B.W., 1964. A morphometric study on the thickness of the pulmonary air-blood barrier. J. Cell. Biol. 21, 367–396. http://dx.doi.org/10.1083/jcb.21.3.367.

Weibel, E.R., Federspiel, W.J., Fryder-Doffey, F., Hsia, C.C., König, M., Stalder-Navarro, V., Vock, R., 1993. Morphometric model for pulmonary diffusing capacity. I Membrane diffusing capacity. Respir. Physiol. 93, 125–149.

Yock, P.G., Popp, R.L., 1984. Noninvasive estimation of right ventricular systolic pressure by Doppler ultrasound in patients with tricuspid regurgitation. Circulation 70, 657—662. http://dx.doi.org/10.1161/01.cir.70.4.657.

Respiratory Physiology & Neurobiology 238 (2017) 59–65

Contents lists available at ScienceDirect

Respiratory Physiology & Neurobiology

journal homepage: www.elsevier.com/locate/resphysiol

Reappraisal of DLCO adjustment to interpret the adaptive response of the air-blood barrier to hypoxia

Egidio Beretta[a,*], Francesca Lanfranconi[a], Gabriele Simone Grasso[a], Manuela Bartesaghi[a], Hailu Kinfu Alemayehu[b], Giuseppe Miserocchi[a]

[a] Dipartimento di Medicina e Chirurgia, Università degli Studi di Milano-Bicocca, Via Cadore, 48 20900 Monza, Italy
[b] Dipartimento di Scienze Mediche e Biologiche, Università degli Studi di Udine, Piazzale M. Kolbe 4, 33100 Udine, Italy

ARTICLE INFO

Article history:
Received 2 May 2016
Received in revised form 11 August 2016
Accepted 29 August 2016
Available online 3 September 2016

Keywords:
Lung diffusive capacity
High altitude
Lung interstitial edema
Lung capillary volume

ABSTRACT

DLCO measured in hypoxia must be corrected due to the higher affinity (increase in coefficient θ) of CO with Hb. We propose an adjustment accounting for individual changes in the equation relating *DLCO* to subcomponents *Dm* (membrane diffusive capacity) and *Vc* (lung capillary volume): $1/DLCO = 1/Dm + 1/\theta Vc$. We adjusted the individual *DLCO* measured in hypoxia (HA, 3269m) by interpolating the $1/DLCO$ to the sea level (SL) $1/\theta$ value. Nineteen healthy subjects were studied at SL and HA. Based on the proposed adjustment, *DLCO* increased in HA in 53% of subjects, reflecting the increase in *Dm* that largely overruled the decrease in *Vc*. We hypothesize that a decrease in *Vc* (buffering microvascular filtration) and the increase in *Dm* (possibly resulting from a decrease in thickness of the air-blood barrier) represent the anti-edemagenic adaptation of the lung to hypoxia exposure. The efficiency of this adaptation varied among subjects as *DLCO* did not change in 31% of subjects and decreased in 16%.

1. Introduction

The high affinity of carbon monoxide (CO) with hemoglobin (Hb) is used to estimate the diffusive properties of the lung (*DLCO*, $ml\,min^{-1}\,mmHg^{-1}$) and, in particular, of its subcomponents namely the diffusion capacity of the air blood barrier (*Dm*, $ml\,min^{-1}\,mmHg^{-1}$) and the volume of pulmonary capillary blood (*Vc*, *ml*) available for the binding of CO with Hb. A linear relationship between *DLCO* and its subcomponents was proposed (Roughton and Foster, 1957) as:

$$\frac{1}{DLCO} = \frac{1}{Dm} + \frac{1}{\theta \cdot [Hb] \cdot Vc} \quad (1)$$

where θ ($ml_{CO}\,min^{-1}\,mmHg^{-1}\,ml_{blood}{}^{-1}$) represents blood conductance for CO which includes diffusion inside red blood cells and reaction with Hb; [Hb] is the ratio between individual hemoglobin concentrations over reference values of hemoglobin concentration for men and women. The relationship of Eq. (1) is experimentally derived by measuring $1/DLCO$ values at increasing O_2 fraction (0.21-0.40-0.60) meant to progressively decrease the CO binding with Hb (θ). A linear regression through the $1/DLCO$ *vs* $1/\theta$ data allows to derive $1/Dm$ (the intercept) and $1/Vc$ (the slope) of Eq. (1). When measurements are done in hypoxia, due to a lower competence with O_2, more sites are available for CO to bind with Hb. Accordingly, an adjustment is required to compare *DLCO* measured in hypoxia to that measured at sea level. American (American Thoracic Society, 1995) and European (MacIntyre et al., 2005) guidelines propose correction for *DLCO* based on data obtained in normobaric hypoxia (Kanner and Crapo, 1986) according to the following equation:

$$DLCO_{adj} = DLCO_{measured} \cdot [1.0 + 0.0035 \cdot (P_AO_2 - 100)] \quad (2)$$

where P_AO_2 (*mmHg*) is alveolar oxygen partial pressure in hypobaric hypoxia. Notably, this approach by definition invalidates Eq. (1) on numerical basis as it neglects potential changes in $1/Vc$ and $1/Dm$ when moving from sea level to hypobaric hypoxia. Actually, recent work (Bartesaghi et al., 2014) emphasized inter-individual differences in $1/Vc$ and $1/Dm$ following exposure to hypobaric hypoxia. In order to maintain the validity of Eq. (1), the aim of the paper is to propose an adjustment for *DLCO* that accounts for inter-individual differences in diffusion subcomponents (slope and intercept of Eq. (1)) measured in hypobaric hypoxia. Based on this rationale we attempted an interpretation of the overall adaptive response of the lung diffusive function in hypobaric hypoxia based on a more thorough evaluation of the individual sea level features of the air-blood barrier.

* Corresponding author.
E-mail address: egidio.beretta@unimib.it (E. Beretta).

http://dx.doi.org/10.1016/j.resp.2016.08.009
1569-9048/

2. Materials and methods

2.1. Subjects

Nineteen healthy caucasian subjects (13 males, 6 females, average age 37 ± 7, BMI 22.0 ± 3.1) underwent to *DLCO* evaluation at sea level (SL, Patm 760 mmHg, P_IO_2=159 mmHg, T 21 °C, 60% relative humidity) and at high altitude (HA, 3269m, Casati Refuge, Italy; Patm 516 mmHg, P_IO_2 107 mmHg, T 21 °C, 40% relative humidity). At HA measurements were performed 6 h after reaching the refuge. The project was approved by the ethical committee of University of Milano Bicocca. Subjects were aware of the experimental procedure and signed an informed consent.

2.2. Measurement of DLCO and subcomponents

Measurement of *DLCO* and subcomponents (QUARK PFT, Cosmed, Roma, Italy) were performed in sitting position at total lung capacity (*TLC*) by single breath method by having subjects to inspire three gas mixtures containing different F_IO_2 (0.2, 0.4 and 0.6, respectively), in addition to the tracer gases (0.3% CH_4 and 0.3% CO). Alveolar volume (*VA*) was determined by CH_4 dilution. As recommended, each measurement was performed at least 6 min after the previous one in order to avoid CO-Hb accumulation. Since most of the variability in *DLCO* measurement is technical rather than physiological, the data were considered valid when *VA* values were within 5% and the regression coefficient of Eq. (1) was >0.8.

Dm and *Vc* were determined from the experimentally derived linear regression as defined by Eq. (1). A blood sample was taken in resting conditions at SL and HA to determine hemoglobin concentration and hematocrit. According to Eq. (1), *DLCO* data were referred to the ratio of individual Hb concentration to reference values for men (14.6 g/dl) and women (13.4 g/dl). This correction is obviously independent of the variability of the *Dm*/*Vc* ratio.

To comply with our previous study, we chose a $1/\theta$ value defined as (Forster, 1987):

$$\frac{1}{\theta} = 0.75 + (0.0057 \cdot P_AO_2) \quad (3)$$

where P_AO_2 (mmHg) is commonly assumed equal to the measured end tidal O_2 pressure.

In order to confirm the validity of the *DLCO* adjustment that we propose, we also considered 1/θ values provided by other references (Reeves and Park, 1992; Stam et al., 1991; Te Nijenhuis et al., 1996).

2.3. The rationale of the individual correction in hypoxia

Fig. 1 presents three cases to explain the rationale of the individual-based *DLCO* adjustment. In case A, no change in regression coefficients of Eq. (1) are hypothesized when moving from sea level (SL, closed circles) to hypobaric hypoxia (HA, open circles): the adjustment accounting for the 1/*DLCO* measured in HA (dashed arrow, for $1/\theta$=1.09 corresponding to P_AO_2 = 60 mmHg) is indicated by the shift (dotted arrow) up to $1/\theta$=1.32 (corresponding to a P_AO_2 = 100 mm Hg). In this case, the 1/*DLCO* value measured in HA is increased by the adjustment, and coincides with the SL value (continuous arrow). Accordingly, the *DLCO* value measured in hypobaric hypoxia is higher than that at SL, but after adjustment becomes equal to the SL value. Thus, in this case, HA does not result in any specific change in oxygen diffusion-transport properties of air blood barrier. For case B, a change in the regression coefficients is hypothesized in HA due to a decrease in 1/*Dm* (corresponding to an increase in *Dm*) and an increase in 1/*Vc* (thus a decrease in *Vc*). The adjustment for $1/\theta$ = 1.32 (dotted arrow) indicates that the individual-based adjusted 1/*DLCO* value is now higher than that

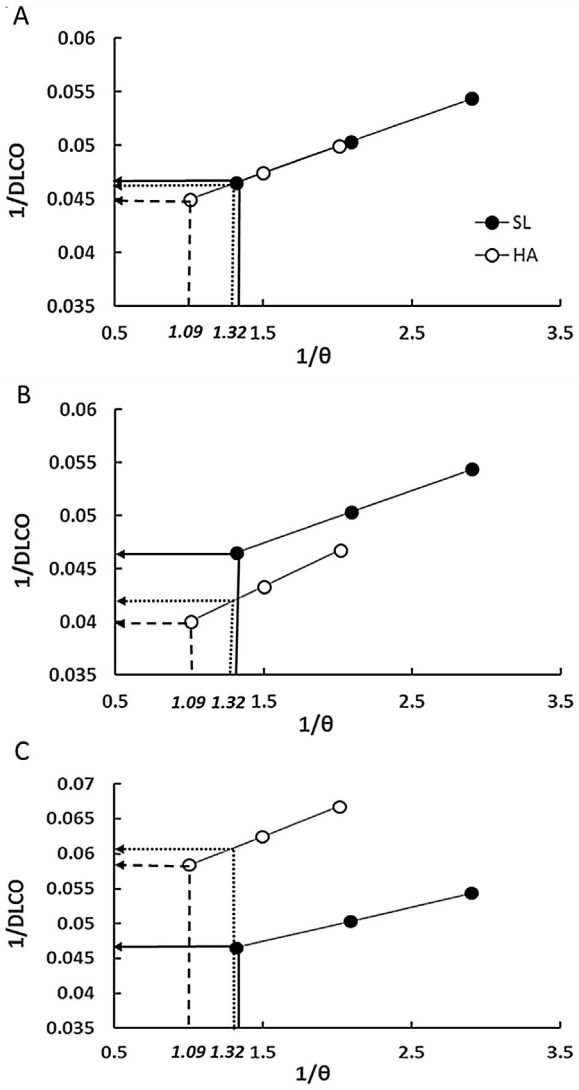

Fig. 1. Principles for the individual-based *DLCO* adjustment in hypoxia. A, B and C represent three cases to explain the concept on which the new adjustment is based considering Eq. (1) when moving from sea level (SL, closed circles) to hypoxia (HA, open circles). Continuous arrow: value of 1/*DLCO* at SL corresponding to $1/\theta$ = 1.32; dashed arrow: value of 1/*DLCO* measured at HA; dotted arrow: adjusted value of 1/*DLCO* for $1/\theta$ = 1.32. A: no change in regression coefficients of the relationship are hypothesized (continuous and dotted arrows overlap); B: shift of HA relationship below the SL one; C: shift of HA relationship above the SL one. 1/*DLCO*: mmHg min ml^{-1}; $1/\theta$: mmHg min ml_{blood} ml_{CO}^{-1}.

measured in HA, but remains lower than that measured at SL. Thus in this case the adjusted *DLCO* value in HA reveals an increase relative to SL. Finally, in case C we hypothesize an increase in 1/*Dm* and in 1/*Vc* (thus a decrease in both *Dm* and *Vc*) in HA. In this case, the adjustment reveals that HA results in an increase in 1/*DLCO*, thus a decrease in *DLCO* relative to SL.

2.4. Standard correction for DLCO in hypoxia

We wished to compare the results of the "individual based correction" to the "standard" current adjustment proposed by guidelines concerning Hb and altitude. We therefore specifically refer to a case where diffusion subcomponents are not available as *DLCO* is only measured at ambient air. Correction for Hb was done using an equation provided by Cotes et al. (1972) that assumes a constant *Dm*/*Vc* ratio equal to 0.7 We also performed Hb correction by inserting in Cotes equation individual values for *Dm*/*Vc*. Finally,

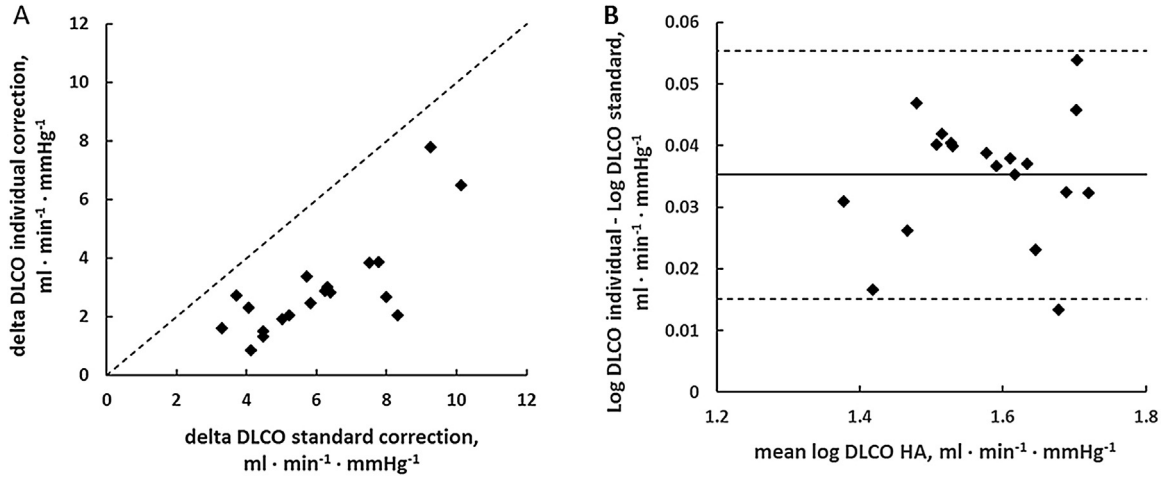

Fig. 2. Comparison between the individual-based and standard *DLCO* adjustment. A: plot of the individual-based adjustment for the *DLCO* measured in hypoxia *vs* the standard adjustment. B: Bland-Altman log plot: the solid line represents the mean difference between the logs of the two DLCO adjustment methods and dotted lines represent the 95% limits of agreement. The bias amounts to 0.035 and the corresponding antilog is 1.085. Antilog of limits of agreements are 1.035 and 1.14.

the correction for altitude was done considering Eq. (2) (MacIntyre et al., 2005).

2.5. Statistical analysis

Regression and correlation analyses were performed using the least squared residuals method. Normality test, Kurtosis and Skewness were assessed by Shapiro-Wilk test utilizing a commercially available software package (Originpro, version 2015, Origin Lab Corporation).

3. Results

3.1. Comparison between individual-based and standard DLCO adjustment

Fig. 2A shows that the standard *DLCO* adjustment (Eq. (2)) exceeds in all subjects the individual-based one (dashed line is the identity line). Fig. 2B shows the Bland-Altman log plot: the solid line represents the mean difference between the logs of the two *DLCO* adjustment methods; the bias amounts to 0.035 and dotted lines represent the 95% log limits of agreement. The antilog of the bias corresponds to 1.085, while the antilog of the limits of agreement are 1.035 and 1.14. Therefore, the standard correction overestimates *DLCO* adjustment, on the average, by 8.5% and in 95% of cases the differences in *DLCO* standard-individual adjustment are in the range 3.5-14%.

3.2. Hypobaric hypoxia induced changes on DLCO adopting the individual-based adjustment

Fig. 3 shows how the individually adjusted *DLCO* values at HA compare with the corresponding *DLCO* values at SL (dashed line is the identity line). Three groups were identified in relation to the observed change in *DLCO*, either increase (open squares), no change (open triangles) or decrease (closed circles). Overall, *DLCO* increased in about 53% of the subjects, it did not change in 31%, while it decreased in the remaining 16%.

Table 1 reports for comparison the *DLCO* adjustment, as well as the corresponding changes in *Dm* and *Vc*, calculated with different 1/θ values as from references indicated. This analysis confirms the

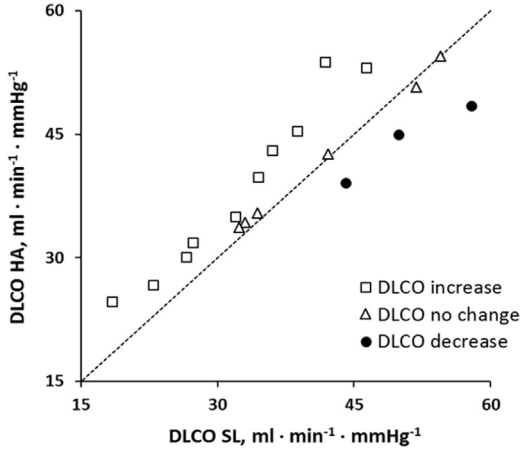

Fig. 3. Hypoxia induced changes on *DLCO* adopting the individual-based adjustment. Relationship between the individually adjusted *DLCO* values at HA *vs* the corresponding *DLCO* values at SL (dashed line is the identity line). Symbols identify groups showing increase, no change or decrease in *DLCO* on exposure to hypoxia.

grouping of the subjects concerning *DLCO* changes in HA, as well as the corresponding changes in diffusion subcomponent.

3.3. Inter-individual differences in lung diffusion properties at sea level and on exposure to hypobaric hypoxia

Fig. 4A shows that the frequency distribution of *DLCO*/*VA* at SL was normal with a coefficient of variation of 0.18; conversely, the distribution of *Dm*/*VA* at SL (Fig. 4B) was not normal due to a degree of skewness and kurtosis. Subjects in the highest range of *Dm*/*VA* are the same that in Fig. 4A lay above the 84 percentile of the normal distribution. Fig. 4C shows that the distribution of *Vc*/*VA* at SL was normal with a high coefficient of variation (0.31).

Fig. 4D–F shows the changes induced by HA on the overall distributions. For *DLCO*/*VA* (Fig. 4D) the distribution remained normal with a lower coefficient of variation (0.12) reflecting, in particular, the decrease of the highest values above 84 percentile at SL. For *Dm*/*VA* (Fig. 4E) the distribution became normal because of the remarkable decrease of the highest values occurring at SL as well as a shift of lowest values towards the mean (the mean value in HA becomes higher than the median at SL). The distribution of *Vc*/*VA*

Table 1
Percent changes of DLCO, Dm and Vc on exposure to hypobaric hypoxia calculated for different 1/θ values.

	Group *DLCO* increase			Group *DLCO* no change			Group *DLCO* decrease		
	Δ%DLCO	Δ%Dm	Δ%Vc	Δ%DLCO	Δ%Dm	Δ%Vc	Δ%DLCO	Δ%Dm	Δ%Vc
Forster	16.4 ± 7.5	46.5 ± 52.3	3.6 ± 54.9	−0.2 ± 2.9	12.4 ± 30.4	−8.1 ± 32.3	−15.6 ± 5.5	−17.7 ± 17.7	−13.4 ± 13.1
Stam	16.6 ± 7.5	19.7 ± 14.4	3.8 ± 55.0	−0.1 ± 3.1	3.0 ± 6.8	−8.1 ± 32.1	−15.6 ± 5.5	−16.0 ± 9.0	−13.6 ± 14.1
Te Nijenhuis	16.9 ± 8.0	35.2 ± 29.6	5.1 ± 56.0	−0.6 ± 3.0	6.7 ± 16.1	−9.5 ± 31.2	−16.3 ± 6.8	−16.8 ± 12.9	−12.6 ± 14.5
Reeves and Park	16.4 ± 7.5	23.1 ± 15.2	3.0 ± 53.9	−0.3 ± 3.1	2.7 ± 6.0	−8.2 ± 31.8	−15.4 ± 5.4	−18.7 ± 6.8	−13.1 ± 14.1

Forster, 1987: $1/\theta = 0.75 + 0.0057 \cdot P_AO_2$.
Stam et al., 1991: $1/\theta = 0.059 + 0.0073 \cdot P_AO_2$.
Te Nijenhuis et al., 1996: $1/\theta = 0.62 + 0.0084 \cdot P_AO_2$.
Reeves and Park, 1992: $1/\theta = 0.0156 + 0.008 \cdot P_AO_2$.

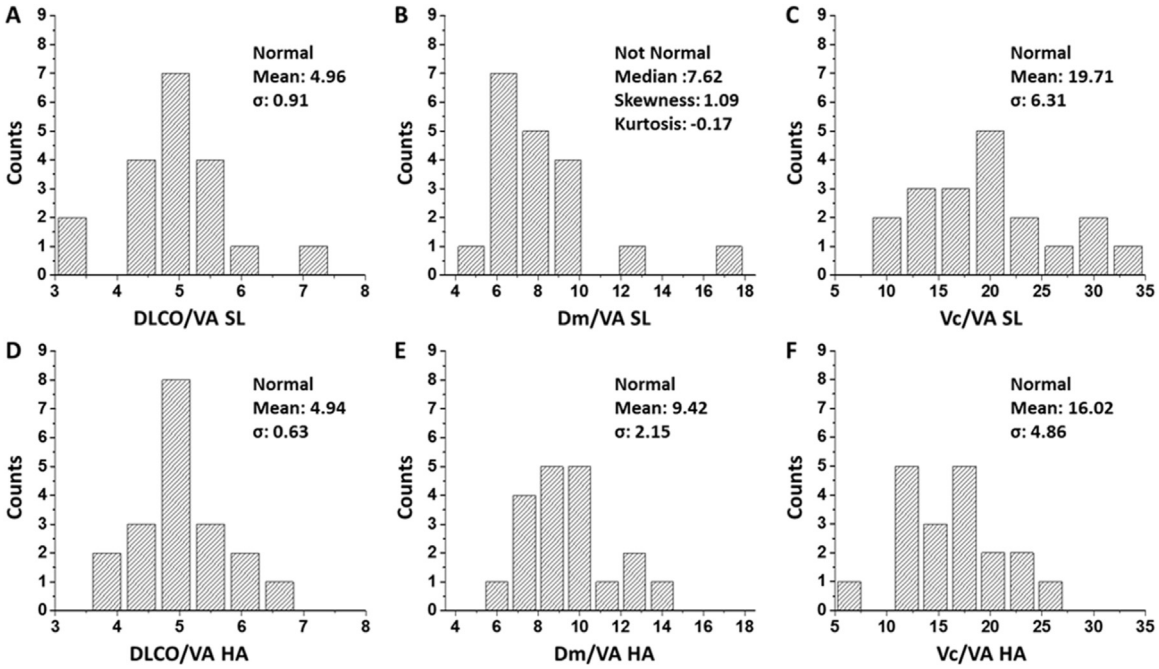

Fig. 4. Distribution of diffusion parameters at SL and HA, normalized to alveolar volume (*VA*). Distribution of *DLCO*/*VA*, *Dm*/*VA* and *Vc*/*VA* at sea level (A, B, C respectively) and in hypoxia (D, E, F respectively). *DLCO*/*VA* and *Dm*/*VA* are expressed as ml min^{-1} mmHg^{-1} L^{-1}; *Vc*/*VA* is expressed as ml L^{-1}.

(Fig. 4F) in HA remained normal but shifted to the left towards lower values with an unchanged coefficient of variation.

At SL, a significant relationship was found by plotting *DLCO* data *vs* the corresponding value of *Dm* by grouping data from all subjects (Fig. 5A); the R^2 value indicates that 75% of the variance of *DLCO* depends upon the individual *Dm* value. Conversely, Fig. 5B shows that *DLCO* poorly correlates with *Vc*. Combining data by multilinear regression analysis, *DLCO* (*ml min*$^{-1}$ *mmHg*$^{-1}$) at SL correlates with *Dm* (*m min*$^{-1}$ *mmHg*$^{-1}$) and *Vc* (*ml*) as:

$$DLCO_{SL} = 5.2 + 0.37Dm_{SL} + 0.06Vc_{SL} (R^2 = 0.88; p < 0.001) \quad (4)$$

Note that the R^2 value increases up to 0.88.

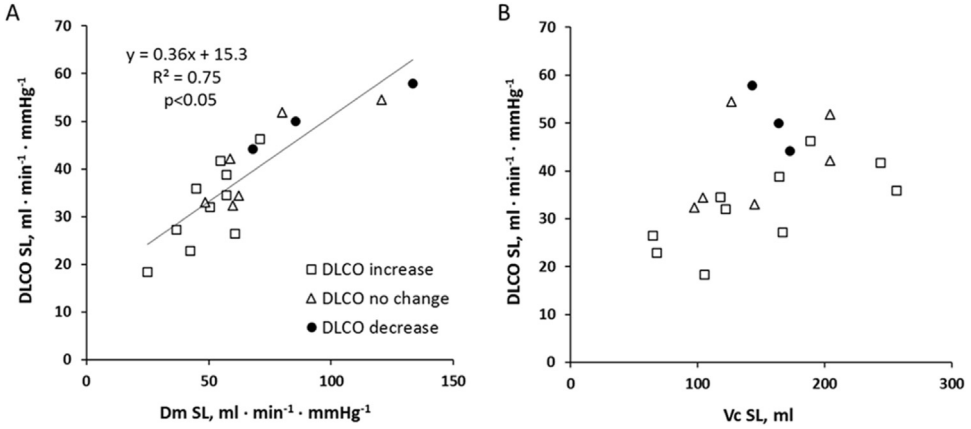

Fig. 5. Dependence of *DLCO* from its subcomponent at sea level. A: regression between *DLCO* values *vs* the corresponding value of *Dm*. B: relationship between *DLCO* values *vs* the corresponding value of *Vc*. Subject grouped as specified in Fig. 3.

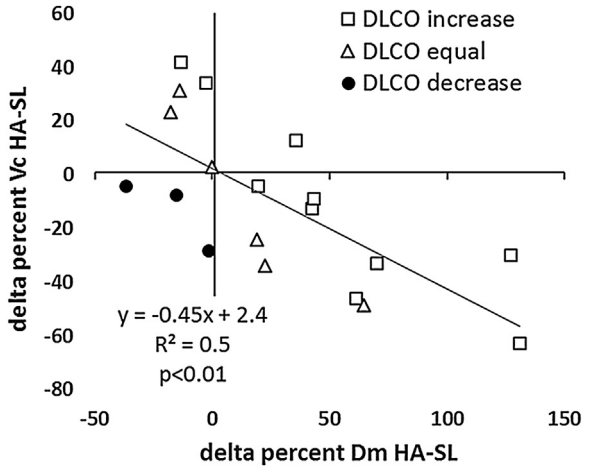

Fig. 6. Hypoxia-induced changes on *Dm* and *Vc*. Delta percent changes induced by hypoxia for *Dm vs Vc*. Subject grouped as specified in Fig. 3.

Fig. 6 reports the inverse relationship between the percent delta changes in *Vc* and *Dm* in HA. Data from the three groups were fitted by a single linear regression. Note that data relative to subjects showing a decrease in *DLCO* lay in quadrant IV.

Fig. 7A allows to appreciate that the change in *DLCO* in HA was directly proportional to the change in *Dm*, while no clear correlation could be found between the changes in *DLCO* and those of *Vc* (Fig. 7B). At individual level, it appears that a decrease in *DLCO* (closed circles) results from combined decrease of both *Dm* and *Vc*.

4. Discussion

The use of the standard adjustment to account for *DLCO* measured in hypoxia has been recommended (American Thoracic Society, 1995; MacIntyre et al., 2005) based on a linear regression obtained by plotting *DLCO* data *vs* P_AO_2 that was varied in normobaric conditions from 120 down to 80 mmHg (Kanner and Crapo, 1986); the regression coefficient of this relationship was low (0.36) due to the low number of subjects (only seven) and the large variability of individual P_AO_2 values for the same P_IO_2. Furthermore, the standard adjustment for Hb assumes a fixed *Dm*/*Vc* ratio equal to 0.7 considered as a "normal" value (Frey et al., 1990; Cotes et al., 1972). Yet, the concept of "normal" is difficult to accept as the coefficient of variation of this ratio amounts to as much as ~50 and 60% of the mean at SL and at HA, respectively. Furthermore, the influence of *Dm/Vc* ratio on Hb correction appears minimal in our subjects as the difference in *DLCO* adjusted values considering either individual *Dm/Vc* ratios or constant value at 0.7 did not exceed 2%.

In the literature, conflicting results have been reported concerning the effect of hypobaric hypoxia exposure on individual values of lung diffusion properties. *DLCO* and subcomponents have in fact been reported to either increase or decrease (Agostoni et al., 2011; de Bisschop et al., 2012; Dehnert et al., 2010; Martinot et al., 2013; Weiskopf and Severinghaus, 1972). The discussion concerning these differences essentially pivoted around exposure time and altitude and the fact of considering average values led to overlook the inter-individual differences in the adaptive response to hypoxia exposure. Such differences were in fact the object of a recent study (Bartesaghi et al., 2014) that reported considerable changes in diffusion subcomponents on exposing subjects to a mild degree of hypobaric hypoxia (P_IO_2 107 mmHg). Based on such differences, the individual-based adjustment that we propose allows now to discuss the potential mechanisms leading to the changes in lung diffusion properties occurring in hypobaric hypoxia, as well as their relationship with the individual morpho-functional features of the air blood barrier at SL.

As data from Fig. 2 show, the standard adjustment overestimates the effect of a greater CO binding to Hb in hypobaric hypoxia, resulting therefore in an abnormal decrease in *DLCO* compared to the SL value. Furthermore, the Bland Altman log plot indicates that the two methods of adjustments are not interchangeable due to an average overestimation of about 10% by the standard adjustment.

4.1. Lung diffusion properties at SL

The value of *DLCO* at SL (Fig. 4A) is proportional to the corresponding *Dm* value (Fig. 5A). On morpho-functional ground, *Dm* might be considered as directly proportional to the surface (*Salv*) of the air blood barrier contributing to gas diffusion and inversely proportional to its thickness (τ), thus $Dm \propto Salv/\tau$. Accordingly, a high *Dm* value might reflect a high number of alveoli and/or a thinner air blood barrier. Although the dependence of *DLCO* on *Vc* appears weaker (Fig. 5B), the inter-individual morphological differences of air blood barrier reflect both the total alveolar number as well as the density of the capillary network supplying the alveoli. Based on the multilinear regression, the relative weight of *Dm* is 6-times greater than that of *Vc* in affecting changes of *DLCO* (Eq. (4)).

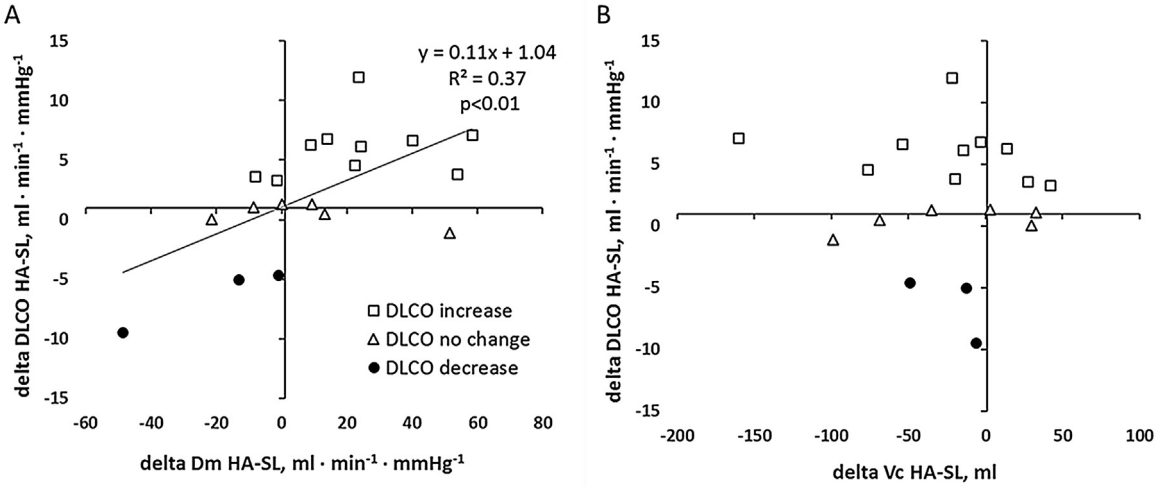

Fig. 7. Dependence of hypoxia-induced *DLCO* delta changes on the corresponding delta changes in its subcomponents. A: changes in *DLCO vs* the corresponding changes in *Dm*. B: changes in *DLCO vs* the corresponding changes in *Vc*. Subject grouped as specified in Fig. 3.

4.2. Lung diffusion adaptive response to HA

An important result of the paper is the opposite changes in *Dm* and *Vc* (Fig. 6) following exposure to HA. This finding is supported by the comparison proposed in Table 1, where different values of $1/\theta$ were adopted. One can recall that inter-individual differences in *Dm*/*Vc* ratio already exist at sea level (Miserocchi et al., 2008; Bartesaghi et al., 2014) and have been interpreted as inborn morpho-functional features of the air-blood barrier, in line with the finding by Aguilaniu et al. (2008) who was unable to relate *Dm*/*Vc* ratio to any covariate. One may comment that the opposite changes in *Dm* and *Vc* reveal a condition of functional adaptation that differs from a pathological condition such as frank edema or atelectasis, where a parallel decrease in *Dm* and *Vc* would maintain *Dm*/*Vc* ratio constant.

We wish to discuss the changes in *Dm*/*Vc* ratio in terms of the anti-edemagenic adaptive response of the lung to counteract an edemagenic condition as occurring on exposure to hypobaric hypoxia (Miserocchi et al., 2001). The decrease in *Vc* implies a parallel decrease in capillary surface that, in turn, would limit microvascular filtration and thus may be regarded as a protective factor against perturbation of lung-water balance. The decrease in *Vc* is in line with the observed increase in intrapulmonary shunting in response to hypoxia, favored by pre-capillary vasoconstriction (Tremblay et al., 2015). Recently, the decrease in alveolar perfusion has been interpreted as the mechanical consequence of the increase in peri-microvascular interstitial pressure during development of interstitial edema (Mazzuca et al., 2016).

The increase in *Dm* (Fig. 7A) that, by and large, overruled the decrease in *Vc* (Fig. 7C) led to an increase in *DLCO* in HA in the majority of subjects (53%, Fig. 3A). It is not surprising that relatively large changes in *Dm* result in minor changes in *DLCO*, though this damping is the mathematical consequence of Eq. (1). An increase in *DLCO* is obviously an advantage in hypoxia as it buffers a restriction in oxygen diffusion due to a decrease in alveolar-venous blood oxygen partial pressure gradient. To explain the increase in *Dm* appears challenging. Yet, it is noteworthy that in interstitial edema a non-homogeneous distribution of extravascular water was found in the thin portion of the air blood barrier, specifically devoted to gas exchange. Indeed, for an increase in extravascular lung water not exceeding 10%, liquid accumulated in endothelial cellular blebs (Conforti et al., 2002; Palestini et al., 2002) resulting in a concomitant thinning of the remaining part of the air blood barrier. In this condition, a realistic estimate of τ was provided by the *harmonic mean* thickness of the tissue-plasma barrier that, compared to the arithmetic and geometric mean, tends to mitigate the impact of the few large outliers (the blebs) and increase the impact of the majority of small ones (Weibel and Knight, 1964; Weibel et al., 1993). The critical dependence of *Dm* from τ is confirmed by the model recently presented by Kang and Sapoval (2016) showing that the diffusion time for CO from alveolar space to Hb molecules is proportional to 1.56 power of the total barrier thickness. In summary, the anti-edemaginic response of the lung may reside in a decrease in τ (favoring an increase in *Dm*) and *Vc* (buffering microvascular filtration).

Clearly, the efficiency of the above anti-edemagenic mechanisms varies among subjects, as *DLCO* did not change in 31% of them and decreased in 16%. This last figure compares well with previously reported data for subjects showing interstitial edema on ascent to 4559 m (15%, (Cremona et al., 2002)) and to 4700 m (12%, (Ge et al., 1997)). In subjects showing no change in *DLCO* in HA a functional balance occurred between the opposite changes in *Dm* and *Vc*. Conversely, subjects decreasing *DLCO* on HA showed a decrease both in *Dm* and in *Vc* (Fig. 6C, quadrant IV); these subjects had a *DLCO* value at SL above 84% percentile, reflecting the highest values of *Dm*, while the corresponding *Vc* values were close to the mean. Possibly, these subjects might be devoid of a high number of alveoli and/or thinner septa. One may speculate that in these subjects the decrease in *Vc* did not fully buffer the edemagenic condition, as a consequence of a high microvascular permeability, as hypothesized by Bartesaghi et al. (2014). It appears tempting to consider the decrease in both *Dm* and *Vc*, and thus in *DLCO*, on exposure to a modest degree of hypoxia as index of individual proneness to develop lung edema.

Conflict of interest

The authors declare that they have no conflict of interest.

Acknowledgments

Financial support by the University of Milano Bicocca, Sports Medicine School Fund and from Resamont 2 project.

References

Agostoni, P., Swenson, E.R., Bussotti, M., Revera, M., Meriggi, P., Faini, A., Lombardi, C., Bilo, G., Giuliano, A., Bonacina, D., Modesti, P.A., Mancia, G., Parati, G., 2011. HIGHCARE investigators, high-altitude exposure of three weeks duration increases lung diffusing capacity in humans. J. Appl. Physiol. 110, 1564–1571, http://dx.doi.org/10.1152/japplphysiol.01167.2010.

Aguilaniu, B., Maitre, J., Glénet, S., Gegout-Petit, A., Guénard, H., 2008. European reference equations for CO and NO lung transfer. Eur. Respir. J. 31, 1091–1097, http://dx.doi.org/10.1183/09031936.00063207.

American Thoracic Society, 1995. Single-breath carbon monoxide diffusing capacity (transfer factor) recommendations for a standard technique–1995 update. Am. J. Respir Crit. Care Med 152, 2185–2198.

Bartesaghi, M., Beretta, E., Pollastri, L., Scotti, V., Mandolesi, G., Lanfranconi, F., Miserocchi, G., 2014. Inter-individual differences in control of alveolar capillary blood volume in exercise and hypoxia. Respir. Physiol. Neurobiol. 190, 96–104, http://dx.doi.org/10.1016/j.resp.2013.08.021.

Conforti, E., Fenoglio, C., Bernocchi, G., Bruschi, O., Miserocchi, G., 2002. Morpho-functional analysis of lung tissue in mild interstitial edema. Am. J. Physiol. Lung. Cell Mol. Physiol. 282, L766–774, http://dx.doi.org/10.1152/ajplung.00313.2001.

Cotes, J.E., Dabbs, J.M., Elwood, P.C., Hall, A.M., McDonald, A., Saunders, M.J., 1972. Iron-deficiency anaemia: its effect on transfer factor for the lung (diffusiong capacity) and ventilation and cardiac frequency during sub-maximal exercise. Clin. Sci. 42, 325–335.

Cremona, G., Asnaghi, R., Baderna, P., Brunetto, A., Brutsaert, T., Cavallaro, C., Clark, T.M., Cogo, A., Donis, R., Lanfranchi, P., Luks, A., Novello, N., Panzetta, S., Perini, L., Putnam, M., Spagnolatti, L., Wagner, H., Wagner, P.D., 2002. Pulmonary extravascular fluid accumulation in recreational climbers: a prospective study. Lancet 359, 303–309, http://dx.doi.org/10.1016/S0140-6736(02)07496-2.

Dehnert, C., Luks, A.M., Schendler, G., Menold, E., Berger, M.M., Mairbäurl, H., Faoro, V., Bailey, D.M., Castell, C., Hahn, G., Vock, P., Swenson, E.R., Bärtsch, P., 2010. No evidence for interstitial lung oedema by extensive pulmonary function testing at 4,559 m. Eur. Respir. J. 35, 812–820, http://dx.doi.org/10.1183/09031936.00185808.

Forster, R.E., 1987. Diffusion of gases across the alveolar membrane. In: Fishman, A.P., Fahri, L.E., Tenney, S.M., Geiger, S.R. (Eds.), Handbook of Physiology, Section 3:The Respiratory System. Vol IV: Gas Exchange. Chapt 5. American Physiological Society, Washington, DC, pp. 71–88.

Frey, T.M., Crapo, R.O., Jensen, R.L., Kanner, R.E., Kass, J.E., Castriotta, R.J., Mohsenifar, Z., 1990. Adjustment of DLCO for varying COHb, and alveolar PO2 using a theoretical adjustment equation. Respir. Physiol. 81, 303–311.

Ge, R.L., Matsuzawa, Y., Takeoka, M., Kubo, K., Sekiguchi, M., Kobayashi, T., 1997. Low pulmonary diffusing capacity in subjects with acute mountain sickness. Chest 111, 58–64, http://dx.doi.org/10.1378/chest.111.1.58.

Kang, M.Y., Sapoval, B., 2016. Time-based understanding of DLCO and DLNO. Respir. Physiol. Neurobiol. 225, 48–59, http://dx.doi.org/10.1016/j.resp.2016.01.008.

Kanner, R.E., Crapo, R.O., 1986. The relationship between alveolar oxygen tension and the single-breath carbon monoxide diffusing capacity. Am. Rev. Respir. Dis. 133, 676–678, http://dx.doi.org/10.1164/arrd.1986.133.4.676.

MacIntyre, N., Crapo, R.O., Viegi, G., Johnson, D.C., van der Grinten, C.P.M., Brusasco, V., Burgos, F., Casaburi, R., Coates, A., Enright, P., Gustafsson, P., Hankinson, J., Jensen, R., McKay, R., Miller, M.R., Navajas, D., Pedersen, O.F., Pellegrino, R., Wanger, J., 2005. Standardization of the single breath determination of carbon monoxide uptake. Eur. Respir. J. 26, 720–735, http://dx.doi.org/10.1183/09031936.05.00034905.

Martinot, J.B., Mulè, M., de Bisschop, C., Overbeek, M.J., Le-Dong, N.N., Naeije, R., Guénard, H., 2013. Lung membrane conductance and capillary volume derived from the NO and CO transfer in high-altitude newcomers. J. Appl. Physiol. 115, 157–166, http://dx.doi.org/10.1152/japplphysiol.01455.2012.

Mazzuca, E., Aliverti, A., Miserocchi, G., 2016. Computational micro-scale model of control of extravascular water and capillary perfusion in the air blood barrier. J.

Theor. Biol., http://dx.doi.org/10.1016/j.jtbi.2016.03.036 (pii. S0022-5193, 30012-1).
Miserocchi, G., Passi, A., Negrini, D., Del Fabbro, M., De Luca, G., 2001. Pulmonary interstitial pressure and tissue matrix structure in acute hypoxia. Am. J. Physiol. Lung Cell. Mol. Physiol. 280, L881–887.
Miserocchi, G., Messinesi, G., Tana, F., Passoni, E., Adamo, S., Romano, R., Beretta, E., 2008. Mechanisms behind inter-individual differences in lung diffusing capacity. Eur. J. Appl. Physiol. 102, 561–568, http://dx.doi.org/10.1007/s00421-007-0625-2.
Palestini, P., Calvi, C., Conforti, E., Botto, L., Fenoglio, C., Miserocchi, G., 2002. Composition, biophysical properties, and morphometry of plasma membranes in pulmonary interstitial edema. Am. J. Physiol. Lung Cell. Mol. Physiol. 282, L1382–1390, http://dx.doi.org/10.1152/ajplung.00447.2001.
Reeves, R.B., Park, H.K., 1992. CO uptake kinetics of red cells and CO diffusing capacity. Respir. Physiol. 88, 1–21.
Roughton, F., Foster, R., 1957. Relative importance of diffusion and chemical reaction rates in determining rate of exchange of gases in the human lung with special reference to true diffusing capacity of pulmonary membrane and volume of blood in the lung capillaries. J. Appl. Physiol. 11, 290–302.
Stam, H., Kreuzer, F.J., Versprille, A., 1991. Effect of lung volume and positional changes on pulmonary diffusing capacity and its components. J. Appl. Physiol. 71, 1477–1488.
Te Nijenhuis, F.C., Lin, L., Moens, G.H., Versprille, A., Forster, R.E., 1996. Rate of uptake of CO by hemoglobin in pig erythrocytes as a function of PO2. J. Appl. Physiol. 81, 1544–1549.
Tremblay, J.C., Lovering, A.T., Ainslie, P.N., Stembridge, M., Burgess, K.R., Bakker, A., Donnelly, J., Lucas, S.J., Lewis, N.C., Dominelli, P.B., Henderson, W.R., Dominelli, G.S., Sheel, A.W., Foster, G.E., 2015. Hypoxia, not pulmonary vascular pressure, induces blood flow through intrapulmonary arteriovenous anastomoses. J. Physiol. 593, 723–737, http://dx.doi.org/10.1113/jphysiol.2014.282962.
Weibel, E.R., Knight, B.W., 1964. A morphometric study on the thickness of the pulmonary air-blood barrier. J. Cell Biol. 21, 367–384.
Weibel, E.R., Federspiel, W.J., Fryder-Doffey, F., Hsia, C.C., König, M., Stalder-Navarro, V., Vock, R., 1993. Morphometric model for pulmonary diffusing capacity: I. Membrane diffusing capacity. Respir. Physiol. 93, 125–149.
Weiskopf, R.B., Severinghaus, J.W., 1972. Diffusing capacity of the lung for CO in man during acute acclimation to 14,246 ft. J. Appl. Physiol. 32, 285–289.
de Bisschop, C., Martinot, J.B., Leurquin-Sterk, G., Faoro, V., Guénard, H., Naeije, R., 2012. Improvement in lung diffusion by endothelin a receptor blockade at highaltitude. J. Appl. Physiol. 112, 20–25, http://dx.doi.org/10.1152/japplphysiol.00670.2011.

MANUSCRIPTS IN PREPARATION

Enhanced peripheral O_2 diffusion by hyperoxia and right-shifted O_2-Hb dissociation curve slows down skeletal muscle $\dot{V}O_2$ kinetics to $\dot{V}O_{2max}$

Bruno Grassi[1,2], Michael C. Hogan[3], William G. Aschenbach[4], Hailu K. Alemayehu[1], Jason J. Hamann[4], Kevin M. Kelley[4], Peter D. Wagner[3], L. Bruce Gladden[4]

1) Department of Medicine, University of Udine, Udine, Italy; 2) Institute of Bioimaging and Molecular Physiology, National Research Council, Milano, Italy; 3) Department of Medicine, University of California San Diego, La Jolla, CA, USA; 4) School of Kinesiology, Auburn University, Auburn, AL, USA.

Corresponding author:
Bruno Grassi, MD PhD
Department of Medicine
University of Udine
Piazzale M. Kolbe 4
I – 33100 Udine; Italy
Tel. +39-0432-494335
E-mail bruno.grassi@uniud.it

ABSTRACT

251

During transitions from rest to contractions of peak metabolic intensity ($\dot{V}O_{2peak}$) enhancement of diffusive O_2 delivery could determine faster skeletal muscle O_2 uptake ($\dot{V}O_2$) kinetics and less fatigue. Isolated canine gastrocnemius muscles *in situ* (n=6) were studied during transitions from rest to 4-min electrically stimulated isometric tetanic contractions corresponding to $\dot{V}O_{2peak}$. Two conditions were compared: 1) normoxia (CTRL); 2) hyperoxia (FIO_2=1.00) + administration of a drug (RSR-13) which right-shifts the Hb-O_2 dissociation curve (Hyperoxia+RSR13). In both conditions muscle was pump-perfused with a constantly elevated blood flow ($\dot{Q}$) and adenosine was infused for vasodilation; arterial (CaO_2) and venous (CvO_2) O_2 concentrations were determined at rest and at 5-7 s intervals during contractions. $\dot{V}O_2$ was calculated as $\dot{Q}\cdot C(a\text{-}v)O_2$. The PO_2 at which 50% of Hb is saturated (P_{50}) and the mean capillary PO_2 ($PcapO_2$) were calculated, respectively, by the Hill equation and by a numerical integration technique. Muscle force (F) and the fatigue index (final/initial F) were not different in the two conditions. P_{50} and $PcapO_2$ were significantly higher (both $P<0.01$) in Hyperoxia+RSR (42.3±6.7 and 218.0±72.6 mmHg, respectively) *vs.* CTRL (32.9±1.9 and 49.0±4.1). $\dot{V}O_2$ kinetics, evaluated by a monoexponential fitting, were slower in Hyperoxia+RSR13 *vs.* CTRL (time delay, TD: 4.4±2.2 *vs.* 9.9±1.7 [x± SD] s [P=0.001]; tau: 12.3±1.9 *vs.* 13.7±4.3 [P=0.373]; mean response time: 16.7±3.2 *vs.* 23.6±3.5 [P=0.003], as a consequence of the longer TD. The delayed $\dot{V}O_2$ kinetics was presumably due to an increased utilization of intramuscular O_2 stores (greater in hyperoxia) and to a delayed activation of oxidative phosphorylation.

INTRODUCTION

During everyday life skeletal muscles continuously face changes in metabolic demand. The intrinsic nature of bioenergetics mechanisms dictates that, following a sudden increase in energy expenditure, skeletal muscle oxidative metabolism is relatively slow to adjust, and follows a kinetics that is usually termed O_2 uptake ($\dot{V}O_2$) "kinetics" (Cerretelli & di Prampero 1986). Innumerable papers and several recent reviews (see *e.g.* Rossiter 2011, Poole & Jones 2012, Murias et al. 2014) have discussed the main characteristics of these kinetics, their relevance in terms of the mechanisms of metabolic regulation and their functional consequences, in physiological and pathological conditions and in sports activities. A slower adjustment of $\dot{V}O_2$ is associated with a greater O_2 deficit, a greater reliance on substrate level phosphorylation, a greater disturbance of "metabolic stability" (Grassi et al. 2011*a*, 2015), resulting in an impaired exercise tolerance.

In the search of the factors dictating the rate of $\dot{V}O_2$ adjustment during metabolic transitions, some years ago our group performed a series of experiments on the isolated dog gastrocnemius preparation (Grassi et al. 1998*a*, 1998*b*, 2000, 2002, 2005, 2011*b*; Zoladz et al. 2008; Goodwin et al. 2012), following the pioneering work on muscle $\dot{V}O_2$ kinetics in that model by Piiper et al. (1968). By allowing the experimental manipulation of convective and diffusive O_2 delivery to the contracting muscle, the studies provided evidence in support of the "tipping point" concept proposed by Poole & Jones (2012): starting from a baseline of "normal" O_2 availability, during transitions from rest to contractions of submaximal intensity the enhancement of convective (Grassi et al. 1998*a*) and diffusive (Grassi et al. 1998*b*) O_2 delivery did not significantly affect skeletal muscle $\dot{V}O_2$ kinetics, suggesting that the latter is mainly dictated by a delayed metabolic activation of oxidative phosphorylation (Grassi 2005). This concept is rather well accepted (Rossiter 2011, Poole & Jones 2012), with some notable exceptions (Murias et al. 2014). More specifically, the delayed activation of oxidative phosphorylation would

be associated with a temporal buffering of energy provision associated with creatine kinase (CK) activity and PCr breakdown (Grassi et al. 2011*b*). On the other hand, a lower than normal O_2 availability (as it may occur in hypoxia or in pathological conditions) would determine a slower muscle $\dot{V}O_2$ kinetics (Goodwin et al. 2012).

The *scenario* could be slightly complicated by the issue of the metabolic intensity of the contractions/exercise. During transitions to contractions corresponding to peak $\dot{V}O_2$ ($\dot{V}O_{2peak}$) convective O_2 delivery played indeed a relatively minor, although significant, role (Grassi et al. 2000), and its enhancement determined a slightly faster muscle $\dot{V}O_2$ kinetics, a smaller O_2 deficit and less fatigue. Thus, in physiological conditions a limiting role of O_2 availability, although relatively minor, could be present during maximal, but not during submaximal contractions.

A "piece of the puzzle" is missing from these earlier studies (Grassi et al. 1998*a*, 1998*b*, 2000): the role of diffusive O_2 delivery during transitions to contractions of maximal metabolic intensity. The aim of the present study was to fill this gap. More specifically, we hypothesized that, starting from a baseline of enhanced convective O_2 delivery (constantly elevated blood flow plus the administration of a vasodilatory drug), during transitions from rest to contractions of maximal metabolic intensity the experimental enhancement of diffusive O_2 delivery (by hyperoxic breathing and by the pharmacological induction of a right-shift of the oxy-hemoglobin dissociation curve [ODC]) would determine faster muscle $\dot{V}O_2$ kinetics and less fatigue. This would confirm a role by O_2 availability in dictating, at least in part, muscle $\dot{V}O_2$ kinetics during maximal contractions.

METHODS

The study was conducted with the approval of the Institutional Animal Care and Use Committee of Auburn University, Auburn, Alabama (USA), where the experiments were performed. Six adult mongrel dogs of either sex (body mass

19.3 ± 4.4 kg, mean ± SD) were anesthetized with pentobarbital sodium (30 mg kg^{-1}), with maintenance doses given as required to maintain a deep plane of surgical anaesthesia, as indicated by a complete absence of pedal, palpebral and corneal reflexes. The dogs were intubated with an endotracheal tube and ventilated with a respirator (Model 613, Harvard). The rectal temperature was maintained at ~37 °C with a heating pad and a heating lamp. After surgical preparation the animals were treated with heparin (1,500 U kg^{-1}). Ventilation was maintained at a level that produced normal values of arterial O_2 and CO_2 partial pressures.

***Surgical preparation*.** The gastrocnemius muscle complex (gastrocnemius + superficial digital flexor), for convenience referred to as "gastrocnemius", was isolated as described previously (Stainsby & Welch 1966). Briefly, a medial incision was made through the skin of the left hindlimb from midthigh to the ankle. The insertion tendons of the sartorius, gracilis, semitendinosus and semimembranosus muscles were cut to allow these muscles to be folded back to expose the gastrocnemius. To isolate the venous outflow from the gastrocnemius, all the vessels draining into the popliteal vein, except those from the gastrocnemius, were ligated. The popliteal vein was cannulated, and the venous outflow was returned to the animal via a jugular reservoir. Venous outflow was returned to the animal via a reservoir attached to a cannula in the left jugular vein. The arterial circulation to the gastrocnemius was isolated by ligating all vessels from the femoral and popliteal artery that did not enter the gastrocnemius. The right femoral artery was also isolated and cannulated for obtaining blood samples. Blood from this artery was passed through tubing to a roller pump (Cole-Parmer Masterflex, Model No. 7520-25, Head Model No. 7016-20) and then through another cannula into the contralateral, isolated popliteal artery supplying the gastrocnemius. Y-connectors positioned before and after the pump allowed either spontaneous perfusion of the gastrocnemius, at the animal's own blood pressure, or controlled flow at any

desired level by adjusting the pump setting. A T-connector in the tubing to the gastrocnemius was connected to a pressure transducer (Narco Biosystems, Model RP-1500) for measurement of muscle perfusion pressure. Arterial blood samples were taken from another T-connector in the cannula exiting the right femoral artery prior to the roller pump.

A portion of the calcaneus, with the two tendons from the gastrocnemius attached, was cut away at the heel and clamped around a metal rod for connection to an isometric myograph via a load cell (Interface SM-250) and a universal joint coupler. The universal joint allowed the muscle to always pull directly in line with the load cell, and thus prevented the application of torque to the cell. The other end of the muscle was left attached to its origin; both the femur and the tibia were fixed to the base of the myograph by bone nails. A turnbuckle strut was placed parallel to the muscle between the tibial bone nail and the arm of the myograph to minimize flexing of the myograph.

The sciatic nerve, which innervates the gastrocnemius, was exposed and isolated near the muscle, doubly ligated and cut between the ties. The distal stump of the nerve, ~1.5-3.0 cm in length, was pulled through a small epoxy electrode containing two wire loops for stimulation. The muscle was covered with saline-soaked gauze and a thin plastic sheet to prevent drying and cooling.

***Experimental design*.** To evoke muscle contractions, the nerve was stimulated by supramaximal square pulses of 4.0-6.0 V amplitude and 0.2 ms duration (Grass S48 stimulator), isolated from ground by a stimulus isolator (Grass SIU8TB). Before each experiment, the muscle was set at optimal length by progressively lengthening the muscle as it was stimulated at a rate of 0.2 Hz, until a peak in developed tension (total tension minus resting tension) was obtained. For the experiments, isometric tetanic contractions were triggered by stimulation with trains of stimuli (4-6 V, 200 ms duration, 50 Hz frequency) at a rate of 1 contraction s^{-1} for a 4-min period. Based on studies of peak $\dot{V}O_2$ in this model

(Kelley et al. 1996, Ameredes et al. 1998), this stimulation pattern should have elicited about 100% of peak metabolic rate for this muscle in the current experiments.

Tetanic contractions were chosen in order to allow a rapid attainment of a steady-state of developed force. Each isometric tetanic contraction lasted 200 ms, and was separated from the following by 1.8 s, during which the muscle was relaxing or relaxed.

For each dog, the experiment consisted of two contraction periods of 4-min duration, preceded by a resting baseline. The contraction periods were separated by at least 35 min of rest. The metabolic transition studied was therefore a rest-to-maximal contractions transition.

Two conditions were compared: 1) A control condition (CTRL), in which the dogs breathed room air and the muscle was pump-perfused at a constant $\dot{Q}$, adjusted 15-30 s before the start of the contraction to a level exceeding that attained in the steady-state of contractions, as determined in a preliminary trial with spontaneous adjustment of $\dot{Q}$. When the blood supply to the gastrocnemius was switched from self-perfused to pump-perfused, at least 15 min were allowed for the hemodynamic parameters to stabilize. In CTRL, 10 mL of saline solution were also infused intravenously over ~3 min before contraction onset. 2) A "treatment" condition (Hyperoxia+RSR13), in which $\dot{Q}$ adjustment was the same described for CTRL, but the dogs inspired from a bag containing 100% O_2, and an intra-arterial administration, over about 15 min before the contraction period, of about 100 ml of half-normal saline solution containing 100 mg kg^{-1} body mass of the sodium salt of the drug 2-(4-{[(3,5-dimethylanilino)carbonyl]methyl}phenoxy)-2-methypropionic acid (RSR13, Allos Therapeutics), an allosteric inhibitor of O_2 binding to hemoglobin (Abraham et al. 1992), was performed. This drug, administred at the same dosage ad in the same experimental preparation as those in the present study, has been previously shown to induce a significant rightward shift of the ODC (Grassi et al. 1998*b*, Richardson et al. 1998) and increase $\dot{V}O_{2max}$

(Richardson et al. 1998), whereas it did not affect muscle $\dot{V}O_2$ kinetics during transitions to contractions of submaximal intensity (Grassi et al. 1998*b*). The order of experimental conditions could not be randomized, because of the duration of the RSR13 effects. In both experimental conditions, to prevent vasoconstriction and inordinate pressure increases with the elevated $\dot{Q}$, 1-2 ml · min^{-1} of a 10^{-2} M adenosine solution (in normal saline) was also infused intra-arterially by a pump, beginning from 15-30 s before the onset of contractions. The adenosine infusion was then continued throughout the contraction period. This dosage of the drug was previously shown to be effective in obtaining a significant vasodilation at the muscle level without causing significant metabolic effects (such as changes in resting $\dot{V}O_2$, $\dot{V}O_2$ at the same submaximal level of contraction, $\dot{V}O_{2peak}$, acid-base status) (Grassi et al. 1998*a*; Grassi et al. 1998*b*; Grassi et al. 2000; Grassi et al. 2011*b*).

We have previously demonstrated in this *in situ* muscle model (Grassi et al. 1998*a*, Grassi et al. 1998*b*, Grassi et al. 2011*b*) that, given sufficient recovery, contractile protocols can be repeated with identical bioenergetics results. The pump-perfused elevated $\dot{Q}$ and adenosine infusion prevented the peripheral vasoconstriction and the reduced $\dot{Q}$ described after the administration of other allosteric inhibitors of O_2-Hb binding (Liard et al. 1993). Muscle perfusion pressure and muscle vascular resistance (see Measurements) where indeed not significantly different in Hyperoxia+RSR-13 compared to CTRL.

At the end of the experiments the dogs were sacrificed with an overdose of pentobarbital. The gastrocnemius was excised and weighed, and the value used to normalize variables per unit of muscle mass, where appropriate.

Measurements. Output from the pressure transducer was recorded on a strip chart recorder while outputs from the load cell and flowmeter (T206, Transonic Systems) were fed through strain gauge and transducer couplers, respectively, into a computerized (PowerComputing PowerBase 240 Macintosh clone) data

acquisition system (GW Instruments Inc., SuperScope II and InstruNet Model 100B D/A input/output system). The load cell reaches 90% of full response within 1 ms, while the flowmeter was set to its highest pulsatile cutoff frequency of 100 Hz; both signals were sampled at a rate of 100 Hz by the computerized data acquisition system. The load cell was calibrated with known weights prior to each experiment. The flowmeter was calibrated with a graduated cylinder and clock during and after each experiment. Vascular resistance was calculated as muscle perfusion pressure (BP_m) divided by $\dot{Q}$.

Peak force was determined for each contraction. The fatigue index (FI) at time *x* was determined as the ratio between peak force determined at time *x* and mean peak force values determined during the first 3 contractions.

Samples of arterial blood entering the muscle and of venous blood from the popliteal vein were drawn anaerobically in heparinized syringes. Since the arterial values varied only slightly throughout each experiment, arterial samples were taken at rest, before the contractions and immediately after the contraction periods. A polyethylene tube (0.8 mm ID, 37 cm length, 0.25 ml total volume including luer hub) was threaded into the popliteal vein cannula to the point where the vein exited the gastrocnemius. This allowed collection of venous blood immediately draining from the muscle. Venous samples were taken at rest (~10 s before the onset of contractions), every 5-7 s during the first 75 s of contractions, and every 30-45 s thereafter until the end of the contraction period. The precise time of each venous sample was recorded.

Blood samples were immediately stored in iced water and analyzed within 30 min of collection. Both arterial and venous blood samples were analyzed at 37 °C for PO_2, PCO_2 and pH by a blood gas, pH, electrolytes, metabolites analyzer (GEM Premier 3000, Instrumentation Laboratories, Lexington, MA), and for hemoglobin concentration ([Hb]) and percent saturation of Hb (SO_2, %) with a CO-Oximeter (IL 682, Instrumentation Laboratories, Lexington, MA), set for dog blood. These

instruments were calibrated before and during each experiment. Dissolved O_2 was also accounted for in the calculation of blood O_2 concentration.

Arterial and venous values of PO_2 and SO_2 were utilized (after correction for temperature, PCO_2 and pH) to plot the ODC for the two conditions. The PO_2 at which 50% of Hb is saturated (P_{50}) was then calculated by using the Hill equation. $\dot{V}O_2$ of the gastrocnemius was calculated by Fick's principle as $\dot{V}O_2 = \dot{Q} \cdot C(a\text{-}v)O_2$, where $C(a\text{-}v)O_2$ is the difference in O_2 concentration between arterial blood (CaO_2) and venous blood (CvO_2). $\dot{V}O_2$ was calculated at discrete time intervals corresponding to the timing of the blood samples. $\dot{V}O_2$ data were also normalized per unit of peak force (see Zoladz et al. 2008), and expressed as ml min^{-1} N^{-1}.

Analysis of $\dot{V}O_2$ kinetics. $\dot{V}O_2$ data were fitted by 3 equations, *i.e.* by equation 1, equation 2 and equation 3. Equation 1 was of the type:

$$y(t) = yBAS + A \cdot [1 - e^{-(t - TDf) / \tau f}] \quad (1)$$

In this equation, y*BAS* indicates the baseline value obtained at rest before contraction onset, A*f* indicates the amplitude between y*BAS* and the steady-state value at the end of the contraction period, TD*f* the time delay and τf the time constant of the function. The suffix *f* indicates that these parameters relate to the "fundamental" component of the $\dot{V}O_2$ kinetics (Rossiter et al. 2011, Poole & Jones 2012).

Equation 2 was of the type:

$$y(t) = yBAS + Af \cdot [1 - e^{-(t - TDf) / \tau f}] + As \cdot [1 - e^{-(t - TDs) / \tau s}] \quad (2)$$

In this equation, A*s,* TD*s* and τs indicate, respectively, the amplitude, the time delay and the time constant of the "slow" component of the kinetics (Rossiter et al. 2011, Poole & Jones 2012).

At times, after the first exponential rise $\dot{V}O_2$ increased linearly without approaching or aiming to a steady-state value. In these case equation 2 does not provide a good fit, and a third equation (equation 3) was utilized, characterized by

an exponential function for the fundamental component and a linear function for the slow component (see *e.g.* Porcelli et al. 2014):

$$y(t) = yBAS + Af \cdot [1 - e^{-(t - TDf) / \tau f}] + S\,[x - TDs] \quad (3)$$

in which S (slope) is the angular coefficient of the linear regression of $\dot{V}O_2$ *vs.* time.

The equation that best fitted the experimental data was determined by the *F* test (see below). That is to say, when equation 2 or equation 3 provided a better fit of data, a slow component of the $\dot{V}O_2$ kinetics was present, superimposed on the fundamental component.

Whereas A*s*, TD*s* and τs values appear devoid of physiological significance, the actual amplitude of the slow component (A's) was estimated as the difference between an average $\dot{V}O_2$ value calculated at the end of the contraction period and the asymptotic value of the fundamental component. The contribution of A'*s* to the total amplitude (A*tot*) of the response (A'*s*/A*tot*) was then calculated (Grassi et al. 2003).

Estimation of mean capillary PO_2. A numerical integration technique was utilized to estimate mean capillary PO_2 after about 15 seconds of contractions (*i.e.* in the time window in which the fast adjustment of $\dot{V}O_2$ occurs), by the use of Fick's law of diffusion and a simple model of capillary exchange (Roca et al. 1989; Hogan et al. 1990). The main assumptions of this calculations are as follows: 1) muscle O_2 diffusive conductance (DmO_2) is constant at each point along the capillary; 2) all residual O_2 in muscle venous blood is explained by diffusion limitation of O_2 transport, on the assumption that arteriovenous O_2 shunts are negligible and $\dot{Q}/\dot{V}O_2$ distribution is relatively homogeneous. The numerical process iteratively determines that value of DmO_2 that produces the measured PvO_2. By the use of the associated PO_2 profile, mean capillary PO_2 can be calculated as an average of all PO_2 values from the arterial to the venous end of the capillary. Mean capillary PO_2 is an estimate of the mean driving pressure for O_2 diffusion.

The numerical integration technique assumes that during maximal exercise mitochondrial PO_2 can be considered sufficiently close to zero to be neglected (Wagner 2012). Richardson et al. (1995) showed that very low intracellular PO_2 levels are reached within 20 s after the beginning of exercise, also in hyperoxia (Richardson et al. 1999).

***Statistical analysis*.** Values were expressed as means ± standard deviations (SD). To determine the statistical significance of differences between two means, a paired Student's *t*-test (two-tailed) was performed. To determine the statistical significance of differences among more than two means, a repeated-measures analysis of variance was performed. A Tukey's *post-hoc* test was utilized to discriminate where significant differences occurred. Data fitting by exponential functions was performed by an iterative least-squares approach. Comparisons between fittings with different exponential models were carried out by *F* test. The area under the curve was calculated by integration. The level of significance was set at $P<0.05$. Data fitting and statistical analyses were carried out by utilizing a commercially available software package (GraphPad Prism, GraphPad Software Inc.).

RESULTS

The mass of the gastrocnemius muscles at the end of the experiments was 84 ± 20 g.

Mean (± SD) values of peak force at discrete times during the contraction period are shown in **Figure 1**. In both conditions the muscles significantly fatigued. Values at the end of the contraction period (259.5 ± 78.6 N $100g^{-1}$ in CTRL, 259.3 ± 79.0 in Hyperoxia+RSR13, no significant difference) were significantly lower than those obtained at the beginning of contractions (413.0 ± 86.6 N $100g^{-1}$ in

CTRL and 396.3 ± 78.6 in Hyperoxia+RSR13, no significant difference). The Fatigue Index at the end of the contraction period was 0.62 ± 0.09 in CTRL and 0.65 ± 0.07 in Hyperoxia+RSR13 (no significant difference). No significant differences between the peak force values in CTRL and in Hyperoxia+RSR13 were observed at any time point. In both conditions the peak force decrease became less steep after the first minute of contractions.

Values at rest and at the end of the contraction period for the main variables pertinent to O_2 transport and utilization, acid-base status and hemodynamics are shown in **Tables 1 and 2.** At rest (Table 1) PaO_2 and PvO_2 values were substantially higher in Hyperoxia+RSR13 *vs.* CTRL, as a consequence of the hyperoxic *vs.* normoxic breathing. Variables related to acid-base status (pH, $PaCO_2$), convective O_2 delivery ([Hb], SO_2, CaO_2, $\dot{Q}$, $\dot{Q}$ CaO_2), O_2 utilization [$C(a-v)O_2$, O_2 extraction, $\dot{V}O_2$] and hemodynamics (perfusion pressure, vascular resistance) were not significantly different between the two conditions. As mentioned in the Methods, $\dot{Q}$ was pump-perfused and it was maintained constant and significantly elevated at rest and throughout the contraction period.
At the end of the contraction period (Table 2) PaO_2 and PvO_2 values were higher in Hyperoxia+RSR13 *vs.* CTRL. For all the other variables no significant differences were observed between CTRL and Hyperoxia+RSR13.

Individual and mean (± SD) values of P_{50} and mean capillary PO_2 determined in the two conditions are presented in **Figure 2**. Values in Hyperoxia+RSR13 were significantly higher than those in CTRL; for P_{50} this was a consequence of the rightward shift of the ODC induced by RSR13, whereas for mean capillary PO_2 the higher values can be attributed to the rightward shift of ODC and to the hyperoxic breathing. Increases of both variables occurred, to a variable degree, in all animals.

A typical individual example of the time-course of $\dot{V}O_2$ *vs.* time of contractions are shown for CTRL and Hyperoxia+RSR13 in **Figure 3**. Data expressed as mL $100g^{-1}$ min^{-1} are shown in the upper panels, whereas data normalized per muscle force (mL min^{-1} N^{-1}) are shown in the lower panels. The best-fit functions (see above) are also shown. For $\dot{V}O_2$/Force (lower panels) the best-fit was represented by equation 2 (in other words a slow component of the $\dot{V}O_2$ kinetics was present); the asymptote of the fundamental component (dashed line) is also shown in the Figure. A slow component was not observed for $\dot{V}O_2$ data (upper panels), in which a steady-state followed the fundamental component of the $\dot{V}O_2$ kinetics (equation 1).

This behavior is confirmed when mean (± SD) data are presented (**Figure 4**): no slow component for $\dot{V}O_2$, a slow component for $\dot{V}O_2$/Force. In the right-hand panels the *x* axis is expanded in order to better appreciate the time courses of the variable during the initial part of the contraction period. Both for $\dot{V}O_2$ and $\dot{V}O_2$/Force the monoexponential increase which characterizes the fundamental component was preceded by a longer delay (TD*f* in equations 1-3) in Hyperoxia+RSR13 *vs.* CTRL.

A slow component was not identified in any dog for $\dot{V}O_2$, and in all dogs (with the exception of one) for $\dot{V}O_2$/Force. In 10 cases out of 11 the slow component was best fit by equation 2, and in one case by equation 3. A'*s*/A*tot* was 0.38 ± 0.12 in CTRL *vs.* 0.23 ± 0.17 in Hyperoxia+RSR13 (P=0.06).

Individual and mean (± SD) values of TD*f*, τf, and mean response time (MRT*f* = TD*f*+τf) of the $\dot{V}O_2$ kinetics are presented in **Figure 5**. TD*f* was significantly longer in Hyperoxia+RSR13 *vs.* CTRL, whereas no significant difference was observed for τf; as a consequence, also MRT*f* values were significantly longer in Hyperoxia+RSR13.

DISCUSSION

In the isolated dog gastrocnemius *in situ* preparation, during metabolic transitions from rest to contractions of peak metabolic intensity ($\dot{V}O_{2peak}$), enhancement of peripheral O_2 diffusion (obtained by hyperoxic breathing and by a right-shifted ODC [Hyperoxia+RSR13]) determined a slower kinetics of adjustment of muscle $\dot{V}O_2$: an unchanged time constant (τ) of the fundamental phase of the kinetics was indeed preceded by a significantly longer time delay (TD) (~10 s, *vs.* ~4 s in CTRL), so that the mean response time (MRT = TD + τ) was longer in Hyperoxia+RSR13 than in CTRL.

How to interpret this observation? Was the delayed $\dot{V}O_2$ increase observed in Hyperoxia+RSR13 attributable to a delayed metabolic activation of oxidative phosphorylation, or was it simply due to the utilization of O_2 stores present in the interstitial space and in the intracellular compartment? These stores would be greater in hyperoxia *vs.* normoxia, and their utilization would not be detected by the calculation of $\dot{V}O_2$ carried out by solving the Fick equation across the muscle. Some estimations and calculations allowed some insights into this issue. First of all, we calculated the areas under the $\dot{V}O_2$ *vs.* time (mL 100 g^{-1} s^{-1}) curves described in the upper-right panel of Figure 4, and obtained the volumes of O_2 (VO_2, in mL 100 g^{-1}) consumed during the first minute of the transition, that is during the period in which most of the changes occur. These values were then expressed in mL of O_2 by taking into account the mass of the muscles, yielding 7.7 mL in CTRL and 6.4 mL in Hyperoxia+RSR13. The difference between the two values (1.3 mL) reflects the area between the two curves in the upper-right panel of Figure 4, and represents the difference between the O_2 deficits in the two conditions.

We then estimated the O_2 stores, present as dissolved O_2 in the interstitial space and in the intracellular compartment, and as O_2 bound to myoglobin (Mb). The volume of O_2 dissolved in the interstitial space was estimated as follows. Muscle volume was estimated on the basis of muscle mass, and by assuming a density of

skeletal muscle of 1.06; interstitial volume was calculated as ~17.5% of muscle volume (Hirai et al. 2018); interstitial PO_2 was estimated to be ~15 mmHg lower than mean capillary PO_2 (Hirai et al. 2018); the solubility of O_2 in the interstitial space was assumed to be the same as in plasma (0.003 mL 100 mL^{-1} $mmHg^{-1}$). For mean capillary PO_2, resting values were assumed to be half-way between the measured PaO_2 and PvO_2, whereas mean capillary PO_2 values during contractions were calculated by the numerical integration technique described above. By these calculations, the differences between interstitial O_2 stores at rest and during contractions were ~0.02 mL in CTRL and ~0.08 mL in Hyperoxia+RSR13. These very small volumes could account for only a tiny fraction of the VO_2 difference (~1.3 mL) between the two curves in the upper-right panel of Figure 4.

Changes in intracellular O_2 stores were estimated as follows. Intracellular volume was estimated to be ~82,5% of muscle volume (Hirai et al. 2018). After assuming a solubility of O_2 in the intracellular space similar to that observed in plasma, we assumed an intracellular PO_2 at rest equal to 34 mmHg in CTRL (Richardson et al. 2006) and ~370 mmHg in Hyperoxia+RSR13 (~50 mmHg less than mean capillary PO_2, as suggested by Richardson et al. 2006), and intracellular PO_2 values during contractions close to zero in both conditions (Richardson et al. 1999). Changes (rest minus exercise) of intracellular O_2 stores (dissolved gas) were ~0.07 mL in CTRL and 0.72 mL in Hyperoxia+RSR13.

In terms of O_2 bound to Mb we assumed a [Mb] (squared brackets denote concentrations) of ~5 mg g^{-1} of muscle (Nemeth et al. 1984). After taking into consideration the O_2 binding capacity of Mb, the total Mb O_2 stores in the muscle would be ~0,56 mL. Assuming a ~50% depletion of these stores from rest to contractions (compatible with an intracellular PO_2 of 2-4 mmHg, both in CTRL and in Hyperoxia+RSR13 [see Richardson et al. 1999]), the depletion (rest – exercise) of Mb O_2 stores would be ~0,28 mL in both experimental conditions.

If we sum up the changes in O_2 stores (dissolved interstitial O_2 + dissolved intracellular O_2 + Mb O_2) occurring between rest and contractions we come up with

a value of 0.36 mL for CTRL, and 1.08 mL for Hyperoxia+RSR13. The difference between the two values would be 0.72 mL, which would correspond to ~50% of the VO_2 difference observed, during the first minute of contractions, between the two curves in the upper-right panel of Figure 4. In other words, enhanced utilization of O_2 stores in Hyperoxia+RSR13 could explain only about half of the greater O_2 deficit observed in this condition. Although we recognize that the calculations described above are based upon several assumptions, we postulate that the remaining half of the greater O_2 deficit in Hyperoxia+RSR13 could be ascribed to a delayed metabolic activation of oxidative phosphorylation.

How could an increased O_2 availability (in terms of dissolved O_2) exert at least a temporary inhibitory role on oxidative phosphorylation? According to Haseler et al. (1998) increases in FIO_2 would increase, in the presence of the same $\dot{V}O_2$, muscle [PCr]. According to a widely accepted theory on the control of mitochondrial respiration (Margaria at al. 1965, Whipp & Mahler 1980, Meyer et al. 1984, Cerretelli & di Prampero 1987), also known with the term "phosphocreatine shuttle" (Meyer et al. 1984), at exercise onset PCr breakdown represents a high-capacitance temporal buffer for the initial demands of ATP turnover. This buffer slows the increase of oxidative phosphorylation (Grassi et al. 2011*b*) by delaying changes in key energetic controlling signals ([ADP], [Pi], [NAD^+], etc.) between sites of ATP hydrolysis in the cytoplasm and sites of oxidative phosphorylation in mitochondria, thereby delaying the finite kinetics of $\dot{V}O_2$ adjustment (Glancy et al. 2008). In other words, the increase in muscle [PCr] following the FIO_2 increase would go in the opposite direction of what observed with creatine kinase (CK) inhibition, which we obtained in a previous study (Grassi et al 2011*b*) on the same experimental model of the present work: in that study, indeed, a decreased [PCr] obtained by CK inhibition was associated with a significantly faster $\dot{V}O_2$ kinetics.

The results of the present study must be interpreted in conjunction with those obtained in a previous study by our group (Grassi et al. 2000), conducted by utilizing the same isolated dog gastrocnemius *in situ* preparation. In that study we demonstrated that, after eliminating all delays in convective O_2 delivery, muscle $\dot{V}O_2$ kinetics to $\dot{V}O_{2peak}$ became slightly but significantly faster, in association with a lower O_2 deficit and less muscle fatigue (Grassi et al. 2000). Thus, during transitions to $\dot{V}O_{2peak}$ convective O_2 delivery limited, at least in part, muscle $\dot{V}O_2$ kinetics. In another study carried out in the same preparation of the present work an enhancement of peripheral O_2 diffusion significantly increased $\dot{V}O_{2peak}$ (Richardson et al. 1998). These studies led us to the working hypothesis of the present work: also peripheral O_2 diffusion could represent a limitation to skeletal muscle $\dot{V}O_2$ kinetics to $\dot{V}O_{2peak}$. The hypothesis was not confirmed by the results: an enhanced peripheral O_2 diffusion actually *slowed* the overall $\dot{V}O_2$ kinetics. If we consider also the previous studies carried out on convective (Grassi et al. 1998*a*) and diffusive (Grassi et al 1998*b*) O_2 delivery during transitions to *submaximal* contractions, the overall *scenario* could be summarized as follows: enhanced convective and diffusive O_2 delivery do not affect skeletal muscle $\dot{V}O_2$ kinetics; the only exception may be the relatively minor role played by convective O_2 delivery during transitions to $\dot{V}O_{2peak}$.

In the present study the combined effects of hyperoxia and of the rightward shift of ODC substantial increased (by ~4-fold on average) mean capillary PO_2. Assuming a mitochondrial PO_2 close to zero (Richardson et al. 1995, Wagner 2012), also in hyperoxia (Richardson et al. 1999), the intervention was likely highly successful in increasing the driving pressure for O_2 from capillaries to mitochondria. RSR13 administration had to be associated with hypoxia, since in normoxia the drug, by producing a rightward shift of ODC would reduce SaO_2, thereby impairing convective O_2 delivery. The enhancement of peripheral O_2 diffusion was obtained starting from an experimental baseline of enhanced

convective O_2 delivery (constantly elevated blood flows from rest, plus the administration of a vasodilatory drug), in order to keep convective O_2 delivery "out of the picture".

Previous studies on the effects of hyperoxia on pulmonary $\dot{V}O_2$ kinetics in humans yielded at least in part different results. Whereas Linnarsson (1974), Hughson & Kowalchuck (1995) and Wilkerson et al. (2006) observed no effects on $\dot{V}O_2$ kinetics, MacDonald et al (1997) observed faster $\dot{V}O_2$ kinetics during heavy-, but not during moderate-intensity exercise. A major limitation of these studies was that they could not determine or make inferences on convective O_2 delivery to muscle. It has been indeed demonstrated that O_2 extraction, as well as blood flow to skeletal muscles, are impeded in hyperoxic dogs (Faithful et al. 1987), possibly as a consequence of intramuscular O_2 restriction and maldistribution (Bredle et al. 1988). In the present study we did not incur into these problems since blood flow was kept constantly elevated and adenosine administration assured vasodilation. Muscle perfusion pressure and vascular resistance were indeed not significantly different in the two experimental conditions (see Table 2).

As in our previous study (Zoladz et al. 2008), also in the present one when $\dot{V}O_2$ *vs.* time was considered no slow component of $\dot{V}O_2$ kinetics was seen. However, since muscles significantly fatigued during the contraction period, after we "normalized" $\dot{V}O_2$ per unit of force a clear slow component appeared. As discussed in previous studies (Zoladz et al. 2008, Jones et al. 2011, Grassi et al. 2015), a decreasing force in the presence of a constant $\dot{V}O_2$ can be considered a sort of a "mirror image" of the traditional slow component. The phenomenon is similar to conditions in which the subject reduces exercise intensity in order to prevent the occurrence of metabolic inefficiency and fatigue (Jones et al. 2011, Grassi et al. 2015). In the present study the relative amplitude of the slow component, with respect to the total amplitude of the response, showed a clear tendency to decrease in Hyperoxia+RSR13 *vs.* CTRL, although the difference did not reach

statistical significance (P=0.06). Considering the relatively low *n*, a type II statistical error cannot be excluded here.

In conclusion, in an isolated canine muscle *in situ* preparation, examined during a metabolic transition from rest to contractions corresponding to $\dot{V}O_{2peak}$, enhancement of peripheral O_2 diffusion by hyperoxia and by a rightward shift of the ODC (Hyperoxia+RSR13) determined a slower overall $\dot{V}O_2$ kinetics, in which an unchanged τ during the fundamental phase was preceded by a longer time-delay. This delayed $\dot{V}O_2$ kinetics was presumably due to an increased utilization of intramuscular O_2 stores (greater in hyperoxia) and to a delayed activation of oxidative phosphorylation.

REFERENCES

Abraham DJ, Wireko FC, Randad RS, Poyart C, Kister J, Bohn BB, Liard JF, Kunert MP. Allosteric modifiers of hemoglobin: 2-(4-{[(3,5-disubstituted anilino)carbonyl]methyl}phenoxy)-2-methyl propionic acid derivatives that lower the oxygen affinity of hemoglobin in red cell suspensions, in whole blood, and *in vivo* in rats. *Biochemistry* 31: 9141-9149, 1992.

Ameredes BT, Brechue WF, Stainsby WN. Mechanical and metabolic determination of $\dot{V}O_2$ and fatigue during repetitive isometric contractions *in situ*. *J Appl Physiol* 85: 1394-1403, 1998.

Bredle DL, Bradley WE, Chapler CK, Cain SM. Muscle perfusion and oxygenation during local hyperoxia. *J Appl Physiol* 65: 2057-2062, 1988.

Cerretelli P, di Prampero PE. Gas exchange in exercise. In: *Handbook of Physiology*, Section 3, *The Respiratory System*, col. IV, *Gas Exchange*. Eds. Fahri LE, Tenney SM, p. 297-339. American Physiological Society, 1987.

Faithful NS, King CE, Cain SM. Peripheral vascular responses to fluorocarbon administration. *Microvasc Res* 33: 183-193, 1987.

Glancy B, Barstow TB, Willis WT. Linear relation between time constant of oxygen uptake kinetics, total creatine, and mitochondrial content in vitro. *Am J Physiol Cell Physiol* 294: C79-C87, 2008.

Goodwin ML, Hernandez A, Lai N, Cabrera ME, Gladden LB. $\dot{V}O_2$ on-kinetics in isolated canine muscle *in situ* during slowed convective O_2 delivery. *J Appl Physiol* 112: 9-19, 2012.

Grassi B. Delayed metabolic activation of oxidative phosphorylation in skeletal muscle at exercise onset. *Med. Sci. Sports Exerc.* 37: 1567-1573, 2005.

Grassi B, Gladden LB, Samaja M, Stary CM, Hogan MC. Faster adjustment of O_2 delivery does not affect $\dot{V}O_2$ on-kinetics in isolated *in situ* canine muscle. *J Appl Physiol* 85: 1394-1403, 1998*a*.

Grassi B, Gladden LB, Stary CM, Wagner PD, Hogan MC. Peripheral O_2 diffusion does not affect $\dot{V}O_2$ on-kinetics in isolated in situ canine muscle. *J Appl Physiol* 85: 1404-1412, 1998*b*.

Grassi B, Hogan MC, Greenhaff PL, Hamann JJ, Kelley KM, Aschenbach WG, Constantin-Teodosiu D, Gladden LB. $\dot{V}O_2$ on-kinetics in dog gastrocnemius in situ following activation of pyruvate dehydrogenase by dichloroacetate. *J Physiol* 538: 195-207, 2002.

Grassi B, Hogan MC, Kelley KM, Aschenbach WG, Hamann JJ, Evans RK, Patillo RE, L.B. Gladden LB. Role of convective O_2 delivery in determining $\dot{V}O_2$ on-kinetics in canine muscle contracting at peak $\dot{V}O_2$. *J Appl Physiol* 89: 1293-1301, 2000.

Grassi B, Hogan MC, Kelley KM, Howlett RA, Gladden LB. Effects of NOS inhibition by L-NAME on oxygen uptake kinetics in isolated canine muscle in situ. *J Physiol* 568: 1021-1033, 2005.

Grassi B, Porcelli S, Salvadego D, Zoladz JA. Slow $\dot{V}O_2$ kinetics during moderate-intensity exercise as markers of lower metabolic stability and lower exercise tolerance. *Eur. J. Appl. Physiol.* 111: 345-355, 2011*a*.

Grassi B, Rossiter HB, Hogan MC, Howlett RA, Harris JE, Goodwin ML, Dobson JL, Gladden LB. Faster O_2 uptake kinetics in canine skeletal muscle *in situ* after acute creatine kinase inhibition. *J Physiol* 589: 221-233, 2011*b*.

Grassi B, Rossiter HB, Zoladz JA. Skeletal muscle fatigue and decreased efficiency: two sides of the same coin? *Exerc Sport Science Rev.* 43: 75-83, 2015.

Haseler LJ, Richardson RS, Videen JS, Hogan MC. Phosphocreatine hydrolysis during submaximal exercise: the effect of FIO_2. *J Appl Physiol* 85: 1457-1463, 1998.

Hirai DM, Craig JC, Colburn TD, Eshima H, Kano Y, Sexton WL, Musch TI, Poole DC. Skeletal muscle microvascular and interstitial PO_2 from rest to contractions. *J Physiol* 596: 869-883, 2018.

Hogan MC, Bebout DE, Wagner PD, West JB. Maximal O_2 uptake in in situ dog muscle during acute hypoxemia with constant perfusion. *J Appl Physiol* 69: 570-576, 1990.

Hughson RL, Kowalchuck JM. Kinetics of oxygen uptake for submaximal exercise in hyperoxia, normoxia, and hypoxia. Can J Appl Physiol 20: 199-211, 1995.

Jones AM, Grassi B, Christensen PM, Krustrup P, Bangsbo J, Poole DC. The slow component of $\dot{V}O_2$ kinetics: mechanistic bases and practical applications. *Med Sci Sports Exerc* 43: 2046-2062, 2011.

Kelley KM, Hamann JJ, Aschenbach WG, Gladden LB. Canine gastrocnemius muscle in situ: $\dot{V}O_{2max}$. *Med Sci Sports Exerc* 28: S62, 1996 (Abstract).

Liard JF, Kunert MP. Hemodynamic changes induced by low blood oxygen affinity in dogs. *Am J Physiol* 264 (*Regulatory Integrative Comp Physiol* 33): R396-R401, 1993.

Linnarsson D. Dynamics of pulmonary gas exchange and heart rate changes at start and end of exercise. *Acta Physiol Scand* 415 (*Suppl*): S1-S68, 1974.

MacDonald M, Pedersen PK, Hughson RL. Acceleration of $\dot{V}O_2$ kinetics in heavy submaximal exercise by hyperoxia and prior high-intensity exercise. *J Appl Physiol* 83: 1318-1325, 1997.

Margaria R, Mangili F, Cuttica F, Cerretelli P. The kinetics of oxygen consumption at the onset of muscular exercise in man. *Ergonomics* 8: 49-54, 1965.

Meyer RA, Sweeney HL, Kushmerick MJ. A simple analysis of the "phosphocreatine shuttle". *Am J Physiol Cell Physiol* 246: C365-C377, 1984.

Murias JM, Spences MD, Paterson DH. The critical role of O_2 provision in the dynamic adjustment of oxidative phosphorylation. *Exerc Sport Sci Rev* 42: 4-11, 2014.

Piiper J, di Prampero PE, Cerretelli P. Oxygen debt and high-energy phosphates in gastrocnemius muscle of the dog. *Am J Physiol* 215: 523-531, 1968.

Poole DC, Jones AM. Oxygen uptake kinetics. *Compr Physiol* 2: 933-996, 2012.

Nemeth PM, Lowry OH. Myoglobin levels in individual human skeletal muscle of different types. *J Histochem Cytochem* 32: 1211-1216, 1984.

Richardson RS, Duteil S, Wary C, Wray DW, Hoff J, Carlier PG. Human skeletal muscle intracellular oxygenation: the impact of oxygen availability. *J Physiol* 571: 415-424, 2006.

Richardson RS, Leigh JR, Wagner PD, Noyszewski EA. Cellular PO_2 as a determinant of maximal mitochondrial O_2 consumption in trained human skeletal muscle. *J Appl Physiol* 87: 325-331, 1999.

Richardson RS, Noyszewski EA, Kendrick KK, Leigh JS, Wagner PD. Myoglobin O_2 desaturation during exercise. Evidence of limited O_2 transport. *J Clin Invest* 96: 1916-1926, 1995.

Richardson RS, Tagore KS, Haseler LJ, Jordan MC, Wagner PD. Increased $\dot{V}O_2$max with a right-shifted Hb-O_2 dissociation curve at constant O_2 delivery in dog muscle in situ. *J Appl Physiol* 84: 995-1002, 1998.

Roca J, Hogan MC, Story D, Bebout DE, Haab P, Gonzalez R, Ueno O, Wagner PD. Evidence for tissue diffusion limitation of $\dot{V}O_2$max in normal humans. *J Appl Physiol* 67: 291-299, 1989.

Rossiter HB. Exercise: kinetic considerations for gas exchange. *Compr Physiol* 1: 203-244, 2011.

Stainsby WN, Welch HG. Lactate metabolism of contracting dog skeletal muscle in situ. *Am J Physiol* 211: 177-183, 1966.

Wagner PD. Muscle intracellular oxygenation during exercise: optimization for oxygen transport, metabolism, and adaptive change. *Eur J Appl Physiol* 112: 1-8, 2012.

Whipp BJ, Mahler M. Dynamics of pulmonary gas exchange during exercise. In: *Pulmonary Gas Exchange*, vol. II, Ed. West JB, pp. 33-96, Academic, New York, 1980.

Wilkerson DP, Berger NJ, Jones AM. Influence of hyperoxia on pulmonary O_2 uptake kinetics following the onset of exercise in humans. *Respir Physiol Neurobiol* 153: 92-106, 2006.

Zoladz JA, Gladden LB, Hogan MC, Nieckarz Z, Grassi B. Progressive recruitment of muscle fibers is not necessary for the slow component of $\dot{V}O_2$ kinetics. *J Appl Physiol* 105: 575-580, 2008.

Table 1. Resting values

		CTRL	Hyperoxia + RSR13	P
PaO_2 (mmHg)		92.0 ± 8.3	532.3 ± 43.3	0.00
PvO_2 (mmHg)		78.7 ± 8.0	310.2 ± 32.3	0.00
$PaCO_2$ (mmHg)		31.8 ± 3.2	31.0 ± 3.9	0.54
pHa		7.41 ± 0.05	7.39 ± 0.06	0.50
[Hb] (g dL^{-1})		16.3 ± 1.8	16.2 ± 2.6	0.79
SaO2 (%)		94.5 ± 0.9	94.6 ± 6.3	0.99
CaO_2 (mL 100 mL^{-1})		21.7 ± 2.4	23.0 ± 4.2	0.26
$C(a\text{-}v)O_2$ (mL 100 mL^{-1})		0.6 ± 0.3	1.4 ± 0.07	0.07
Q (mL min^{-1} $100g^{-1}$)		110.1 ± 32.0	110.9 ± 33.2	0.38
Q CaO_2 (mL min $100g^{-1}$)		25.0 ± 7.6	24.5 ± 5.3	0.87
Fractional O_2 extraction		0.03 ± 0.01	0.06 ± 0.02	0.09
VO_2 (mL min^{-1} $100g^{-1}$)		0.6 ± 0.4	1.4 ± 0.5	0.07
Perfusion pressure (mmHg)		140.3 ± 21.7	145.7 ± 22.0	0.52
Vascular resistance (mmHg mL^{-1} 100g min)		1.46 ± 0.80	1.52 ± 0.9	0.10

Table 2. Values during the last minute of contractions

		CTRL	Hyperoxia + RSR13	P
PaO_2 (mmHg)		95.2 ± 16.3	543.2 ± 35.3	0.00
PvO_2 (mmHg)		27.7 ± 3.7	43.7 ± 14.2	0.04
$PaCO_2$ (mmHg)		31.4 ± 2.4	31.0 ± 3.0	0.80
pHa		7.41 ± 0.05	7.39 ± 0.06	0.46
[Hb] (g dL^{-1})		16.3 ± 2.0	15.8 ± 2.9	0.38
SaO2 (%)		94.7 ± 1.0	95.8 ± 4.9	0.60
CaO_2 (mL 100 mL^{-1})		21.8 ± 2.7	22.8 ± 4.5	0.37
$C(a\text{-}v)O_2$ (mL 100 mL^{-1})		14.6 ± 2.4	10.5 ± 5.7	0.13
Q (mL min^{-1} $100g^{-1}$)		110.1 ± 32.0	110.9 ± 33.2	0.38
Q CaO_2 (mL min $100g^{-1}$)		23.3 ± 5.0	24.2 ± 5.2	0.48
Fractional O_2 extraction		0.67 ± 0.08	0.58 ± 0.10	0.02
VO_2 (mL min^{-1} $100g^{-1}$)		15.7 ± 4.6	13.8 ± 4.0	0.12
Perfusion pressure (mmHg)		123.4 ± 12.2	124.8 ± 17.3	0.71
Vascular resistance (mmHg mL^{-1} 100g min)		1.27 ± 0.63	1.31 ± 0.8	0.64

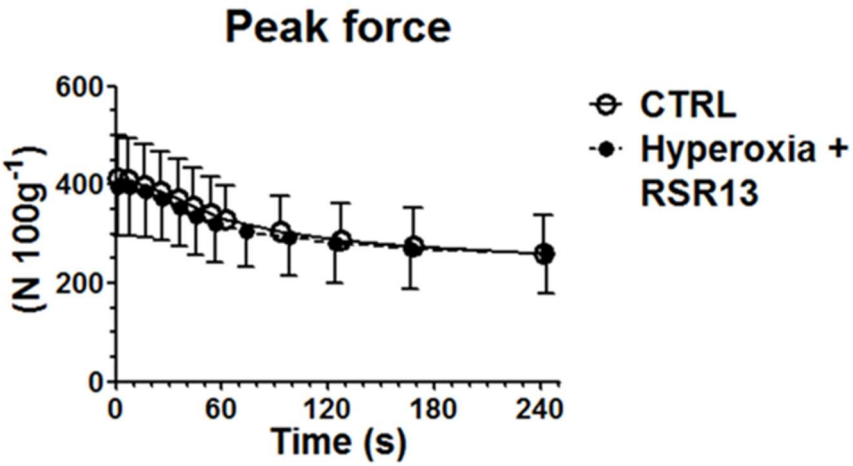
Peak force
600
400
200
0
(N 100g-1)
0
60
120
180
240
Time (s)
CTRL
Hyperoxia +
RSR13

Figure 1

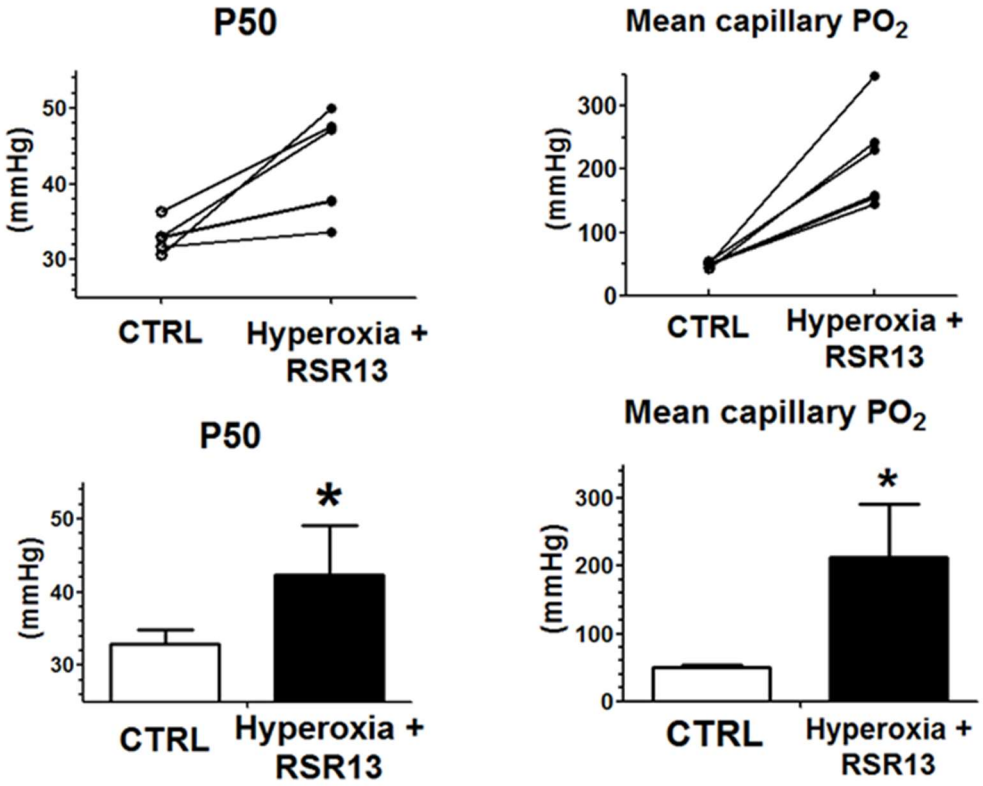
P50
(mmHg)
50
40
30
CTRL
Hyperoxia + RSR13
Mean capillary PO_2
(mmHg)
300
200
100
0
CTRL
Hyperoxia + RSR13
P50
(mmHg)
50
40
30
*
CTRL
Hyperoxia + RSR13
Mean capillary PO_2
(mmHg)
300
200
100
0
*
CTRL
Hyperoxia + RSR13

Figure 2

Figure 3

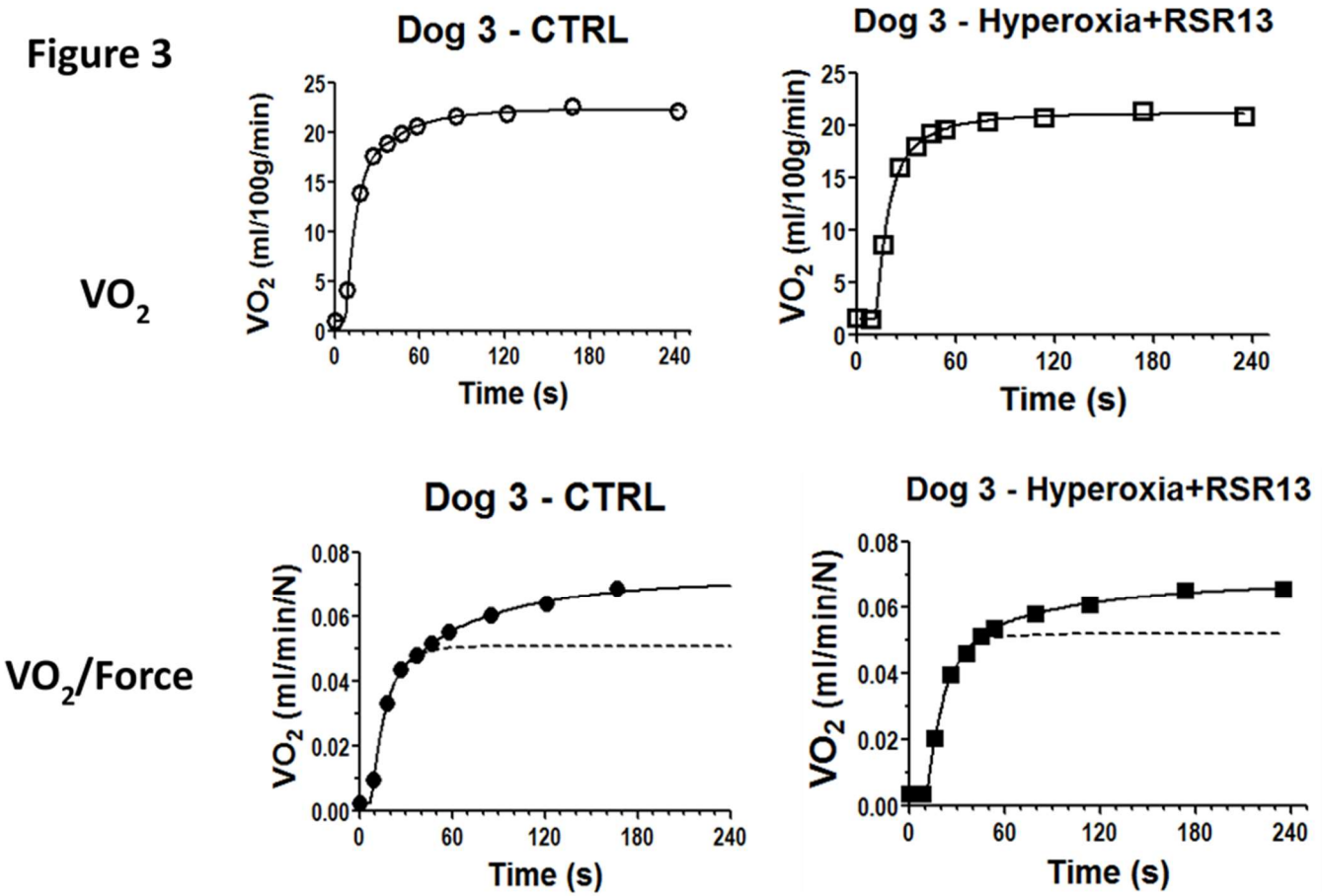
VO2
Dog 3 - CTRL
Dog 3 - Hyperoxia+RSR13
VO2 (ml/100g/min)
Time (s)
VO2/Force
VO2 (ml/min/N)

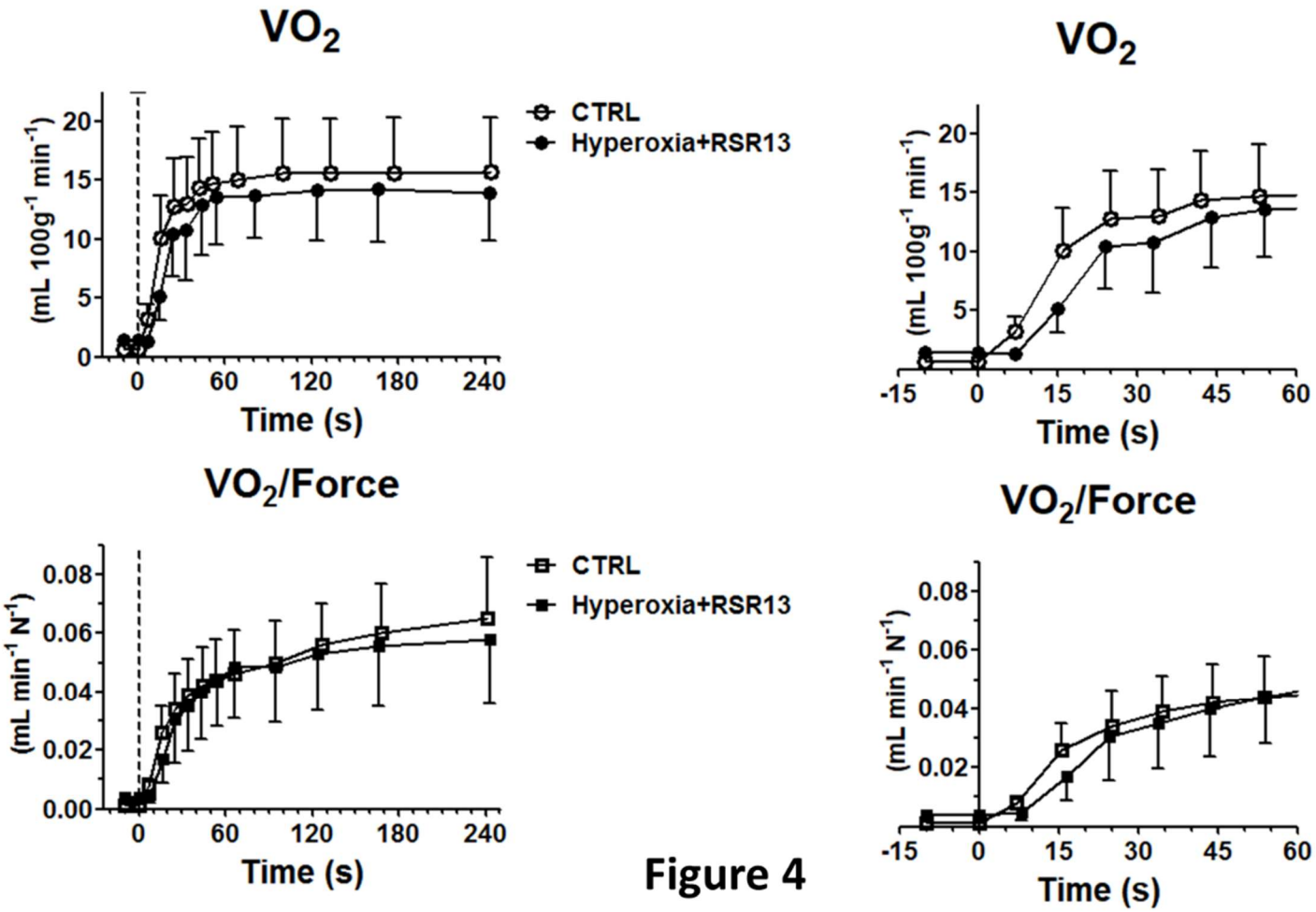
VO2
(mL 100g-1 min-1)
0
5
10
15
20
0
60
120
180
240
Time (s)
CTRL
Hyperoxia+RSR13
VO2/Force
(mL min-1 N-1)
0.00
0.02
0.04
0.06
0.08
0
60
120
180
240
Time (s)
CTRL
Hyperoxia+RSR13
VO2
(mL 100g-1 min-1)
0
5
10
15
20
-15
0
15
30
45
60
Time (s)
VO2/Force
(mL min-1 N-1)
0.02
0.04
0.06
0.08
-15
0
15
30
45
60
Time (s)

Figure 4

Figure 5

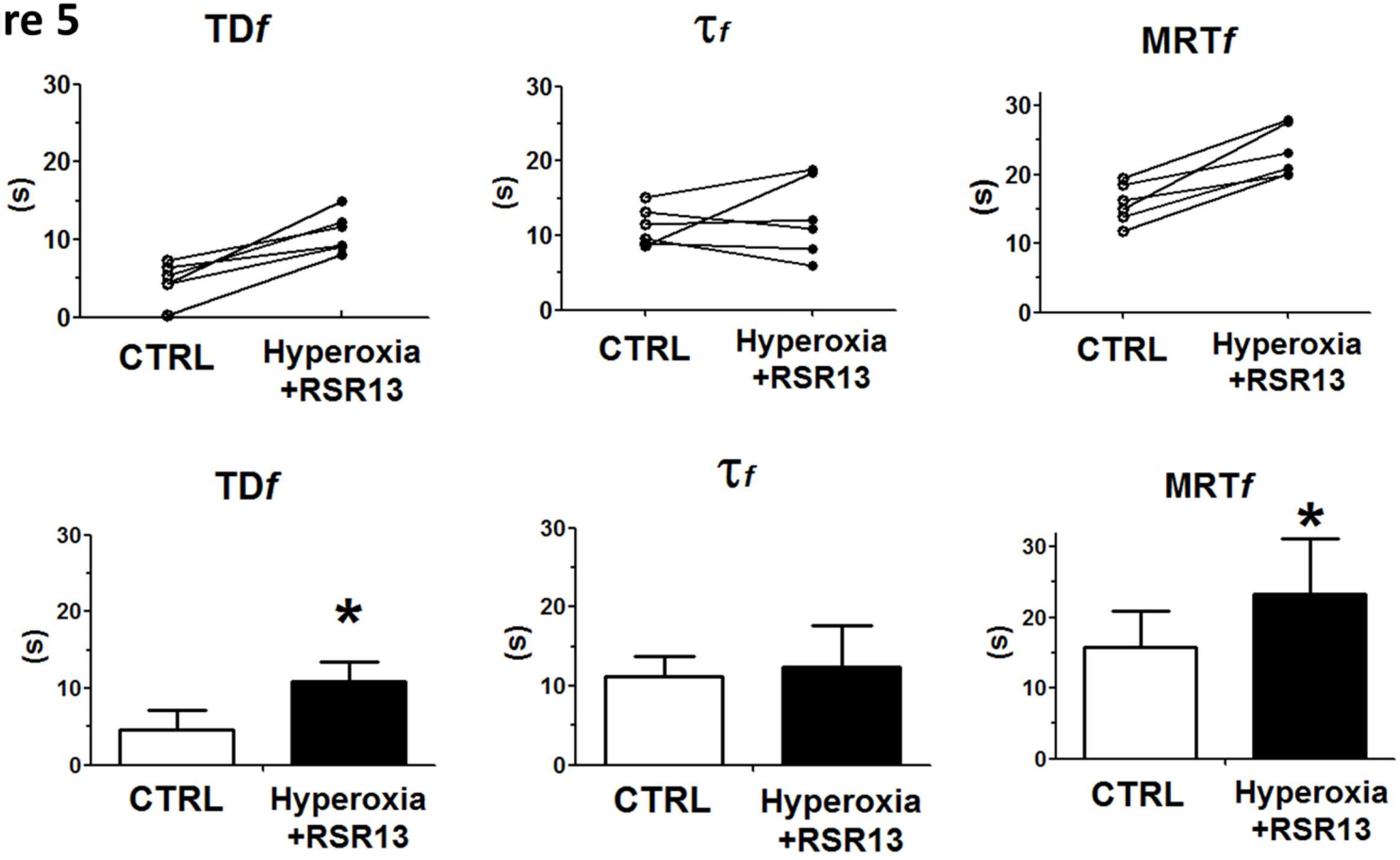

Changes in skeletal muscle oxidative capacity after a trail running race

Giovanelli Nicola[1,2], Biasutti Lea[1,2], Salvadego Desy[1,2], Hailu Kinfu Alemayehu[1,2], Grassi Bruno[1,2], Lazzer Stefano[1,2]

1. Department of Medicine, University of Udine, Udine, Italy
2. School of Sport Sciences, University of Udine, Udine, Italy

Running title: Muscle oxygenation and trail running

Keywords: NIRS; downhill running; eccentric; ultra-endurance; mountain running

Corresponding Author:
Nicola Giovanelli
University of Udine
Department of Medical Area
P.le Kolbe 4
33100 Udine, Italy
Phone: (+39) 0432 494300
e-mail: nicola.giovanelli@uniud.it

Introduction

Trail-running is defined by the International Tail Running Association (ITRA) *"[…]a pedestrian race open to all, in a natural environment (mountain, desert, forest, plain…) with minimal possible paved or asphalt road […]"* (www.i-tra.org). The racecourses can reach and exceed the 200 km of length with more than 20000 m of elevation gain. In particular, races longer than the classical marathon distance are defined ultra-trails (UTs). Trail- and ultra-trail running become more popular among amateur and professional runners and they present significant differences in elevation gain, with multiple up- and downhill sections. Whereas uphill sections stress to a greater extent aerobic metabolism, in downhill sections, as a consequence of the repeated and forceful eccentric contractions muscle damage and inflammation responses ensue (Saugy et al., 2013). In the last few years several physiological aspects of trail running have been studied, such as the cost of running or cycling, the neuromuscular alterations and the biomechanical changes following trail-running races (Lazzer et al., 2014; Savoldelli et al., 2017; Temesi et al., 2014; Vernillo, Savoldelli, et al., 2016). More recently, the availability of new portable or wearable devices allowed the determination of other physiological parameters, also during sport activities. For example, near-infrared spectroscopy (NIRS) is a non-invasive method for the evaluation of skeletal muscle oxidative metabolism and can be used to evaluate the tissue oxygenation dynamics under different conditions (Grassi & Quaresima, 2016). In particular, during the last few years, NIRS has been used to evaluate exercise intensity and muscle oxygenation dynamics in different sport situations (Born, Stoggl, Swaren, & Bjorklund, 2016; S. Jones et al., 2017; Snyder & Parmenter, 2009; Vernillo, Brighenti, et al., 2016). Snyder & Parmenter (2009) proposed to use NIRS to determine the maximal steady state running intensity since the results were comparable to those obtained from blood lactate concentration test. Thus, it may be appropriate for determining exercise training intensity. Born et al. (2016) monitored the intensity during a trail-running event comparing the heart rate and the NIRS-obtained parameters. They suggested that NIRS is more accurate than heart rate to monitor running intensity, in particular when the exercise is performed on hilly terrain.

Vernillo, Brighenti, et al. (2016) showed that an UT (330 km, 24000 m of elevation gain) leads to an alteration in the balance between O_2 delivery ($Q'O_2$) and O_2 utilization ($V'O_2$) within the working muscles at submaximal (1 and 1.5 W/kg) intensity. They proposed that the continuous concentric and eccentric contractions, due to the up- and downhill sections, impaired the microcirculatory function. The effects of downhill running on muscle oxidative functions in rats were investigated

by Kano et al. (2005). These authors observed that, one and three days after a downhill run to exhaustion, the capillary hemodynamic and the $Q'O_2/V'O_2$ matching were still compromised. Moreover, Kano et al. (2005) suggested that the fiber damage after eccentric exercise is the main determinant for these impairments. Also, Fernstrom et al. (2007) studied the functional aspects of mitochondria isolated from muscle biopsies before and after a 24-h ultra-endurance exercise performed at ~60% of $V'O_2max$, demonstrating that after ultra-endurance exercise also mitochondrial efficiency is reduced.

To our knowledge the study of Vernillo, Brighenti, et al. (2016) is the first one in which NIRS has been used for the evaluation of the muscle oxidative metabolism before and after an UT. However, these authors used a protocol that does not provide information on the maximal capacity to oxidize substrates by the skeletal muscle, since the exercise they analyzed was a submaximal whole-body exercise (cycling at 1 and 1.5 W/kg). Thus, the purpose of the present study was to evaluate the effects of a trail-running race on muscle oxidative function by measuring pulmonary gas exchange variables and muscle fractional O_2 extraction. Measurements were carried out during an incremental one-leg knee extension (KE) exercise performed before and after a trail-running competition. This exercise utilizes a relatively small muscle volume (the quadriceps muscle of one leg, ~3 kg), thereby reducing substantially any limitation to oxidative metabolism deriving from central-cardiovascular O_2 delivery and allowing any limitation intrinsic to the muscle to become fully manifest (Salvadego et al., 2011). We hypothesize a significant impairment of skeletal muscle oxidative function following the race, with specific reference to the maximal capacity of O_2 extraction and to the relationship between O_2 uptake and O_2 delivery.

Materials and Methods

Subjects

Thirty-two subjects were enrolled in this study as participants in the "Trail dei 3 Castelli" (www.trail3castelli.com), but only eighteen athletes (mean ± SD; age: 36.8 ± 9.2 y; maximal oxygen uptake [$V'O_{2max}$]: 64.3 ± 6.3 $ml \cdot kg^{-1} \cdot min^{-1}$) (Table 1) completed the race and were evaluated before (PRE) and after (POST) the competition. The participants were experienced ultra-endurance runners (5.9 ± 3.2 years of ultra-endurance experience, 78.9 ± 39.2 $km \cdot week^{-1}$). The experimental protocol was conducted according to the Declaration of Helsinki and it was approved by the Ethics Committee of the University of Udine. Before the study began, the purpose and objectives were

carefully explained to each participant and written informed consent was obtained from all of them.

Experimental protocol

Athletes enrolled in the present study participated to a 32-km race with 2000 m of elevation gain (n=9), or to 50 km race with 3500 m of elevation gain (n=9). Racecourses included several up- and downhill sections (**Figure 1**). Participants were invited twice to the laboratory during the week before the race (PRE) in order to perform an incremental uphill running test (day 1) and an incremental exercise by utilizing a one-leg knee extensor (KE) ergometer (day 2), previously described and used by our group (Salvadego et al., 2013; Salvadego et al., 2011). The KE exercise was repeated as soon as possible after the end of the race (8±4 min, POST).

Physiological measurements

Anthropometry. We measured the body mass (BM) to the nearest 0.1 kg with a manual weighing scale (Seca 709, Hamburg, Germany) before and after the race. Stature was measured to the nearest 0.001 m on a standardized wall-mounted height board. Then, we calculated the body mass index (BMI). Moreover, we calculated the lean (fat-free) volume of the right lower limb using the Jones and Pearson method (P. R. Jones & Pearson, 1969), which is based on the summation of truncated cones.

Incremental uphill running test. During the week before the race, maximal oxygen uptake ($V'O_{2max}$), maximal heart rate (HR_{max}) and maximal vertical velocity ($V_{vert}max$) were determined during a graded exercise test on a treadmill (Saturn, HP Cosmos, Germany) under medical supervision. After a ten-minutes warm-up at self-selected speed, athletes started the test at the speed of 6 $km \cdot h^{-1}$ and a slope of 0.10. Every two minutes we increased the slope of the treadmill by 0.02 until 0.24, which is the maximum slope that the treadmill can reach. After this step, we increased the speed by 0.5 $km \cdot h^{-1}$ until the volitional exhaustion of the subject. We choose this protocol because it allowed to increase the vertical velocity linearly by ~3.2 $m \cdot s^{-1}$ every two minutes. During the test, we measured oxygen uptake ($V'O_2$), carbon dioxide production ($V'CO_2$), ventilation (V'E), tidal volume (V'T), and respiratory frequency (fR) breath-by-breath using a portable metabolic unit (K4 b^2, Cosmed, Italy). Before every test, we calibrated the volume and gas analyzers using a 3-L calibration syringe and calibration gas (16.00 $\%O_2$ and 4.00% CO_2),

respectively. During the tests, we recorded heart rate (HR) with a dedicated device (Polar, Kempele, Finland).

One-leg knee extensor incremental test. During the week before the race and as soon as possible (8±4 min) after the finish of the race, athletes underwent an incremental KE exercise on an ergometer that was previously used by our group (Salvadego et al., 2013; Salvadego et al., 2011). We measured the time to exhaustion, the peak power (Ppeak), the muscle oxygenation dynamics by using NIRS and the cardiorespiratory parameters ($V'O_2$, $V'CO_2$, V'E, VT, fR and HR) by using the metabolimeter (K4 b^2, see above). Subjects were seated on an adjustable seat, and the angle of the hip was maintained at ∼90° by a safety belt. We attached the right leg to a lever arm and participants were instructed to actively extend the leg from 90° to 175°. This range of motion was limited by two blocks specifically arranged. The return of the leg to the starting position was performed passively (i.e. no contraction was required). Before each test, athletes familiarized with testing procedures. After an initial 3 min of unloaded KE exercise an operator adjusted the workload every minute by increasing the workload by ∼8 $W \cdot min^{-1}$ (8.4±3.2 $W \cdot min^{-1}$) (see Ref. (Salvadego et al., 2011) for details). Throughout the test, the active KE and passive knee flexion cycle was carried out 40 times per minute as imposed by a metronome. During each cycle (total duration of 1.5 s), KE lasted ∼1 s. Thus, muscle contraction corresponded ∼65% of the duty cycle. Athletes performed the exercise until the exhaustion, which was defined as the inability to maintain the imposed workload at the required frequency despite vigorous encouragements by the operators. During the incremental test we evaluated the oxygenation changes in *vastus lateralis* muscle by near-infrared spectroscopy (NIRS, PortaLite, Artinis, The Netherlands) (see Grassi & Quaresima (2016) for a recent review on the method). NIRS was used for measuring the micromolar changes in oxygenated (Hb)+myoglobin (Mb) concentrations Δ[oxy(Hb+Mb)], and in deoxygenated [Hb+Mb] Δ[deoxy(Hb+Mb)], with respect to an initial value arbitrarily set equal to zero and obtained during the resting condition preceding the test. Δ[deoxy(Hb + Mb)] is relatively insensitive to changes in blood volume and has been considered an estimate of skeletal muscle fractional O_2 extraction (ratio between O_2 consumption and O_2 delivery) (Ferreira, Poole, & Barstow, 2005). Values of Δ[deoxy(Hb+Mb)] were obtained as a percentage of the values of maximal muscle deoxygenation obtained during a transient ischemia of the limb by a pressure cuff inflation (at 300–350 mmHg), maintained until Δ[deoxy(Hb+Mb)] reached a plateau. Δ[deoxy(Hb+Mb)] kinetics during the incremental tests were fitted by a sigmoid function, as

previously presented by other authors (Ferreira, Koga, & Barstow, 2007). Then, we calculated the mean values of cardiorespiratory parameters and muscle oxygenation variables during the last 20 s of each workload.

Statistical analysis

Statistical analyses were performed using PASW Statistic 18 (SPSS Inc., IL, USA) with significance set at $P<0.05$. All results are expressed as means ± SD. Normal distribution of the data was tested using the Shapiro-Wilk test. Sphericity (homogeneity of covariance) was verified by the Mauchly's test. Differences in anthropometric characteristics and metabolic parameters of two groups, before (PRE) and at the end (POST) of the race, were studied with General Linear Model repeated measures of the main effects of group (G: Short vs Long), time (T: PRE *vs* POST) and group x time interaction. Since no significant effects of distance race was observed on reported parameters, the two groups were pooled together to further analyze the changes of metabolic and mechanical parameters by General Linear Model repeated measures.

Results

Age, BM pre- and post- race, stature, BMI, quadriceps muscle mass (QM), $V'O_2max$, HR max, $V_{vert}max$ and race time of the eighteen participants in the study are reported in **Table 1**. BM decreased by -2.1 ± 1.6%, $p<0.001$ in POST *vs.* PRE. The range position among the athletes participating in the study was 1^{st}-132^{nd} (04:59:07 ± 01:16:30, hh:mm:ss) in the 32-km race (total of 143 finishers) and 1^{st} – 84^{th} (08:17:53 ± 1:23:40, hh:mm:ss) in the 50-km race (total of 84 finishers).

Pulmonary gas exchange during incremental KE exercise. Peak values of the main cardiorespiratory variables determined at exhaustion are presented in **Table 2,** along with the peak power and time to exhaustion of the KE exercise. V'Epeak and HRpeak suggest that the exercise was not maximal from a cardiorespiratory perspective; in particular, HRpeak was markedly lower than the maximal values obtained during the incremental uphill running test, both in PRE (-54.7±6.8%; $p<0.001$) and in POST (-49.0 ± 5.1%; $p<0.001$). V'Epeak, V'Tpeak and $V'O_2peak$ (L/min) were significantly lower at POST vs. PRE (-17.4 ± 10.9%, -18.2 ± 14.6% -23.9 ±9.0%, respectively, $p<0.001$). Moreover, $V'O_2peak$ at POST was lower than $V'O_2$ at the same workload at PRE (-8.4 ± 15.6%, $p=0.049$, Figure 2). When $V'O_2peak$ was normalized for the quadriceps muscle mass, values were still significantly

lower (by -24.7 ± 8.2%, p<0.001) in POST vs. PRE. Peak power output and time to exhaustion decreased significantly (by -23.7 ± 14.3% and -18.3 ± 11.3%, respectively, p<0.005) after the race (Tab. 2). No differences were observed for the other peak variables. $V'O_2$ values *vs.* work rate are shown in Figure 2. $V'O_2$ values were grouped for discrete workload intervals, which were determined to have, in each interval, each subject represented by one data point. When the subject had more than one "original" data point in the interval, mean individual values were calculated, both for the *x* and *y* variables, and were taken in consideration to obtain the figure (Salvadego et al., 2011). The same was done with Δ[deoxy(Hb+Mb)] (see below). No significant differences between values in PRE and POST were observed at the 3 lowest work rates. $V'O_2$ values were significantly lower in POST *vs.* PRE at the work rate corresponding to about 60 watts.

Near-infrared spectroscopy. The dynamics of Δ[deoxy(Hb+Mb)] as a function of workload during incremental KE exercise PRE- and POST the race are described in **Figure 3**. Both in PRE and in POST, Δ[deoxy(Hb+Mb)] values increased following a sigmoid-like pattern, approaching a plateau within the last one or two workloads. Values did not differ significantly in PRE vs. POST at the submaximal work rates, however in POST the increase as a function of workload, from unloading to peak, was much less pronounced (from 20.2 ± 10.1 to 64.5 ± 21.1% of limb ischemia at PRE to 16.9 ± 12.7 to 44.0 ± 18.9% at POST). Peak Δ[deoxy(Hb+Mb)] values were significantly lower at POST (by -31.2±20.5%; p<0.001).

Discussion

The main result of the present study shows that a few minutes after a trail running competition lasting between ∼3 and ∼11 hours the participants experienced a marked impairment of oxidative function intrinsic to skeletal muscle. This impairment is to ascribe to a reduced peak $V'O_2$ and peak fractional O_2 extraction (Δ[deoxy(Hb+Mb)]) of *vastus lateralis* muscle determined during an incremental one-leg KE exercise.

KE exercise allows a "functional isolation" of the knee extensor muscle group (i.e. the *vastus lateralis*), and the cardiac involvement during KE does not reach maximal values even at peak exercise intensity (Salvadego et al., 2013). In fact, in the present study participants reached exhaustion at relatively low HR values (corresponding to about 50% of the peak values determined during the incremental running test), confirming the absence of any cardiovascular limitation during KE. In the present study, $V'O_2$peak was significantly lower after the race (-23.9±9.0%)

compared with PRE, and this was associated with lower peak power output (-23.7±14.3%) and early exercise interruption (see Tab 2).

At submaximal loads there were no differences in $V'O_2$ in POST vs. PRE, suggesting that the exercise economy was not negatively affected by the race. This result is in agreement with other studies (Vernillo, Brighenti, et al., 2016; Vernillo, Savoldelli, et al., 2016; Vernillo et al., 2014) that did not report an alteration in oxygen cost of cycling or walking after an UT of 330 km. However, other authors (Gimenez, Kerherve, Messonnier, Feasson, & Millet, 2013; Lazzer et al., 2014) reported an increased O_2 cost of running following UT; the increase was related to exercise duration or distance covered. The conflicting results of these studies may be attributed, at least in part, to the different type of exercise (walking/running 330 km vs. a multi-stage competition or treadmill running) and/or to the time elapsed between the end of the race and the arrival of the subjects at the laboratory for the test (Vernillo, Savoldelli, et al., 2016).

To our knowledge there are no studies in which the $V'O_2$peak was measured immediately after an ultra-endurance event but we can speculate that this parameter is negatively affected by the fatigue state occurred after this type of exercise (Millet et al., 2011). During a pilot study in which we involved three subjects, we compare the power output and the $V'O_2$ during an incremental test before and after an ultra-endurance cycling race of 606 km with 16000 m of elevation gain (Ultracycling Dolomitica). The peak power and the systemic $V'O_2$peak after the race were ∼40% and ∼25% lower than before the race, respectively. As well, Kasikcioglu et al. (2006) and Sierra et al. (2016) reported a decrease in $V'O_2$peak during an incremental test one and three days after a marathon. Some authors suggested that decrease in $V'O_2$peak after a long-lasting effort may be attributed to a deceleration in the muscle oxygen kinetics (Kasikcioglu et al., 2006) or some degree of “cardiac fatigue” (Douglas, O'Toole, Hiller, Hackney, & Reichek, 1987; Sierra et al., 2016).

In the present study muscle mass was not affected by the race, and thus the observed impairment in $V'O_2$peak was substantially qualitative, presumably related to functional impairments intrinsic to the muscle fibers. Millet et al. (2011) reported that after an UT of 166 km and 9500 m of elevation gain the maximal voluntary contraction of the knee extensor muscles was markedly reduced, and was mainly associated with an early development of central fatigue. In particular, these authors reported a reduction in voluntary activation measured during KE exercise. It is also known that the repeated eccentric contractions during downhill running induce muscle damage and neuromuscular alterations, with a decreased central drive and strength loss (Giandolini et al.,

2015). In fact, UT induces muscle damage and inflammation (Millet et al., 2011) which could affect the contractility proprieties. Thus, the repeated downhill sections occurring during the competition may have affected KE performance by acting both at peripheral and central level. Moreover, prolonged exercise can induce an accumulation of metabolites within the muscle fibers (Millet et al., 2011; Overgaard, Lindstrom, Ingemann-Hansen, & Clausen, 2002), which can disrupt the Ca^{2+} release and uptake pathways in the sarcoplasmatic reticulum with a consequent failure of the excitation-contraction coupling (Amann & Calbet, 2008). Overall, these alterations may lead to a lower force production during KE exercise, lower peak power and an early exhaustion of the subjects.

In this study Δ[deoxy(Hb+Mb)] was utilized to estimate fractional O_2 extraction at the *vastus lateralis* muscle, in other words the ratio between intramuscular increases in $V'O_2$ and O_2 delivery (Ferreira et al., 2007). Δ[deoxy(Hb+Mb)] did not change in POST (*vs.* PRE) at submaximal work rates. Considering that at these work rates $V'O_2$ was not different in the two conditions, it can be concluded that also O_2 delivery was unaffected. Peak values of O_2 extraction were significantly lower in POST (44.0 ± 18.9% of limb ischemia) than in PRE (64.5±21.1%), in conjunction with a percentage-wise similar decrease in $V'O_2$peak. Again, this observation suggests a substantially maintained O_2 delivery, also at peak exercise, pointing to alterations more specifically related to muscle fibers as the potential cause of the observed oxidative impairment.

At a first glance, these findings may appear in contradiction with those obtained by Vernillo, Brighenti, et al. (2016) after an UT of 330 km and 24000 m of elevation gain; these authors found an increase in muscle deoxygenation during low-intensity cycling and attributed this response to an impaired intramuscular $Q'O_2/V'O_2$ matching consequent to the eccentric loads that characterize the downhill sections in such races. An association between eccentric exercise and impaired matching between $Q'O_2$ and $V'O_2$ was indeed demonstrated by Davies et al. (2008) in physically active men during severe-intensity cycling and by Kano et al. (2005) in rats during moderate-intensity downhill running and was explained by an altered capillary hemodynamics. The apparent discrepancy between the responses observed in this study at submaximal work rates with those observed by Vernillo, Brighenti, et al. (2016) are presumably due to the peculiarity of the exercise protocol proposed in the present study. Indeed, KE exercise recruits a small portion of the legs muscles and cardiovascular limitations in O_2 delivery are absent or significantly reduced compared to what observed in cycling exercise or treadmill running (Richardson et al., 1993). In

other words, the adopted exercise protocol allowed us to identify the impairments in oxidative metabolism, more strictly related to muscle fibers, deriving from the race.

Of note, the results of the present study are similar to those observed in healthy young men after a 35-days bed rest period (Porcelli et al., 2010; Salvadego et al., 2011), suggesting that two opposite stimuli such as a trail running race and chronic physical inactivity can induce a similar substantial muscle dysfunction and a subsequent marked exercise limitation. Differently from the bed rest studies, in this study after the race there was not loss of muscle mass, while a parallel decrease in $V'O_2$peak and Δ[deoxy(Hb+Mb)] peak was evident. These findings suggest the occurrence of qualitative constraints after a trail running race, which may involve the contractile function, such as a different recruitment of motor units towards the less oxidative and less resistant fast twitch fibers (Ferreira, McDonough, Behnke, Musch, & Poole, 2006), and/or the metabolic function, such as a reduced mitochondrial respiration. No biochemical or molecular analyses of muscle samples were performed in this study. However, it can be hypothesized that a decrease in mitochondrial efficiency could have occurred after the race, as previously observed after a 24-h ultra-endurance exercise at ∼60% of $V'O_2$max by Fernstrom et al. (2007), possibly a consequence of an increased oxidative stress (Tonkonogi, Walsh, Svensson, & Sahlin, 2000). Oxidative stress and inflammation are present in mountain marathon and ultra marathon (Da Ponte et al., 2017; Mastaloudis, Leonard, & Traber, 2001; Mrakic-Sposta et al., 2015; Rowlands et al., 2012) even if they may be counterbalanced by increased antioxidant defenses (Mastaloudis et al., 2001).

In conclusion, in the present study we provide evidence of a substantial impairment in skeletal muscle oxidative metabolism following a trail running exercise of 3-11 hours, possibly related to muscle damage from repeated eccentric contractions. In association with other mechanisms leading to impaired force generation, central fatigue, oxidative stress and damage, the impairment of skeletal muscle oxidative metabolism is likely responsible of the reduced exercise capacity and tolerance during and following these races.

References

Amann, M., & Calbet, J. A. (2008). Convective oxygen transport and fatigue. *J Appl Physiol (1985), 104*(3), 861-870. doi:10.1152/japplphysiol.01008.2007

Born, D. P., Stoggl, T., Swaren, M., & Bjorklund, G. (2016). Running in Hilly Terrain: NIRS is More Accurate to Monitor Intensity than Heart Rate. *Int J Sports Physiol Perform*, 1-21. doi:10.1123/ijspp.2016-0101

Da Ponte, A., Giovanelli, N., Antonutto, G., Nigris, D., Curcio, F., Cortese, P., & Lazzer, S. (2017). Changes in cardiac and muscle biomarkers following an uphill-only marathon. *Res Sports Med*, 1-12. doi:10.1080/15438627.2017.1393750

Davies, R. C., Eston, R. G., Poole, D. C., Rowlands, A. V., DiMenna, F., Wilkerson, D. P., . . . Jones, A. M. (2008). Effect of eccentric exercise-induced muscle damage on the dynamics of muscle oxygenation and pulmonary oxygen uptake. *J Appl Physiol (1985), 105*(5), 1413-1421. doi:10.1152/japplphysiol.90743.2008

Douglas, P. S., O'Toole, M. L., Hiller, W. D., Hackney, K., & Reichek, N. (1987). Cardiac fatigue after prolonged exercise. *Circulation, 76*(6), 1206-1213.

Fernstrom, M., Bakkman, L., Tonkonogi, M., Shabalina, I. G., Rozhdestvenskaya, Z., Mattsson, C. M., . . . Sahlin, K. (2007). Reduced efficiency, but increased fat oxidation, in mitochondria from human skeletal muscle after 24-h ultraendurance exercise. *J Appl Physiol (1985), 102*(5), 1844-1849. doi:10.1152/japplphysiol.01173.2006

Ferreira, L. F., Koga, S., & Barstow, T. J. (2007). Dynamics of noninvasively estimated microvascular O2 extraction during ramp exercise. *J Appl Physiol (1985), 103*(6), 1999-2004. doi:10.1152/japplphysiol.01414.2006

Ferreira, L. F., McDonough, P., Behnke, B. J., Musch, T. I., & Poole, D. C. (2006). Blood flow and O2 extraction as a function of O2 uptake in muscles composed of different fiber types. *Respir Physiol Neurobiol, 153*(3), 237-249. doi:10.1016/j.resp.2005.11.004

Ferreira, L. F., Poole, D. C., & Barstow, T. J. (2005). Muscle blood flow-O2 uptake interaction and their relation to on-exercise dynamics of O2 exchange. *Respir Physiol Neurobiol, 147*(1), 91-103. doi:10.1016/j.resp.2005.02.002

Giandolini, M., Horvais, N., Rossi, J., Millet, G. Y., Morin, J. B., & Samozino, P. (2015). Acute and delayed peripheral and central neuromuscular alterations induced by a short and intense downhill trail run. *Scand J Med Sci Sports*. doi:10.1111/sms.12583

Gimenez, P., Kerherve, H., Messonnier, L. A., Feasson, L., & Millet, G. Y. (2013). Changes in the Energy Cost of Running during a 24-h Treadmill Exercise. *Med Sci Sports Exerc, 45*(9), 1807-1813. doi:10.1249/MSS.0b013e318292c0ec

Grassi, B., & Quaresima, V. (2016). Near-infrared spectroscopy and skeletal muscle oxidative function in vivo in health and disease: a review from an exercise physiology perspective. *J Biomed Opt, 21*(9), 091313. doi:10.1117/1.JBO.21.9.091313

Jones, P. R., & Pearson, J. (1969). Anthropometric determination of leg fat and muscle plus bone volumes in young male and female adults. *J Physiol., 204*(2), 63P-66P.

Jones, S., D'Silva, A., Bhuva, A., Lloyd, G., Manisty, C., Moon, J. C., . . . Hughes, A. D. (2017). Improved Exercise-Related Skeletal Muscle Oxygen Consumption Following Uptake of Endurance Training Measured Using Near-Infrared Spectroscopy. *Front Physiol, 8*, 1018. doi:10.3389/fphys.2017.01018

Kano, Y., Padilla, D. J., Behnke, B. J., Hageman, K. S., Musch, T. I., & Poole, D. C. (2005). Effects of eccentric exercise on microcirculation and microvascular oxygen pressures in rat spinotrapezius muscle. *J Appl Physiol (1985), 99*(4), 1516-1522. doi:10.1152/japplphysiol.00069.2005

Kasikcioglu, E., Arslan, A., Topcu, B., Sayli, O., Akhan, H., Oflaz, H., . . . Meric, M. (2006). Cardiac fatigue and oxygen kinetics after prolonged exercise. *Int J Cardiol, 108*(2), 286-288. doi:10.1016/j.ijcard.2005.03.014

Lazzer, S., Taboga, P., Salvadego, D., Rejc, E., Simunic, B., Narici, M. V., . . . di Prampero, P. E. (2014). Factors affecting metabolic cost of transport during a multi-stage running race. *J Exp Biol, 217*(Pt 5), 787-795. doi:10.1242/jeb.091645

Mastaloudis, A., Leonard, S. W., & Traber, M. G. (2001). Oxidative stress in athletes during extreme endurance exercise. *Free Radic Biol Med, 31*(7), 911-922.

Millet, G. Y., Tomazin, K., Verges, S., Vincent, C., Bonnefoy, R., Boisson, R. C., . . . Martin, V. (2011). Neuromuscular consequences of an extreme mountain ultra-marathon. *PLoS One, 6*(2), e17059. doi:10.1371/journal.pone.0017059

Mrakic-Sposta, S., Gussoni, M., Moretti, S., Pratali, L., Giardini, G., Tacchini, P., . . . Vezzoli, A. (2015). Effects of Mountain Ultra-Marathon Running on ROS Production and Oxidative Damage by Micro-Invasive Analytic Techniques. *PLoS One, 10*(11), e0141780. doi:10.1371/journal.pone.0141780

Overgaard, K., Lindstrom, T., Ingemann-Hansen, T., & Clausen, T. (2002). Membrane leakage and increased content of Na+ -K+ pumps and Ca2+ in human muscle after a 100-km run. *J Appl Physiol (1985), 92*(5), 1891-1898. doi:10.1152/japplphysiol.00669.2001

Porcelli, S., Marzorati, M., Lanfranconi, F., Vago, P., Pisot, R., & Grassi, B. (2010). Role of skeletal muscles impairment and brain oxygenation in limiting oxidative metabolism during exercise after bed rest. *J Appl Physiol (1985), 109*(1), 101-111. doi:10.1152/japplphysiol.00782.2009

Richardson, R. S., Poole, D. C., Knight, D. R., Kurdak, S. S., Hogan, M. C., Grassi, B., . . . Wagner, P. D. (1993). High muscle blood flow in man: is maximal O2 extraction compromised? *J Appl Physiol, 75*(4), 1911-1916.

Rowlands, D. S., Pearce, E., Aboud, A., Gillen, J. B., Gibala, M. J., Donato, S., . . . Tarnopolsky, M. A. (2012). Oxidative stress, inflammation, and muscle soreness in an 894-km relay trail run. *Eur J Appl Physiol, 112*(5), 1839-1848. doi:10.1007/s00421-011-2163-1

Salvadego, D., Domenis, R., Lazzer, S., Porcelli, S., Rittweger, J., Rizzo, G., . . . Grassi, B. (2013). Skeletal muscle oxidative function in vivo and ex vivo in athletes with marked hypertrophy from resistance training. *J Appl Physiol, 114*(11), 1527-1535. doi:japplphysiol.00883.2012 [pii]10.1152/japplphysiol.00883.2012

Salvadego, D., Lazzer, S., Marzorati, M., Porcelli, S., Rejc, E., Simunic, B., . . . Grassi, B. (2011). Functional impairment of skeletal muscle oxidative metabolism during knee extension exercise after bed rest. *J Appl Physiol, 111*(6), 1719-1726. doi:japplphysiol.01380.2010 [pii] 10.1152/japplphysiol.01380.2010

Saugy, J., Place, N., Millet, G. Y., Degache, F., Schena, F., & Millet, G. P. (2013). Alterations of Neuromuscular Function after the World's Most Challenging Mountain Ultra-Marathon. *PLoS One, 8*(6), e65596. doi:10.1371/journal.pone.0065596

Savoldelli, A., Fornasiero, A., Trabucchi, P., Limonta, E., La Torre, A., Degache, F., . . . Schena, F. (2017). The Energetics during the World's Most Challenging Mountain Ultra-Marathon-A Case Study at the Tor des Geants(R). *Front Physiol, 8*, 1003. doi:10.3389/fphys.2017.01003

Sierra, A. P., da Silveira, A. D., Francisco, R. C., Barretto, R. B., Sierra, C. A., Meneghelo, R. S., . . . Stein, R. (2016). Reduction in Post-Marathon Peak Oxygen Consumption: Sign of Cardiac Fatigue in Amateur Runners? *Arq Bras Cardiol, 106*(2), 92-96. doi:10.5935/abc.20150148

Snyder, A. C., & Parmenter, M. A. (2009). Using near-infrared spectroscopy to determine maximal steady state exercise intensity. *J Strength Cond Res, 23*(6), 1833-1840. doi:10.1519/JSC.0b013e3181ad3362

Temesi, J., Rupp, T., Martin, V., Arnal, P. J., Feasson, L., Verges, S., & Millet, G. Y. (2014). Central fatigue assessed by transcranial magnetic stimulation in ultratrail running. *Med Sci Sports Exerc, 46*(6), 1166-1175. doi:10.1249/MSS.0000000000000207

Tonkonogi, M., Walsh, B., Svensson, M., & Sahlin, K. (2000). Mitochondrial function and antioxidative defence in human muscle: effects of endurance training and oxidative stress. *J Physiol, 528 Pt 2*, 379-388.

Vernillo, G., Brighenti, A., Limonta, E., Trabucchi, P., Malatesta, D., Millet, G. P., & Schena, F. (2016). Effects of Ultratrail Running on Skeletal Muscle Oxygenation Dynamics. *Int J Sports Physiol Perform*. doi:10.1123/ijspp.2015-0745

Vernillo, G., Savoldelli, A., Skafidas, S., Zignoli, A., La Torre, A., Pellegrini, B., . . . Schena, F. (2016). An Extreme Mountain Ultra-Marathon Decreases the Cost of Uphill Walking and Running. *Front Physiol, 7*, 530. doi:10.3389/fphys.2016.00530

Vernillo, G., Savoldelli, A., Zignoli, A., Trabucchi, P., Pellegrini, B., Millet, G. P., & Schena, F. (2014). Influence of the world's most challenging mountain ultra-marathon on energy cost and running mechanics. *Eur J Appl Physiol, 114*(5), 929-939. doi:10.1007/s00421-014-2824-y

Table 1. Physical characteristics of the participants and race time.

Runners (n:18)						
Age (years)	36.8	±	9.2	[23	-	56]
BM (kg) PRE	68.1	±	8.1	[46	-	82]
BM (kg) POST	66.7	±	8.3	[44	-	82]
Stature (m)	1.75	±	0.07	[1.54	-	1.83]
BMI ($kg \cdot m^{-2}$)	22.1	±	1.6	[18.8	-	25.3]
QM (kg)	1.94	±	0.35	[1.35	-	2.40]
$V'O_2max$ ($ml \cdot kg^{-1} \cdot min^{-1}$)	64.3	±	6.3	[55.3	-	77.5]
HRmax (bpm)	179.0	±	9.5	[163	-	198]
$V_{vert}max$ ($m \cdot s^{-1}$)	0.42	±	0.07	[0.33	-	0.55]
Race time (hh:mm:ss)	06:32:39	±	02:08:15	[03:20:15	-	10:48:50]

All values are means ± SD.

BM: body mass; BMI: body mass index; $V'O_2max$: maximal oxygen uptake; HRmax: maximal heart rate; QM: quadriceps muscle mass; $V_{vert}max$: maximal vertical velocity.

Table 2. Peak physiological parameters during the one-leg knee extensor exercise measured before (PRE) and after (POST) the race.

	PRE	POST	P
V'Epeak (L·min^{-1})	55.1 ± 14.5	45.8 ± 14.9	0.001
V'Tpeak (L)	1.73 ± 0.40	1.39 ± 0.32	0.001
V'O_2peak (L·min^{-1})	1.63 ± 0.37	1.24 ± 0.32	0.001
fRpeak (breaths·min^{-1})	32.9 ± 7.0	33.5 ± 7.6	0.566
Rpeak	0.96 ± 0.09	0.91 ± 0.08	0.164
HRpeak (beats·min^{-1})	126.9 ± 1.5	116.6 ± 13.5	0.085
V'O_2peak /QM (ml·min^{-1}·100g^{-1})	83.50 ± 12.70	63.1 ± 13.1	0.001
Ppeak (W)	79.5 ± 15.5	58.5 ± 17.5	0.002
Time to exhaustion (min:sec)	08:43 ± 01:27	07:00 ± 01:34	0.002

All values are means ± SD.

V'Epeak: peak ventilation; V'Tpeak: peak tidal volume; V'O_2peak: peak oxygen uptake; fRpeak: peak respiratory frequency; Rpeak: peak respiratory exchange ratio; HRmax: maximal heart rate; QM: quadriceps muscle mass; Ppeak: peak power.

Figure 1. Race profiles for the 32 km (2000 m elevation gain, A) and 50 km (3200 m elevation gain, B).

A.

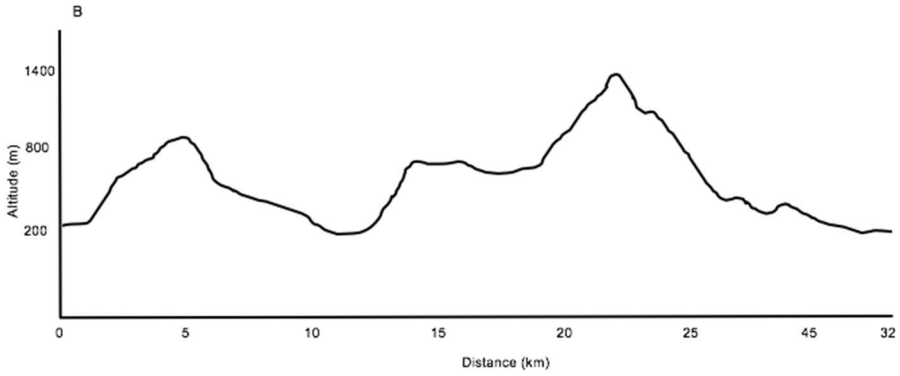

B.

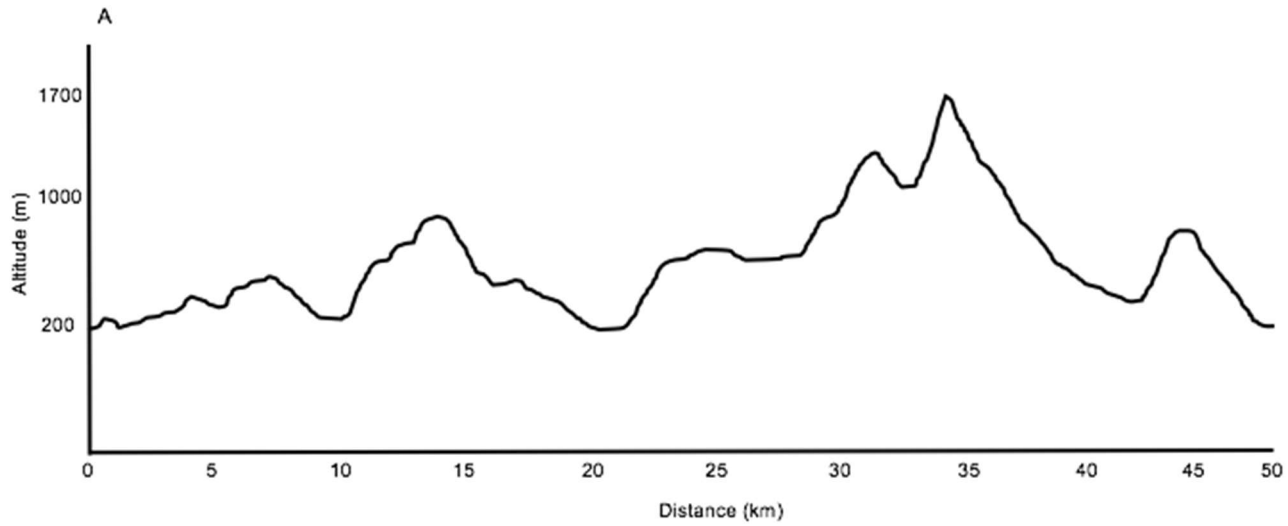

Figure 2. Oxygen uptake as a function of work rate during one-leg knee extensor exercise before (PRE, black squares) and after (POST, white dot) the race. All values are means ± SD.

* : p<0.001 compared to the last workload at POST.

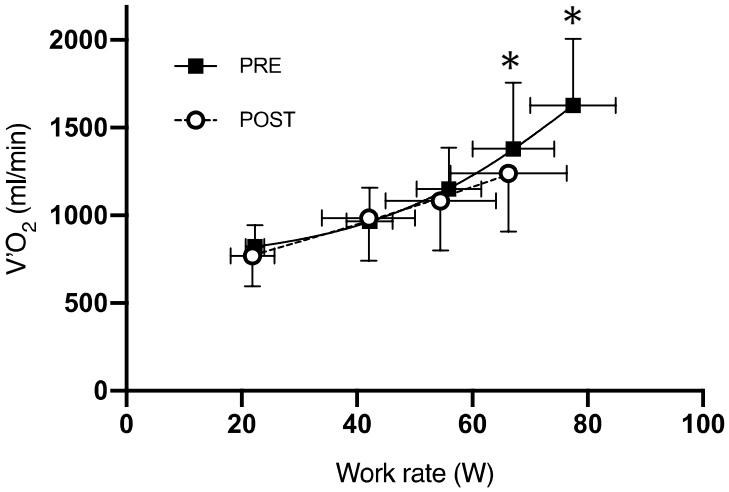

Figure 3. Deoxygenated hemoglobin and myoglobin Δ[deoxy(Hb+Mb)] measured by NIRS as a function of work rate during one-leg knee extensor exercise before (PRE, black squares) and after (POST, white dot) the race. The percentage is related to the maximum value obtained during a transient limb ischemia induced at the end of the test. All values are means ± SD. * : p<0.001 compared to the last workload at POST.